NIST GCR 02-832

Flammability Characteristic of Painted Concrete Blocks

Jason Dreisbach
University of Maryland
College Park, MD 20742

National Institute of Standards and Technology
Technology Administration, U.S. Department of Commerce

NIST GCR 02-832

Flammability Characteristic of Painted Concrete Blocks

Prepared for
U.S. Department of Commerce
Building and Fire Research Laboratory
National Institute of Standards and Technology
Gaithersburg, MD 20899-8661

By
Jason Dreisbach
University of Maryland
College Park, MD 20742

April 2002

U.S. Department of Commerce
Donald L. Evans, Secretary

Technology Administration
Phillip J. Bond, Under Secretary for Technology

National Institute of Standards and Technology
Arden L. Bement, Jr., Director

Notice

This report was prepared for the Building and Fire Research Laboratory of the National Institute of Standards and Technology under Contract number 60NANB8D0085. The statement and conclusions contained in this report are those of the author and do not necessarily reflect the views of the National Institute of Standards and Technology or the Building and Fire Research Laboratory.

FLAMMABILITY CHARACTERISTIC OF PAINTED CONCRETE BLOCKS

By

Jason Dreisbach

Thesis submitted to the Faculty of the Graduate School of the
University of Maryland, College Park in partial fulfillment
of the requirements for the degree of
Master of Science,
2001

Advisory Committee

Professor Frederick Mowrer, Chair
Professor James Quintiere
Professor James Milke

ACKNOWLEDGEMENTS

I would like to thank the Department of Fire Protection Engineering, especially Dr Mowrer, for helping me through this process. May our paths cross again.

Thank you to my family and especially Katie for being understanding and fully supportive.

TABLE OF CONTENTS

LIST OF FIGURES

LIST OF TABLES

ABSTRACT

Title of Thesis: FLAMMABILITY CHARACTERISTICS OF PAINTED CONCRETE BLOCK

Degree Candidate: Jason S. Dreisbach

Degree and Year: Master of Science in Fire Protection Engineering, 2001

Thesis directed by: Dr. Frederick W. Mowrer, Associate Professor, Department of Fire Protection Engineering

The flammability characteristics of painted concrete blocks exposed to incident heat fluxes were studied using the Cone calorimeter. Samples of concrete block were painted with 2, 4, 6, 8, and 10 coats of interior oil-based or latex paint over one coat of latex based primer and subjected to heat fluxes ranging from 35 kW/m^2 to 85 kW/m^2. Critical heat fluxes were found for the different coating levels and types of paint. The ASTM E1321 analysis methodology was used to evaluate ignition temperatures and those values were compared with surface temperatures measured using thermocouples imbedded in the surface of some painted samples. The calculated and measured values for effective ignition temperature differed by a factor of 2 or more, with the calculated values being higher. A new method for determining the effective ignition temperature based on handbook material properties, the heat conduction equation and ignition time found better agreement with measured surface temperature data when using appropriate

values for radiative absorptivity. Quintiere's flame spread parameter, b, was used to evaluate the propensity for flame spread on painted concrete block surfaces. This propensity was found to be small for the range of heat fluxes and coating levels considered. Based on the tests of painted concrete block performed, it appears that the release of water vapor from the concrete block might effect ignition via dilution of the flammable vapor above the surface.

I. INTRODUCTION

The flammability characteristics of interior wall and ceiling finishes are an important aspect of building fire safety. **As** noted in the NFPA Fire Protection Handbook, these interior finishes represent large surfaces over which flame can spread [13. Such flame spread can escalate a small fire to much larger intensity, leading to room flashover, or it can serve as a pathway for fire to spread from one object to another.

For the past 50 years, the flammability characteristics of interior wall and ceiling finishes have been regulated in the United States by means of an index-based fire test method commonly known as the "tunnel test" [2]. The tunnel test method provides a comparative ranking of materials based on their performance under the conditions specified in the test standard. Unfortunately, performance in the tunnel test may not correlate with actual performance in the field, so efforts have been undertaken to develop more predictive methods for evaluating the flammability characteristics of interior wall and ceiling finishes.

Predictive methods for evaluating the flammability characteristics of interior wall and ceiling finishes are based on theoretical models of flame spread [3, 4, 5] that make use of fundamental material flammability properties [4, 9] derived from small-scale fire test methods, such as the Cone Calorimeter [6] and the LIFT apparatus [7]. These theoretical models demonstrate the critical nature of flame spread, particularly for thin combustible surfaces applied to noncombustible substrates. This means that small differences in exposure conditions or in material properties can lead to large differences in actual flame spread performance.

Theoretical models of flame spread on a surface consider flame spread as a sequence of ignitions on fuel elements. In this respect, flame spread will occur if the burning duration of a burning element of the surface is longer than the time to ignition of an adjacent element. If true, then flame spread is expected. If false, then localized burnout is expected. In theory, there is a fine line separating these two regimes.

The purpose of this work is to evaluate the flammability characteristics of painted concrete block and to derive appropriate material flammability properties for painted concrete block that can be used for flame spread modeling. Painted concrete block is a popular interior finish in many buildings, particularly in educational, institutional and multi-family residential facilities, so the implications of this work can have an impact on the evaluation of fire safety in facilities with painted concrete block surfaces.

The flammability characteristics of painted concrete block were evaluated by subjecting 100 mm by 100 mm by 50 mm specimens coated with primer and various layers of paint on one surface to testing in the Cone Calorimeter [6]. Samples coated with one layer of latex primer and with two to ten coats of latex- and oil-based interior paints were evaluated. Imposed heat fluxes ranging from 35 to 85 kW/m^2 were used.

Effective material flammability properties were derived from the Cone Calorimeter test results. Based on analysis of test results along with some specially instrumented Cone Calorimeter tests, it was determined that the standard methods for evaluating effective material flammability properties will yield erroneous results for painted concrete block. Alternative methods for evaluating these properties are developed and presented.

II. BACKGROUND

McGraw and Mowrer [13] investigated the flammability of painted gypsum wallboard using the cone calorimeter. Tests were run on samples with two through eight coats of latex paint over one coat of primer at incident heat fluxes ranging from 25 kW/m^2 to 75 kW/m^2. The flame-spread model developed by Quintiere and coworkers [3, 4, 5] was used to evaluate the potential for flame spread over painted gypsum wallboard. This study determined flame spread might occur for high heat fluxes and high coating levels. Also, by comparing the ratio of ignition time to burning duration, a critical heat flux required for flame spread was found for thin materials. This study did not conclude a dependence of coating level on the propensity to spread flame.

Mowrer [14] has recently presented more data and analysis on oil based painted gypsum wallboard. This study found that blistering at the surface occurred for oil-based paint while being exposed to an incident heat flux. This decreased the ignition time of the sample by a factor of 3-4 because the thin flammable material separated from the gypsum making it essentially thermally thin as opposed to thermally thick when attached to the gypsum throughout the test. In this analysis, the ignition response parameter (IRP) and the specific ignition energy (SIE) were used to attempt to characterize the ignition phenomenon of blistered samples. The cause and verification of blistering on other materials was left as a question.

Torero and Mowrer [11] have studied interpretation of ignition test data and applicability of **ASTM** E1321 methods for evaluating material properties. Their analysis included interpretation of short and long time solutions for non-dimensional surface temperature and determined that the testing conditions specified by the LIFT procedure fell in between those two solutions. Testing of PMMA samples showed in-depth conduction of approximately 30% of the external heat flux. This led to the conclusion that an evaluation of the in depth conduction during the test is warranted for the testing conditions in order to more accurately determine ignition temperatures.

Delichatsios et. al. [12] have studied the use of ignition time data for calculating material properties and critical heat flux. This study evaluated the method described in ASTM E1321 for determining thermal inertia and critical heat flux, or ignition temperature. The study reformulated the heating theory to include significant surface reradiation and convective losses and found that the method of plotting the square root of ignition time on the x-axis to obtain "effective" properties is a zeroeth order approximation of theory. Their improvements led to a more accurate representation of reality, however, with approximations, the equations are not fully applicable to all testing conditions. They have therefore proposed a modification of the testing procedures used to study ignition. They proposed the surface of the sample be covered with a thin layer of carbon black to simulate the effects of smoke deposition and to ensure all heat to the sample is absorbed via conduction. This would mean the absorption coefficient and emissivity would exactly equal unity and determination of thermal properties would not be influenced by the uncertainty in these parameters.

Janssens and Dillon **[8]** have studied the use of small-scale test data for determining material and flammability properties for materials and their use in predicting performance in full-scale fire scenarios. The material properties were calculated using a modified formulation of the typical ignition theory that accounted for a variable convection coefficient. The properties that were calculated and small-scale test data from the cone calorimeter were used in a model to predict the performance of interior finish material in the ISO 9705 Room/Corner Test [10]. Dillon et al [9] used the LIFT apparatus [7] procedure for determining material properties to fit into a similar model of the ISO 9705 test. The methods of both of these studies did not fundamentally modify the technique prescribed by **ASTM** E1321, but rather adjusted the technique in order to use the available data. The results were "effective" material properties for the condition tested and assumptions made. The authors of both of these studies claimed reasonable accuracy in the large-scale prediction using these effective properties. However, no attempt was made to validate assumptions at the small-scale level where material properties were derived.

111. THEORY

This chapter presents the ignition and flame spread theories used to evaluate the flammability characteristics of painted concrete block. These theories indicate the material flammability properties needed to evaluate the potential for ignition and flame spread.

IGNITION THEORY

In order to predict the ignition of a solid surface, it is typical to assume that a material will ignite when it reaches a unique effective ignition temperature, T_{ig}. This implies that the material will be inert up to the effective ignition temperature, then will release an ignitable concentration of vapors at the fuel surface when the effective ignition temperature is reached.

The surface of a material will heat up if exposed to an incident heat flux. The rate of heating of this surface depends on the intensity of the incident heat flux and the material's thermal properties. The rate of heating also has some length scale dependence, and therefore, materials are generally classified as either thermally thin or thermally thick. Most building materials, including painted concrete block, represent thermally thick materials.

The ASTM E 1321 (LIFT apparatus) test method and interpretation represents the most widely used presentation of ignition theory [7]. This theory assumes a semi-infinite solid. The heat conduction equation is solved for a semi-infinite solid exposed to a constant incident heat flux with convective heat losses at the surface to obtain a nondimensional temperature rise at the surface of:

$$\frac{\Delta T_s}{\Delta T_c} = 1 - exp\left(\frac{t}{t_c}\right) erfc\left(\sqrt{\frac{t}{t_c}}\right) \tag{1}$$

where $\Delta T_c = \frac{\alpha \dot{q}''_{inc}}{h_t}$ and $t_c = \frac{k\rho c}{h_t^2}$. The term h_t represents the total heat transfer coefficient at the surface and is intended to include surface convection and reradiation losses from the surface, i.e., **h,** $= h_c + h_r$. The characteristic temperature rise at the surface, ***AT,,*** represents the maximum surface temperature under conditions of no conduction into the material. The characteristic time constant, *t,* **,** represents the time for the solid to thermally relax. The energy balance at the surface under condition of no conduction can be expressed as:

$$\alpha \dot{q}''_{inc} = h_c(T_c - T_o) + \varepsilon\sigma(T_c^4 - T_o^4) = h_t(T_c - T_o)\,. \tag{2}$$

In the calculation method for determining ignition temperature in ASTM E 1321, the left hand side of Equation 2 is set equal to the critical heat flux for ignition $\dot{q}''_{cr}$, which is defined as the minimum incident heat flux at which ignition occurs within the 20 minute standard test time. ***An*** iterative approach must be used to solve Equation 2 due to the nonlinearity of the reradiative term. Equation 2 was solved using the Newton-Raphson Method to produce the equilibrium surface temperatures and associated heat transfer coefficients shown in Figure 1 and Table 1:

Table 1 : Characteristic Temperatures and Total Heat Transfer Coefficients

αq_{inc} (kW/m2)	ΔT_c	h_t
0	0	
10	289	0.035
20	426	0.047
30	518	0.058
40	589	0.068
50	647	0.077
60	697	0.086
70	740	0.095
80	779	0.103
90	815	0.110
100	847	0.118

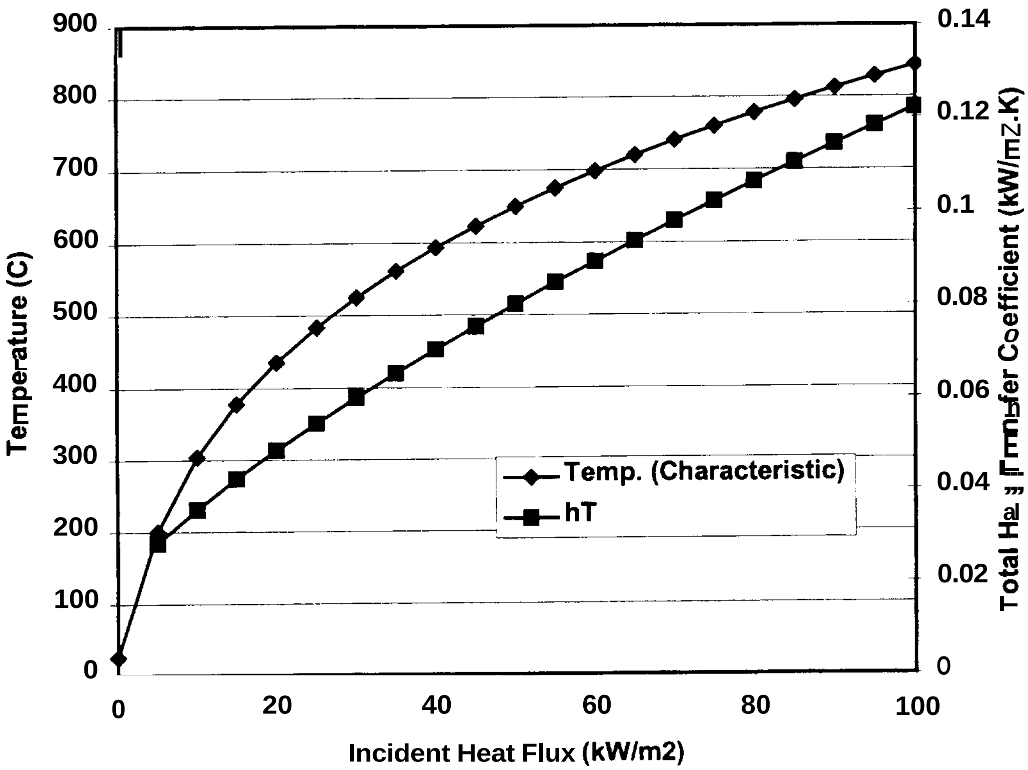

Figure 1: Equilibrium Surface Temperature as a Function of Incident Heat Flux

Figure 1 shows the characteristic surface temperature and total heat transfer coefficient as a function of incident heat flux. A constant value of 0.015 $kW/m^2.K$ is used for the convective heat transfer coefficient. This plot is similar to the plot in the ASTM E1321 standard.

This approach to determining an effective ignition temperature tends to overpredict the actual ignition temperature because it ignores the effect of conduction into the material on the surface energy balance. After long times, conduction will not necessarily go to zero as assumed in the ASTM E1321 methodolgy; instead, it will approach a steady-state value greater than zero that will depend on the conductivity and thickness of the material and any additional layers of material behind the surface material. The actual quasi-steady energy balance at the surface can be expressed as:

$$\alpha\dot{q}''_{inc} = h_c(T_s - T_o) + \varepsilon\sigma(T_s^4 - T_o^4) + h_k(T_s - T_o) \qquad (3)$$

where h_k represents a conductive heat transfer coefficient. This coefficient can be represented in general for a single material as:

$$h, = \left(\frac{k}{\delta}\right).$$

δ represents the thermal penetration depth and $\boldsymbol{k}$ is the thermal conductivity dependent on the material. At short times, the thermal penetration depth will vary according to the relation $\delta \sim \sqrt{\alpha t}$ **,** where $a = \boldsymbol{k} / \rho c$ is the thermal diffusivity of the material. At long times, the thermal penetration depth will become equal to the thickness of the material. By substitution, the conductive heat transfer coefficient at short times is expected to vary as:

$$h_k \sim \sqrt{\frac{k\rho c}{t}} ,$$

with the proportionality constant to be determined.

For an assembly with multiple layers of different materials, the conductive heat transfer coefficient becomes:

$$h_{k,eq} = \frac{1}{\sum_i 1/h_{k,i}} .$$

This quasi-steady formulation of conduction represents a theoretical limit, since fire tests are normally not conducted until steady state conditions occur. This discussion attempts to demonstrate that the method of determining the effective ignition temperature by the critical heat flux will tend to overestimate the actual ignition temperature, with the magnitude of the difference increasing with the relative magnitude of the conduction term.

FLAME SPREAD THEORY

The focus of this work with respect to flame spread is on the potential for concurrent flow or wind-aided flame spread. Opposed flow flame spread is not addressed. In general, wind-aided flame spread represents a much greater hazard than does opposed flow flame spread. The model propounded by Quintiere and coworkers [3, 4, 5] is used for this analysis. Mowrer and Williamson [15] applied this model to the evaluation of textile wall coverings adhered to gypsum wallboard, while McGraw and Mowrer [13] and Mowrer [14] have applied this model to evaluation of latex- and oil-based painted gypsum wallboard.

The Quintiere model considers the potential for flame spread in terms of the ignition and burnout of surface elements as they are subjected to heat fluxes imposed by the flame and external sources. The details of the model and its simplifying assumptions are described elsewhere [3, 4, 5]. What is significant for the present discussion is that this flame spread model produces a dimensionless "flammability parameter," defined as:

$$b = k_f \dot{Q}'' - \left({t_{ig}}/{t_b} \right) - 1 . \qquad (4)$$

According to the Quintiere model, acceleratory upward flame spread will occur when the value of the flammability parameter is positive, while decay to extinction is expected if its value is negative. Steady fire propagation is expected if the flammability parameter evaluates exactly as zero.

The terms in the flammability parameter equation need to be evaluated. The flame length parameter, k_f, is typically considered to have a value of 0.01 m^2/kW, based on the assumption that the flame length varies linearly with the heat release rate. The heat release rate per unit area, Q'', is typically considered to be the peak heat release rate per unit area for the material. Based on heat transfer theory for a semi-infinite solid, the ignition time, t_{ig}, is typically approximated as:

$$t_{ig} = \frac{\pi}{4} k \rho c \left[\frac{\Delta T_{ig}}{\dot{q}''} \right]^2 , \qquad (5)$$

where $\dot{q}''$ is the incident heat flux at the surface of the material. This is the solution to the semi-infinite heat conduction equation for the case of no surface convection or reradiation. The burning duration, t_b, is typically approximated as:

$$t_b = \frac{Q''}{\dot{Q}''}$$

where Q'' represents the total heat release per unit area, which is also the area under the heat release rate per unit area versus time curve.

Methods have been developed to assess these flammability parameters from Cone Calorimeter data. For thin combustible surfaces over noncombustible substrates tested in the Cone Calorimeter, it is fairly common to obtain results similar to those illustrated inFigure **2,** where the heat release rate rises quickly to a sharp peak value, then descends rapidly back to zero or a near-zero value.

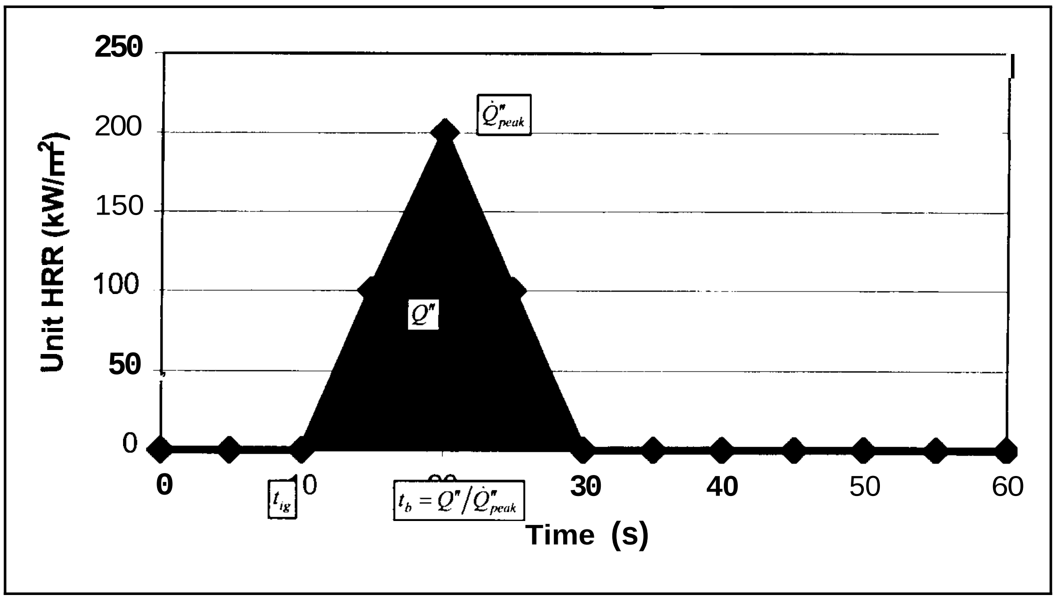

Figure 2: Data Used for Calculation of b

The total heat release, Q'', is the area under the heat release rate curve. This curve is estimated as approximately triangular and, therefore, the area can be calculated simply as one half the base multiplied by the height. The energy released by the fuel burning must be great enough and the duration of release must be long enough to heat the adjacent material to cause ignition and for the fire to spread. Therefore, if the burning duration is long and/or the heat release rate high, b would be greater than zero. Conversely, if the burning duration is approximately equal to or less than the ignition delay time, then flame spread is unlikely based on the Quintiere analysis method.

McGraw and Mowrer [13] suggested that an alternative way to evaluate the potential for flame spread on thin materials adhered to noncombustible substrates is to simply compare the time to ignition with the burning duration. If the burning duration of a burning element is less than the time to ignition of an adjacent element, then localized burnout is expected. Otherwise, flame spread to the adjacent element would be expected. This relationship is similar to the Quintiere flame spread parameter; it can be expressed as:

$\frac{t_b}{t_{ig}} > 1$ for flame spread to occur. Substituting relationships for these individual times and rearranging will lead to a critical heat flux for flame spread:

$$\frac{t_b}{t_{ig}} = \dot{q}''_{critical} = \left(\frac{\pi}{4} \frac{k\rho c\left(T_{ig} - T_o\right)^2}{\rho\delta L} \right)^{-1} \dot{q}''_{net} > 1 \tag{6}$$

According to Equation 6, the ratio of times should vary linearly with the imposed heat flux, with the slope related to the material properties. This time ratio can also be estimated as a function of thermal properties and the square of Tewarson's thermal response parameter (TRP) [19] for thermally thick materials [14]:

$$\frac{t_b}{t_{ig}} = \frac{\dot{q}''_{net}}{\dot{q}''_{critical}} \left(\frac{\rho\delta\Delta H_v}{(TRP)^2} \right) \dot{q}''_{net} > 1 \tag{7}$$

IV. EXPERIMENTAL PROCEDURE

Two different sets of tests were performed in this study. The first set of tests used the cone calorimeter [6]. The other set of tests involved measurement of mass and sample surface, midpoint and back face temperatures under heating from a cone heater. The goal of these tests was to get a direct measure of ignition temperature and approximate conduction through the sample.

The initial procedure for testing painted concrete block followed the procedure of past testing of painted interior wall materials, specifically, the test procedure for painted gypsum wallboard [13]. There were 2 types of paint (oil-based and latex), 5 coating levels (2, 4, 6, **8,** 10 coats plus 1 coat of primer for each), **3** heat fluxes (35, 50 and 75 kW/m^2) and 3 samples for each configuration. Also, additional samples would be needed for an investigation into the critical heat fluxes needed for ignition. All the tests were conducted in the Cone Calorimeter following NFPA 271[6]. The data acquired were then used to evaluate flammability characteristics and the potential for flame spread on painted concrete block surfaces for a range of typical fire scenario heat fluxes.

168 samples were made from 21 8"x16"x 2" (0.20m x 0.41m x 0.05m) concrete patio blocks. Patio blocks were used because they were easier to cut into cone calorimeter samples than hollow concrete blocks while having similar properties. A wet saw was used to cut the blocks into **8** samples per block. After the samples were cut, they were allowed to dry for 30 days or more in the open air inside **a** lab before the mass was measured and the samples were painted. After the mass for each sample was

measured, the density was calculated by dividing the measured mass by the measured volume.

Subsequently, the first 90 samples were painted. All samples received one coat of primer. The primer was a "block filler." Three different paint manufacturers were contacted and all suggested the primer be a thick primer known as a block filler used to smooth the surface of the concrete before painting, in order to increase the adherence of the paint to the surface of the concrete block. The specific block filler used was Duron© Block Kote, which is a latex block filler. After the primer was applied, 45 samples were painted with latex paint, specifically, Duron© Ultra Deluxe Interior Acrylic Latex Semi-Gloss Enamel in white, and 45 samples were painted with oil-based paint, specifically, Duron© Dura Clad Alkyd Gloss Enamel, Urethane Modified in white. The total mass was measured after the final coat was applied to the sample. The mass of paint added for each coat (paint application rate) was not measured for these 90 samples. The incidental mass loss due to normal handling of these samples represented a problem to consistent and meaningful mass data because the addition of mass was so small compared to the total mass and minor loss of concrete aggregate due to handling had a relatively large effect on the mass measurements. For this reason, the samples were handled as little as possible and the mass data was taken after the final coat was applied. However, the average application rate could still be calculated

Once the painting was complete, testing commenced. The initial tests were run at a heat flux of 35 kW/m^2. No ignition occurred at this heat flux for any samples that were painted and the procedure was modified because the needed data could not be collected without ignition. Testing for the critical heat flux needed for ignition was started. The testing was done via trial and error in the Cone Calorimeter. The heat flux was increased by 5 kW/m^2 if the coating level did not ignite until ignition and continuous flaming was observed. No verification tests have been performed at this point. The result is a critical heat **flux** range for ignition.

After the critical heat fluxes were found, the procedure to obtain the needed data was revised. Instead of using the heat fluxes of 35, 50 and 75 kW/m^2 specified in the initial test procedure, the heat fluxes for testing were determined from the critical heat fluxes found earlier. Specifically, tests were run at 10 kW/m^2 and 20 kW/m^2 above the critical heat flux for Latex painted samples (the critical heat fluxes were higher for those samples), up to 85 kW/m^2. The following heat fluxes were used for testing both types of painted samples:

- 10 coat samples were tested at *65* and 75 kW/m^2;
- 8 coat samples were tested at 65 and 75 kW/m^2;
- 6 coat samples were tested at 75 and 85 kW/m^2;
- **4** coat samples were tested at 75 and 85 kW/m^2;
- 2 coat samples were tested at 85 kW/m^2.

The second set of tests took place after the first set of tests was completed. This set of tests involved painting ten more samples, five with latex paint and five with oil-based paint. For these tests type K thermocouples were imbedded in the surface of the sample. To do this, the thermocouples were positioned on the middle of the surface and painted over with one coat of primer and six or ten coats of paint. Three samples for each type of paint received ten coats and two samples of each type received six coats. Painting the thermocouple in to the surface allowed them to stay affixed on the surface of the sample imbedded in the coating of paint. **A** hole at the midpoint of the depth of the sample was drilled to the middle of the length and during testing a thermocouple was positioned in that hole to measure the temperature in the middle of these samples. **A** thermocouple was also placed under the sample at the back face between the sample and the insulating backing material to measure the back face temperature during testing. The mass of the sample was also measured during these tests.

V. DATA AND ANALYSIS

In this chapter, the data collected during this study will be presented, along with analysis of the results. The data collected includes ignition and flammability characteristics. The analysis focuses on using and comparing standard methods versus new methods for determining these characteristics.

Before the data are presented, the literature material properties will be described. The SFPE Handbook [16] lists the thermal properties for cinder concrete including density, ; thermal conductivity, *k;* specific heat, c; and thermal diffusivity . Table 2 summarizes these properties.

Table 2: Material Properties from SFPE Handbook [16]

Property		*k*	c	
Units	kg/m^3	W/m.C	kJ/kg.C	m^2/s
Concrete, cinder	1900-2300	0.76	0.88	8.2-6.8(10^{-7})

Part of the test procedure included weighing and measuring each sample for mass and volume prior to painting in order to calculate the actual density of the blocks used. The block data is summarized in Figure 3 and Figure 4 below. Figure 3 shows the surface area of each sample, while Figure 4 shows the density of each sample. Samples had surface areas less than the nominal 100 cm^2 cone samples because they were cut from larger samples. The samples are smaller due to the width of the saw blade.

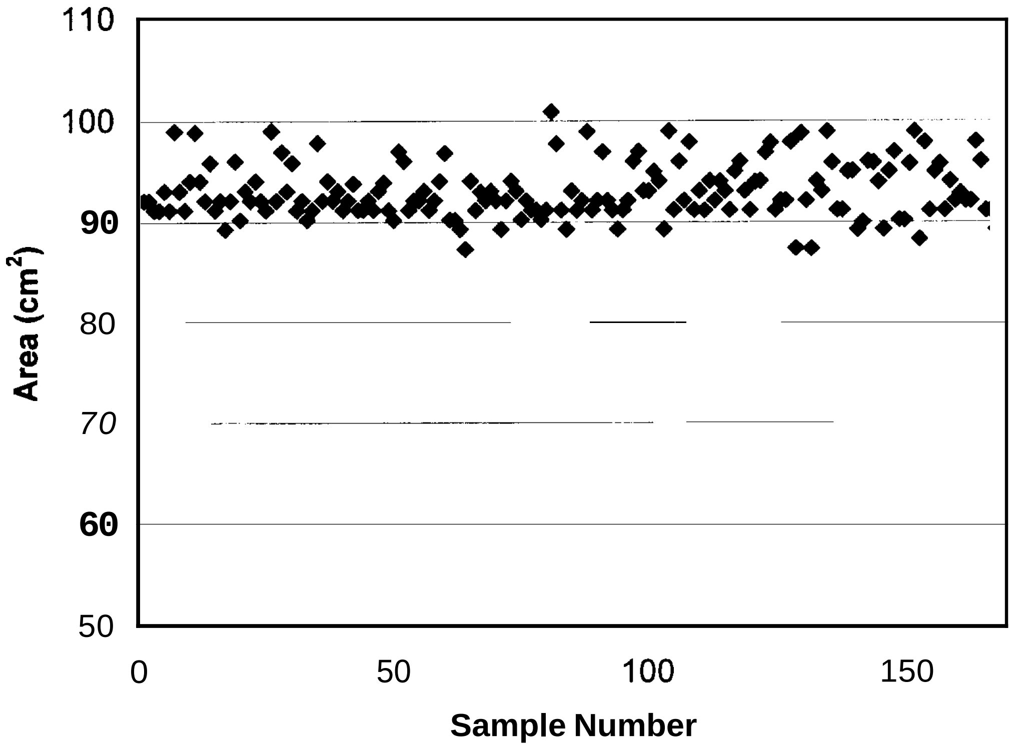

Figure 3: Surface Area of Samples

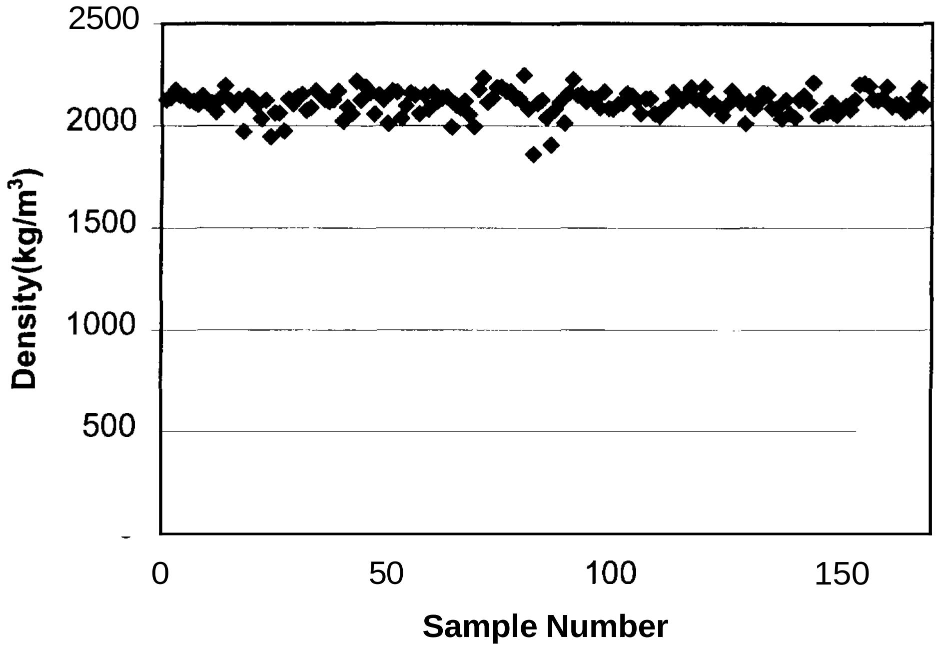

Figure 4: Density of Samples

The surface area of the actual samples ranged from 87.3 cm^2 to 100.88 cm^2, with an average area of 93.07 cm^2. The thickness of all samples was 4.1 cm. The average density was found to be 2110 kg/cm^3, with a minimum of 1860 kg/cm^3 and a maximum of 2250 kg/cm^3. This is consistent with the quoted density of concrete block in the SFPE Handbook [16] ranging between 1900 g/cm^3 and 2300 g/cm^3.

Since the application rate of paint for the first 90 samples was not measured directly after each coat of paint was added, the application rate was estimated. The total mass of paint added per unit area was divided by the number of coats plus one to account for the primer coat. The application rates for different coating levels are shown in Figure 5 and Figure 6.

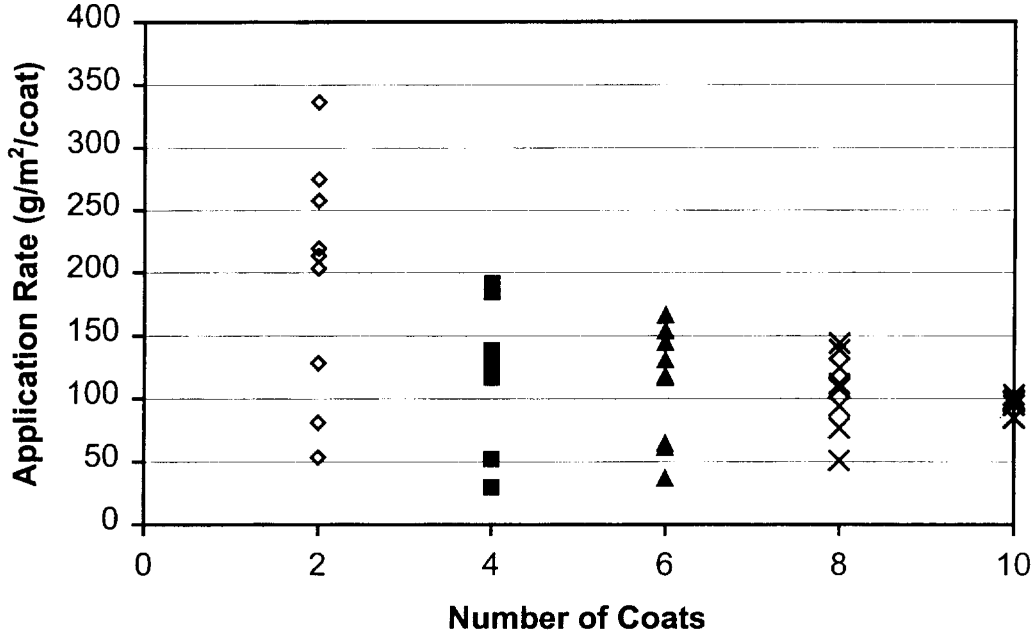

Figure 5: Application Rate by Coating Level for Latex Painted Samples

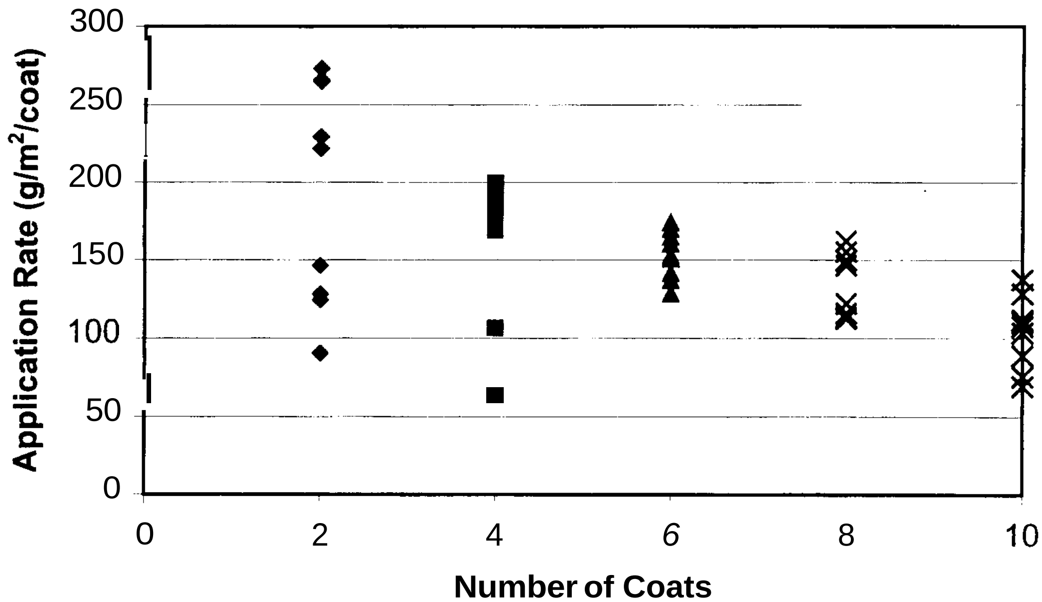

Figure 6: Application Rate by Coating Level for Oil-based Painted Samples

These plots show significant scatter in the application rates. However, they show that the average rates decrease as the number of coats increase. This can be attributed to a "filling" effect each coat has on the surface of the block. More paint is added in the lower coats because the surface of the block is not flat and the paint is able to travel into the cracks and crevasses. **As** more coats are added, the cracks and crevasses fill up and the surface becomes flatter. Figure 7 and Figure **8** show the total paint mass for each sample as a function of number of coats.

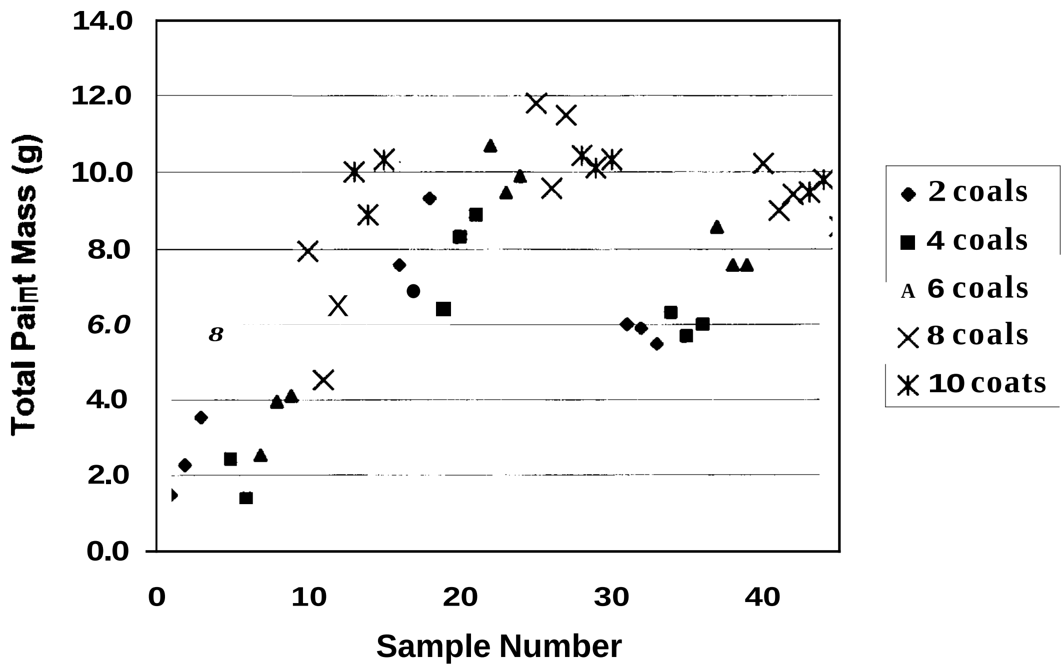

Figure 7: Total Paint Mass - Latex

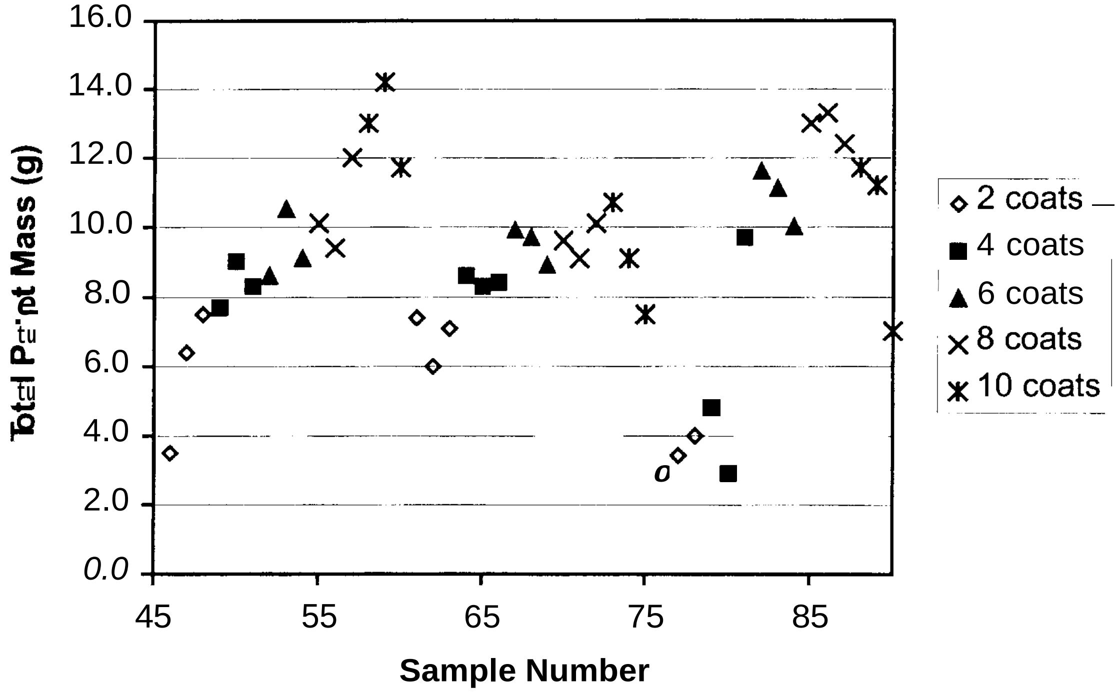

Figure 8: Total Paint Mass - Oil Based

Further study on the application rate was also conducted on samples that were not tested. Twenty-four samples were painted with latex paint. For these samples, the mass of the samples was measured after every coat, including the primer coat. The data from these measurements indicated the same average trend of a decrease in paint application of latex with an increase in number of coats.

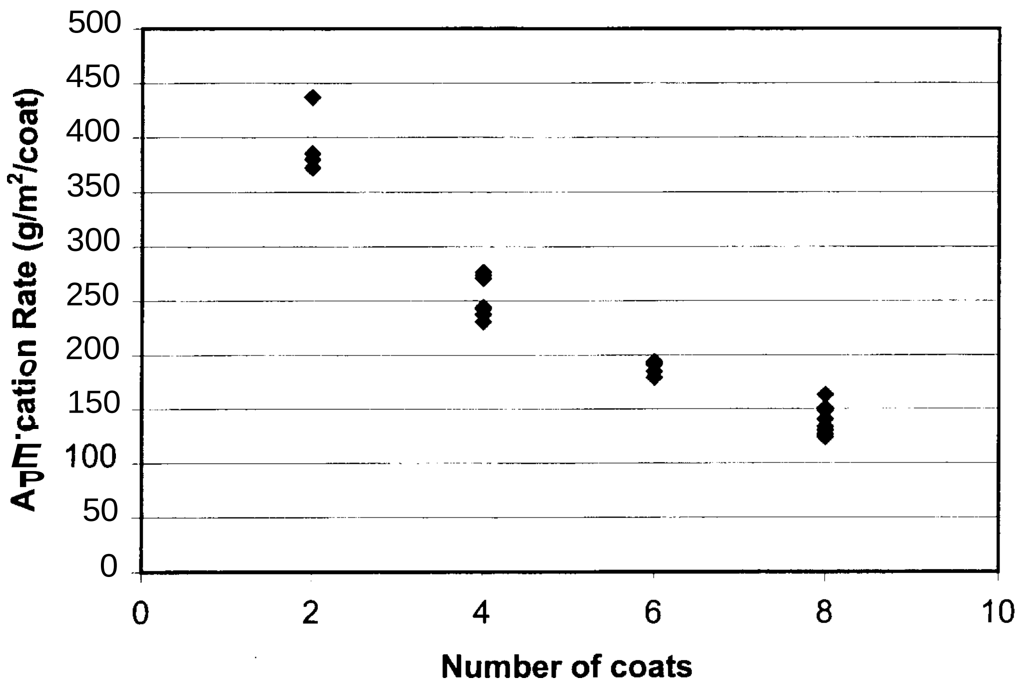

Figure 9: Application Rate by Coating Level for Latex Painted Samples

As described in Chapter IV, the test procedure included determination of the critical heat flux for ignition. This was done through trial and error in the Cone Calorimeter. The heat flux was adjusted in increments of 5 kW/m^2 until a test with no ignition and a test with ignition took place. This led to a critical heat flux measured within 5 kW/m^2. The testing showed that the critical heat flux is dependent on the type of paint, as well as the number of coats of paint on the sample. Table 3 summarizes the critical heat fluxes found.

	Latex	Oil-based
Coats	kW/m^2	kW/m^2
10	*50-55*	45-50
8	*50-55*	*50-55*
6	*60-65*	*50-55*
4	*70-75*	*60-65*
2	80-85	**NA**

Tests for the critical heat flux for 2 coats of oil-based paint were not conducted due to mechanical difficulties with the cone calorimeter. These results show that the critical heat flux for ignition varies significantly with the coating level. They also show that the critical heat flux for latex paint is greater than oil-based paint, again depending on the number of coats. It should be noted that a repeat test of samples with 8 coats of oil-based paint indicated one test with ignition and one test without ignition at *50* kW/m^2. The critical heat flux values listed above were higher than anticipated based on the results of previous studies with painted wall materials [13].

Based on these critical heat fluxes, more tests were conducted to evaluate the burning characteristics of painted concrete block. The tests were run at 10 kW/m^2 and 20 kW/m^2 above the critical values for the latex painted samples, depending on coating level, since critical heat flux levels for latex were higher. Samples with **4, *6*,** 8 and 10 coats were tested at *75* kW/m^2. **A** summary of the test data is provided in Appendix A.

Since all coating levels for both types of paint were tested at *75* kW/m^2 (except 2 coats), that data is considered for comparison purposes. Figure 10 and Figure 11 show comparisons between coating levels and ignition time and peak heat release rate.

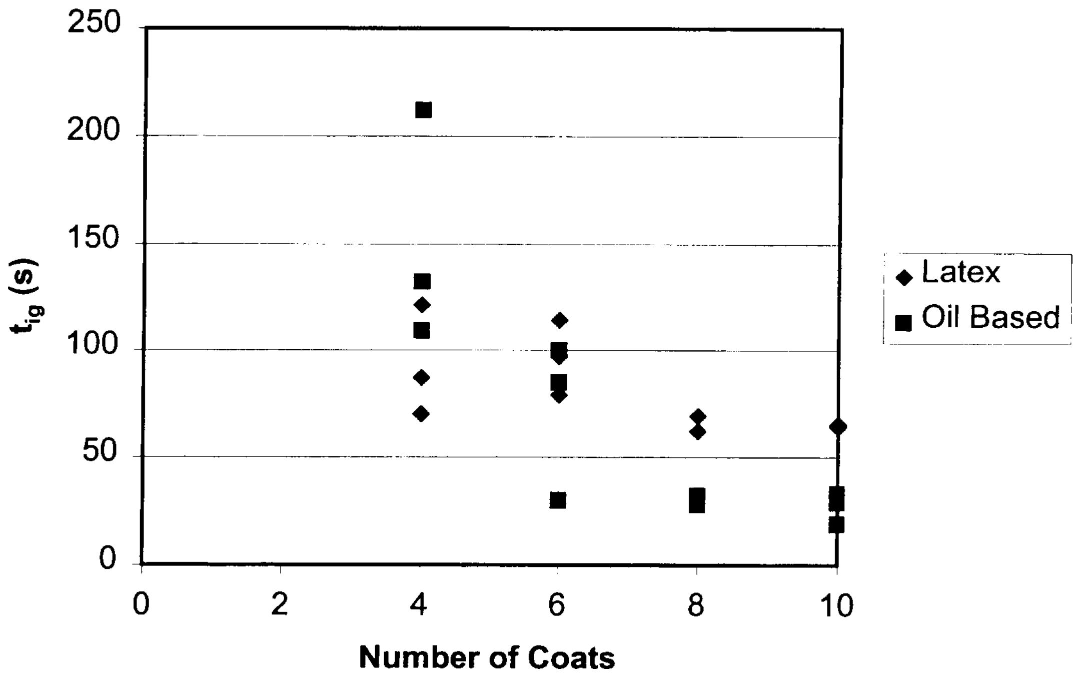

Figure 10: Ignition Time as a Function of Number of Coats at 75 kW/m^2

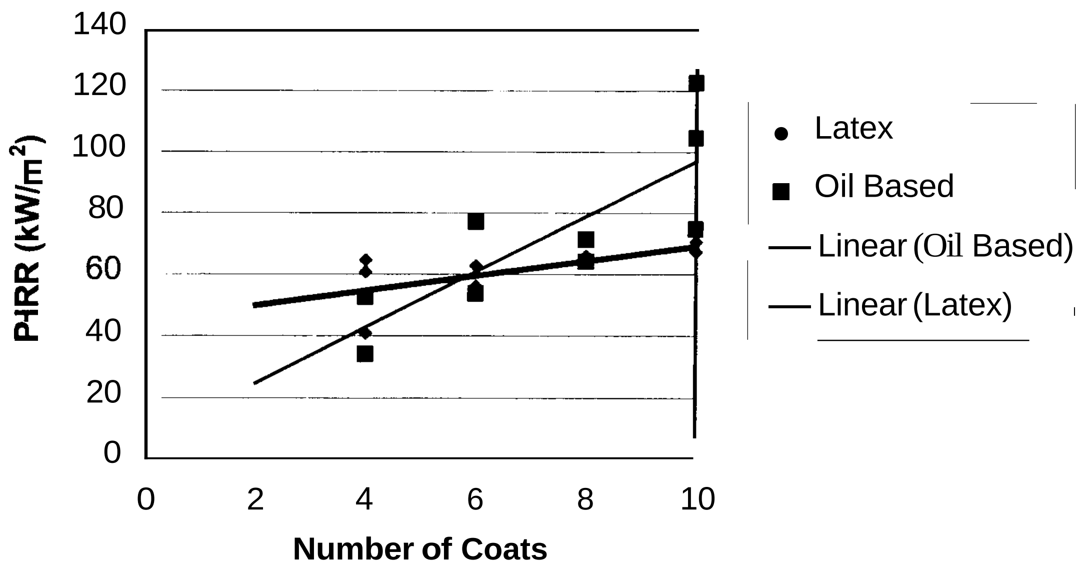

Figure 11: Peak Heat Release Rate as a Function of Number of Coats at 75 kW/m^2

Figure 10 and Figure 11 indicate that the ignition and burning properties depend on the number of coats of paint. The trends show generally that ignition time decreases as number of coats increase and that peak heat release rate increases as number of coats increase. The rate of decrease in ignition time for oil-based paint is much higher than that rate for latex paint. The variation of ignition times for low coating levels indicate that the tested heat flux is close to the critical heat flux for ignition for those coating levels. This suggests that the critical heat flux is coating level dependent. Also, the rate of increase in peak heat release rate is much higher for oil-based paint than for latex.

To look at the problem more closely, ignition times and peak heat release rates versus total mass of paint were considered, as opposed to number of coats.

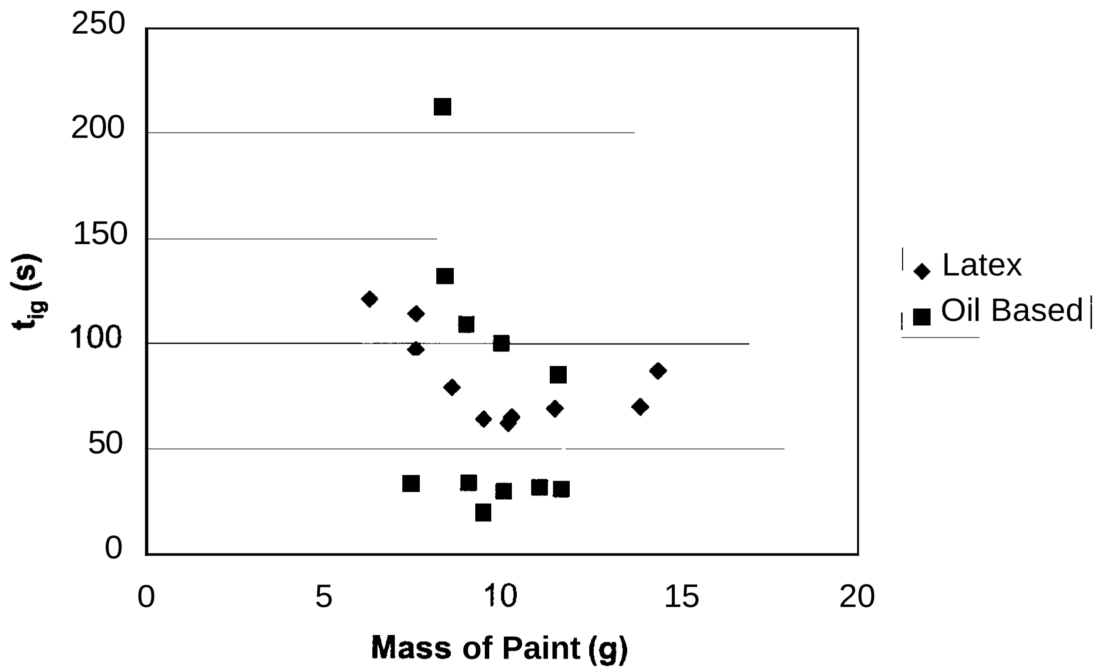

Figure 12: Ignition Time as a Function of Total Mass of Paint at 75 kW/m^2

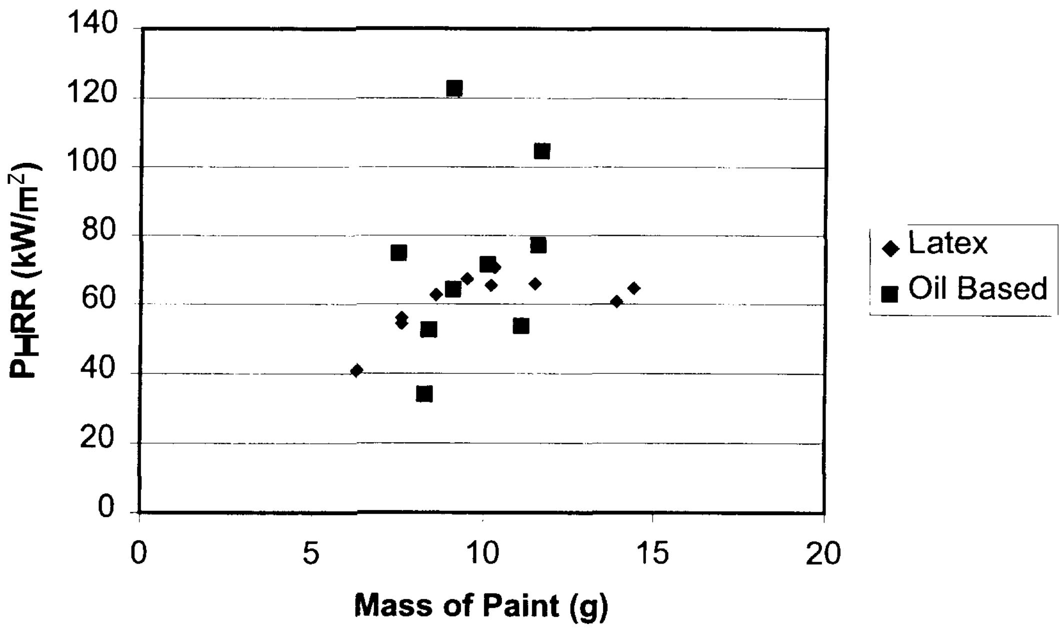

Figure 13: Peak Heat Release Rate as a Function of Total Mass of Paint at 75 kW/m^2

Figure **12** and Figure 13 are less revealing as to relationships between amount of paint and ignition and heat release rate, especially for oil-based painted samples. The trends for the latex painted samples are the same as the trends over number of coats, although much less pronounced. Also, there do not seem to be any trends for the oil-based painted samples and no conclusions can be made about the ignition time and heat release rate dependence on total mass of paint.

A key part of this study focused on effective ignition temperatures of the painted concrete block. Ignition temperatures are represented as a material property in general. This means that ignition temperatures of different samples of the same material are assumed to be the same. Ignition temperatures are used to calculate flammability characteristics and serve a major role in predicting flame spread. It is important therefore that ignition temperature estimations be fairly accurate. Two methods for determining ignition temperature of painted concrete block were used in this study. The first was an indirect calculation using critical heat flux for ignition as determined during testing. The second was a direct measurement using thermocouples on the surface of the samples. Upon comparing these two estimated temperatures, the heat conduction theory was revisited and another method for determining effective ignition temperatures from the data collected is proposed.

The ignition temperature was first determined using the calculation method described in ASTM E1321. The theory for this calculation was described in Chapter III. The determination of a characteristic ignition temperature uses the critical heat flux for ignition. Since the critical heat flux varied depending on type of paint and number of coats, the characteristic ignition temperatures varied also according to type of paint and number of coats. Therefore, one ignition temperature for a type of paint is not a valid assumption to make for this analysis. One must also know how many coats of paint have been applied to a given wall to evaluate its ignition temperature, based on the results of this study. Figure 1 was used to evaluate ignition temperatures via calculation.

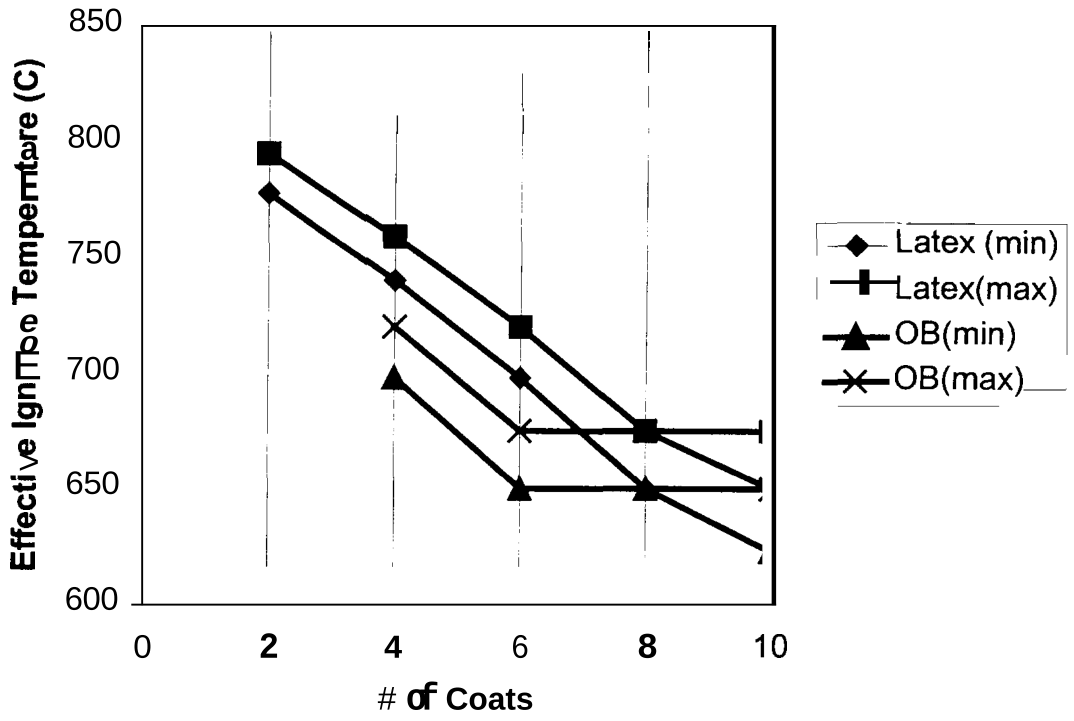

Figure 14: Characteristic Temperature (ignition) Calculated From Critical Heat Flux as a Function of Number of Coats

The "min" and "max" lines in Figure 14 indicate the critical heat flux range of 5 kW/m^2 associated with the testing procedure followed. Characteristic ignition temperature decreases as number of coats increase, and the calculated ignition temperatures are lower for oil-based paint. Also shown in Figure 14 is the magnitude of the calculated ignition temperatures. Depending on number of coats, latex paint ignited between 650°C and 800°C, while oil-based paint ignited between 625°C and 725°C, based on the methodology presented in ASTM E1321.

In an attempt to verify these ignition temperatures and study the applicability of the ASTM E1321 calculation method, ignition temperatures were directly measured using imbedded thermocouples located at the surface of 10 painted samples under an incident heat **flux** of 75 kW/m^2. The procedure was described in Chapter IV. Figure 15 and Figure 16 show the acquired data.

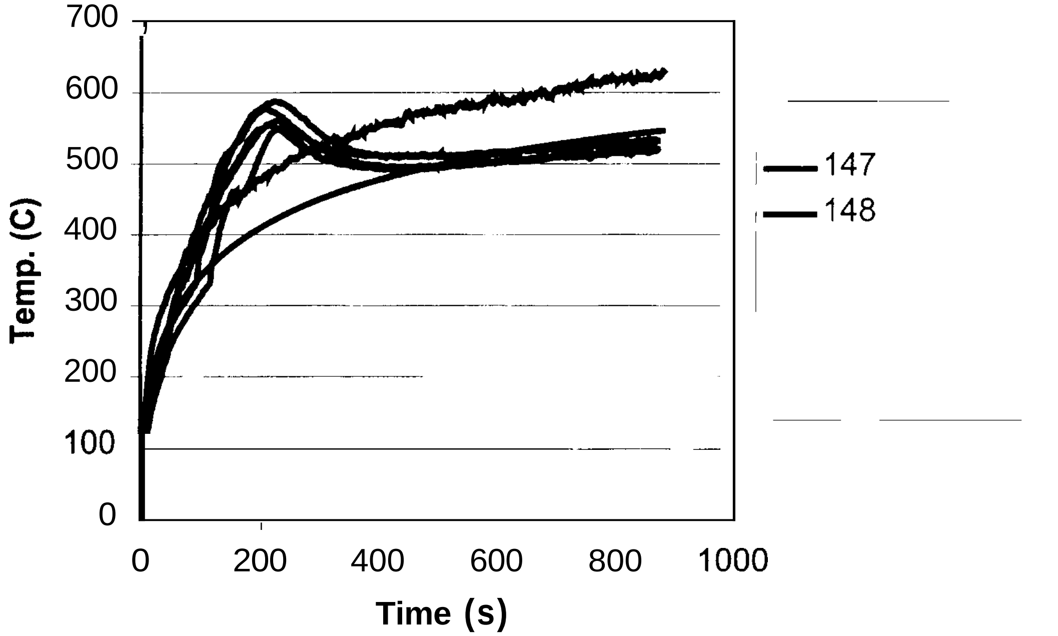

Figure 15: Surface Thermocouple Data for Latex Samples at 75 kW/m^2

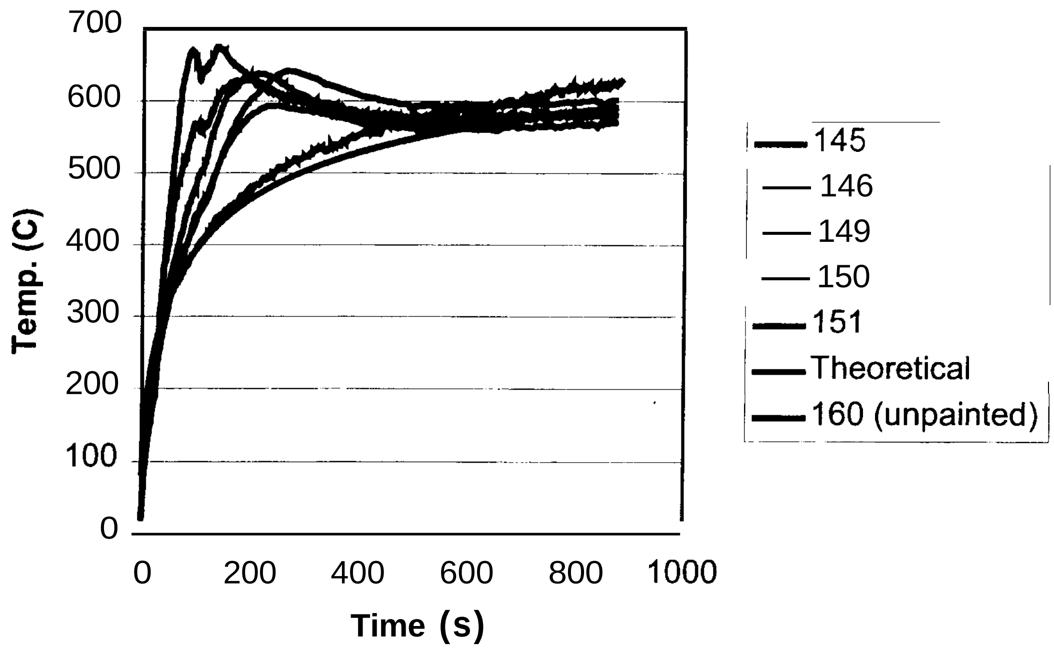

Figure 16: Surface Thermocouple Data for Oil Based Samples at 75 kW/m^2

In Figure 15 and Figure **16,** the surface temperature data is plotted for all the samples of the two types of paint. Also plotted is the surface temperature data of an unpainted sample. These plots show that the surface temperature data for samples with the same type of paint are fairly consistent with one another. The theoretical curves shown on these plots will be discussed later. Data from the individual tests, as well as five thermocouple tests of unpainted samples are given in Appendix B.

The ignition times were also measured during these tests; these ignition times are shown in Table **4.**

Table 4: Measured Ignition Times for Thermocoupled Tests

Sample #	# of Coats	Paint	Ignition Time(s)
144	10	Latex	43
148	10	Latex	55
152	10	Latex	34
147	6	Latex	90
153	6	Latex	113
149	10	OB	14
150	10	OB	21
145	10	OB	11
151	6	OB	***27***
146	6	OB	31

Using these ignition times, actual ignition temperatures can be read directly from the surface temperature data. One can see from the representative graphs above that the ignition temperatures are much lower, even with the error associated with thermocouples measuring surface temperature, than the calculated ignition temperatures. This data was used to determine ignition temperatures for samples with 10 coats and with 6 coats. Figure 17 shows this data.

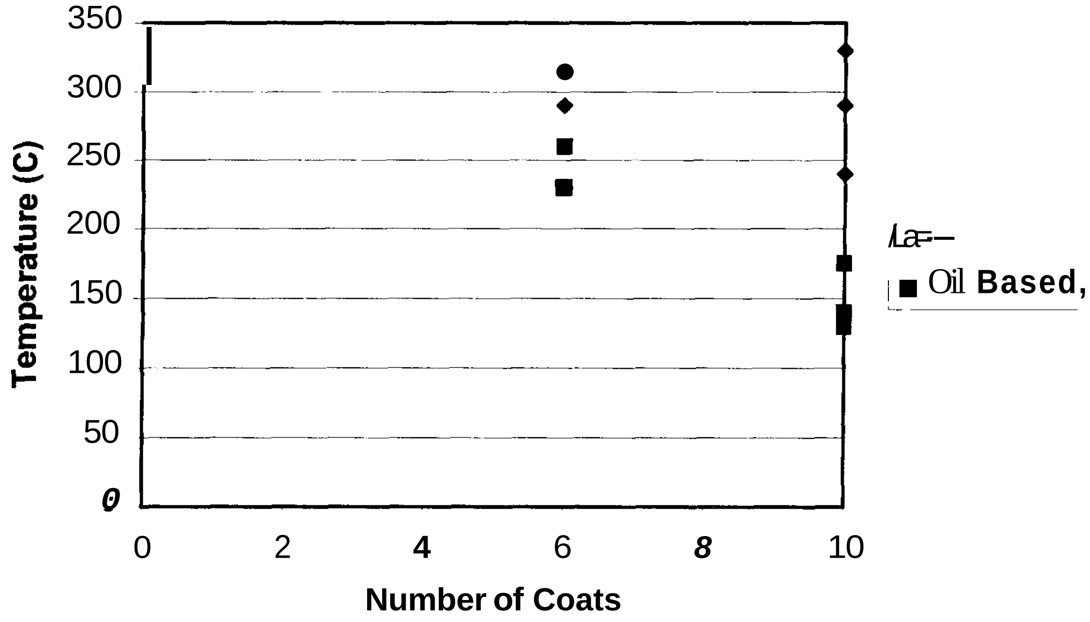

Figure 17: Measured Surface Temperatures at Ignition of Painted Samples at 75 kW/m2 as a Function of Number of Coats

Measured ignition temperatures for latex ranged from a low of 240°C to a high of 330°C, while the range for oil-based paint was 130°C to 240°C. These values are less than half the values calculated based on the ASTM E1321 method, suggesting that this method should be reevaluated.

The term that is neglected in the analysis to calculate the ignition temperature is the conduction term. Neglecting the effect of conduction through the solid during heating translates to a higher surface temperature, which can be seen from the differences in calculated effective ignition temperatures and measured ignition temperatures. To reevaluate the ASTM E1321 calculation method, the analytical solution to the semi-infinite conduction equation was reconsidered:

$$\frac{\Delta T_s}{\Delta T_c} = 1 - exp\left(\frac{t}{t_c}\right) erfc\left(\sqrt{\frac{t}{t_c}}\right). \qquad (1)$$

Equation 1 estimates the surface temperature of a particular material with given thermal properties subject to an imposed heat flux with surface convection. For this analysis, the material properties from the SFPE Handbook [16] are used to estimate this surface temperature.

In order to use this equation, some other properties and characteristics must be determined. The absorptivity, a, of the surface receiving the incident heat flux must be determined to evaluate the fraction that is absorbed to heat the material. The surface of the material in this study was white latex or oil-based paint. The ASHRAE Handbook apsorptivity value for white enamel paint is given as -0.9[18]. This indicates that approximately 90% of the incident heat flux is absorbed into the surface, with the remaining fraction reflected. The absorptivity of a material is used in the solution for surface temperature as function of heat flux, which is shown graphically in Figure 1. This heat balance equation can also be used to solve for h_t, the total heat transfer coefficient. This coefficient relates the characteristic temperature rise and characteristic time to the incident heat flux as given by $AT, = \frac{\alpha \dot{q}''_{inc}}{h_t}$ and $t, = \frac{k\rho c}{h_t^2}$. Using the handbook thermal properties, the heat equation solution can be used to find the surface temperature as a function of time. Figure **18** compares this equation to measured surface temperature of an unpainted concrete block sample at 75 kW/m^2.

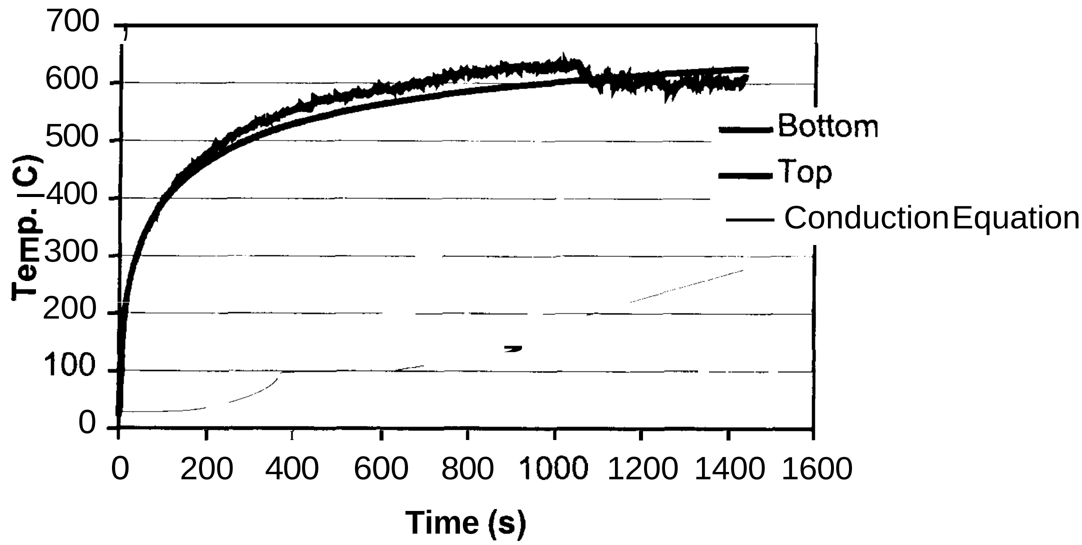

Figure 18: Measured versus Calculated Surface Temperature of Unpainted Sample at 75 kW/m^2

Figure 18 shows that the measured and calculated temperatures fall on top of one another for early times. Again, it is noted that the conduction equation is using handbook values for the thermal properties of concrete block and white paint. This suggests that the conduction equation used with handbook properties can approximate the surface temperature curve of a material under an imposed heat flux.

The conduction equation was compared with the temperature data of painted samples. These curves are shown in the plots of measured temperatures (Appendix B) as well as in Figure 15 and Figure 16. In Figure 15, the theoretical curve has been calculated using $a = \varepsilon = 0.7$ instead of 0.9. The conduction equation fits the measured temperature data better with this approximation. The physical justification for a lower absorptivity and emissivity for latex painted samples is that the residue left after burning is a white powdery substance, as opposed to a black resin type of residue left on the oil-based samples. The white powdery residue would cause the surface to reflect more of the incident energy than the black residue, and therefore the surface would not reach the same surface temperature for long times. The lower value for α and ε also lead to good agreement between the conduction equation and measured temperatures for shorter times. This analysis neglects the effect of temperature, and therefore, wavelength on the absorptivity. The local divergence of the measured temperature data from the conduction equation for times from 100s to 400s in Figure 15 and Figure 16 can be explained as the temperature increase associated with the flame heat flux after ignition has occurred. The conduction equation used in this analysis does not account for this additional incident flux. However, after the sample has burned out, the measured temperature converges back to the conduction equation approximation.

The curves of the heat conduction equation solution estimate very closely the temperature rise at the surface according to the thermocouple measurements. The plots indicate that the heat conduction equation is predicting the heat **up** of the surface of painted concrete block with reasonable accuracy using handbook values for thermal properties and estimates of absorptivity. This agreement suggests that effective ignition temperatures can **be** estimated using handbook thermal properties, the heat conduction equation and measured ignition times. **A** summary graph of calculated effective ignition temperatures using this method for all samples in this study is given in Figure 19.

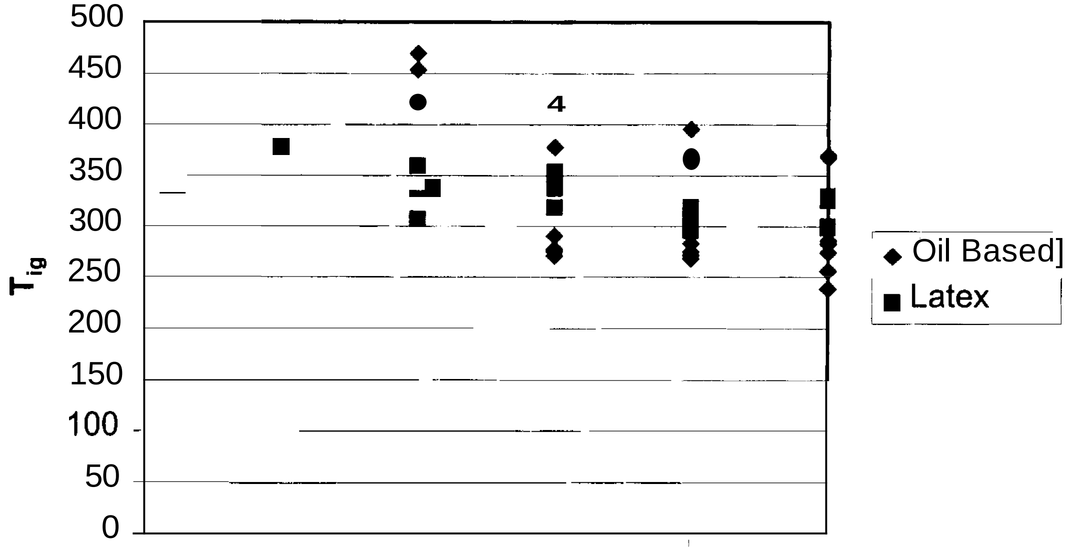

Figure 19: Calculated Effective Ignition Temperatures as a Function of # of Coats

The effective ignition temperatures shown in Figure 19 indicate reasonable consistency. There are a number of data points for oil-based paint in the region between 250°C and 300°C. The data points for oil-based paint outlying this region correspond to low coating levels and tests close to the critical heat flux values. The latex painted data points indicate fair consistency and average 325°C. These values are much closer to the measured ignition temperatures than the calculated values that used the critical heat flux based on the method prescribed in ASTM E1321.

Figure 20 shows a plot measured surface of an unpainted sample exposed to 75kW/m^2. Also shown on this plot is the heat conduction equation, and two short time solutions as given in ASTM E1321 as:

$$t = \frac{\pi}{4} k\rho c \left[\frac{T_s - T_\infty}{\alpha \dot{q}''} \right]^2 .$$

The two short time solutions correspond to two different values of kpc, one twice the other. The short-term solution using twice kpc would be the approximation for a material with a given ignition temperature of 300°C which ignites at a time of approximately 37 seconds. This means that using the short term solution to derive effective material properties would results in a difference of a factor of two from the actual individual values found in the handbook. The other short term solution shows that this approximation does not do a good job estimating surface temperature above 250°C or for time greater than 20 seconds. This is compared to the heat conduction equation which estimated very closely the surface temperatures in the early as well as later domains.

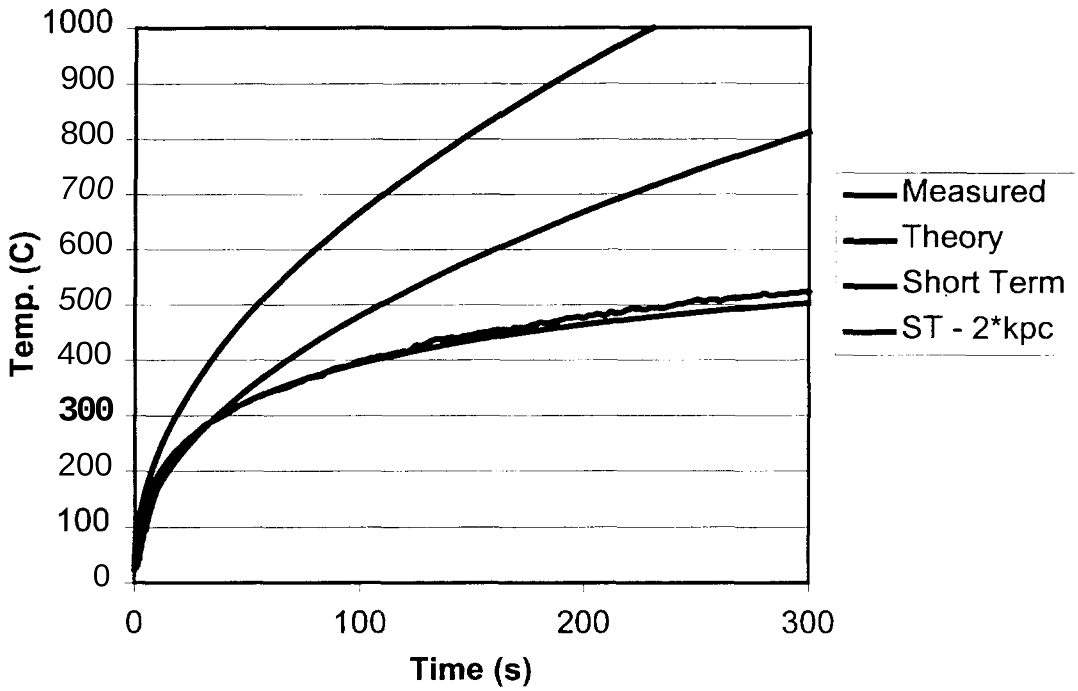

Figure 20: Surface Temperature of Unpainted Sample

Quintiere's flammability parameter, b, was used in order to study the potential for flame spread on the surface of painted concrete block. The theoretical description of this parameter was described in Chapter 111. The heat release curves acquired from Cone Calorimeter testing were used for determination of characteristic heat release rate and total heat release. Figure 21 and Figure 22 are examples of these curves.

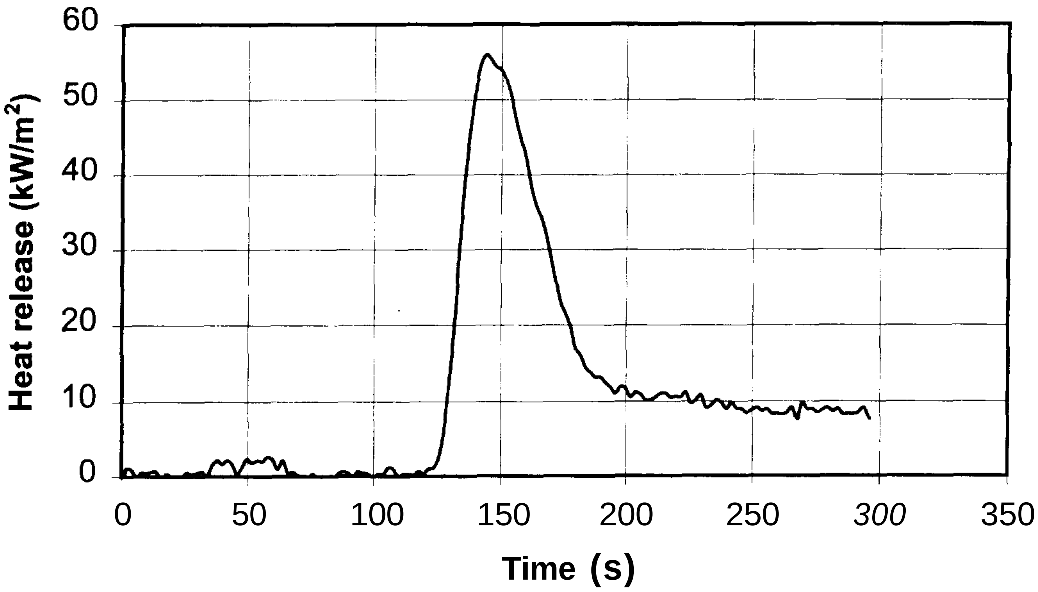

Figure 21: Heat Release Rate per Unit Area - Sample #38 (6 Coats Latex, 75kW/m²)

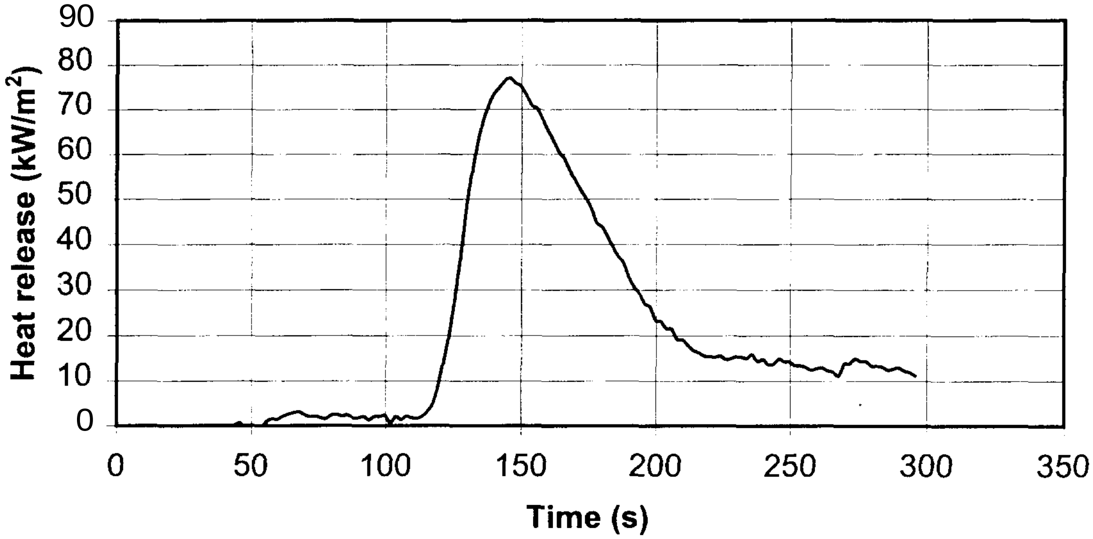

Figure 22: Heat Release Rate per Unit Area - Sample #83 (6 Coats Oil-based, 75kW/m^2)

These curves are typical of all samples tested. The estimation of a triangular shape is a good approximation. Therefore, the burning duration is calculated by the procedure described in Chapter 111, where the total area under the triangular curve is divided by the peak heat release rate per unit area. This calculation was verified by measuring the approximate duration of burning during testing. The measured and calculated values agreed very well. Using the linearized flame length parameter, k_f, equal to 0.01, the b number was calculated.

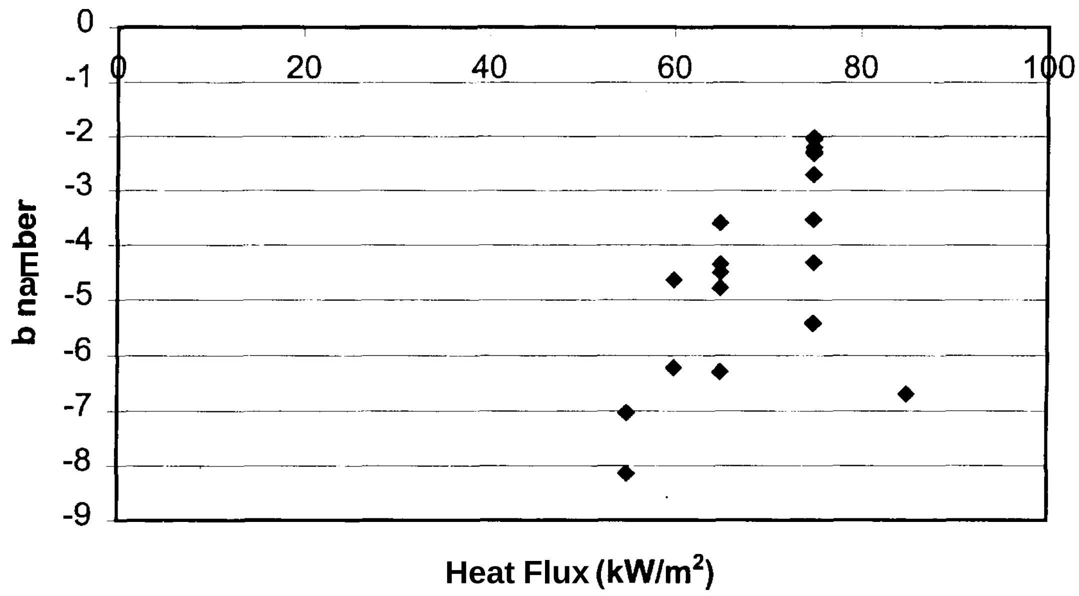

Figure 23: b number as a Function of Heat Flux for Latex Painted Samples

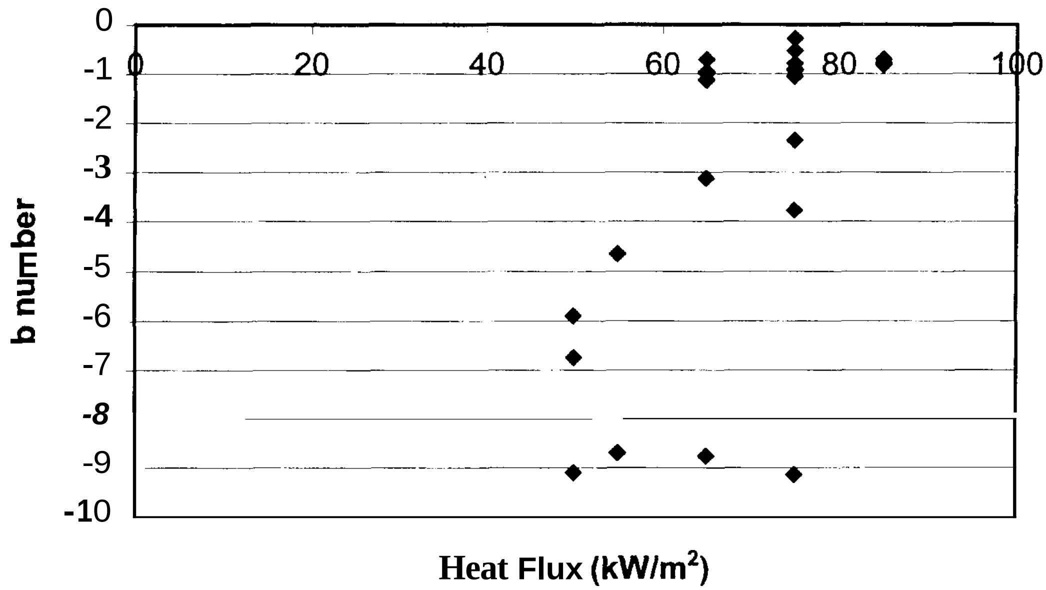

Figure 24: b number as a Function of Heat Flux for Oil Based Painted Samples

Figure **23** and Figure **24** indicate that for all tests performed, the b number was negative, and therefore indicates that flame spread was not likely in any particular configuration of coating level and heat flux. The trend is that as heat flux increases, the b number becomes less negative suggesting that flame spread may occur at higher heat flux levels. However, the scatter of the data signifies the dependence of coating level on the propensity to spread.

VI. DISCUSSION

The standard method used to deduce a material's effective ignition temperature does not account properly for some of the physics in some situations. At heat fluxes near a critical heat flux, conduction into the material may not be zero, and may, in fact, account for a significant amount of the heat losses compared to the incident heat flux. This proposition requires further study. However, it is apparent from the measured ignition temperature data acquired within this study that the LIFT test calculation method overpredicts the ignition temperature of painted concrete block. This is important in the use of this material property in analyses using fire modeling software. For example NIST’s Fire Dynamics Simulator (FDS) [17] requires input of a characteristic ignition temperature for materials to be evaluated for ignition and flame spread. If an ignition temperature of approximately 700°C is used for a material, instead of an ignition temperature of 250°C, that material might not ignite in the model when realistically, there is a possibility of ignition and/or flame spread. The results might conclude no ignition or flame spread, when there actually is a chance for it. This might lead to an incorrect hazard evaluation. It is important in light of this possible inaccuracy to revisit, especially for complex materials, the process of evaluating the ignition temperatures for those materials. It is not practical to directly measure those temperatures for many materials so a more thorough theoretical evaluation of the heat loss conditions at the surface of a material at ignition is necessary. This analysis was carried out using the heat conduction equation and handbook material properties. The results from Chapter V showed that this equation could approximate the surface temperature rise for painted concrete block. The following could be used as a procedure for evaluating ignition temperatures using the conduction equation for thermally thick materials:

1) Use appropriate handbook values of absorptivity/emissivity, ***k***, ρ, c for the material being tested;

2) Solve Equation 2 for appropriate heat fluxes to find ΔT_c and $h_{t,max}$ (this solution is iterative; Newton-Raphson Method used here);

3) Measure time to ignition for material being tested at a range of heat fluxes;

4) Solve Equation 1 using handbook property values, estimated characteristic temperature rise, ΔT_c, maximum total heat transfer coefficient, $h_{t,max}$, and measured time to ignition data.

A further illustration of the inaccuracies of the ASTM E1321 calculation method would be to find, from the theoretical Temperature vs. Incident Heat Flux curve the critical heat flux for ignition given the measured ignition temperatures from this study. If ignition temperatures are assumed to be between 200°C and 350°C, the critical heat flux falls between 5-15 kW/m^2. In some cases, these critical heat fluxes are one-fifth the experimentally determined critical fluxes.

This result could indicate another problem not accounted for in the theory. If a thin flammable material is adhered to a noncombustible substrate, the material properties for conduction are used in temperature evaluations because it is assumed that the thin material will not affect the heating of the solid. This assumption is valid in many cases. However, when determining the ignition of an assembly like painted concrete block, or in general, temperature at the surface is not the only determining factor. Therefore, the definition of ignition in general is revisited.

For ignition to occur via a pilot energy source, the surface of the material must 1) reach a temperature by which that material chemically decomposes; 2) release the products of decomposition; 3) mix with the ambient gases to form a flammable mixture; 4) reach the pilot source before that mixture is diluted out of the flammable limits. The parts of this process that are not accounted for in the general ignition analysis are 3) and 4). The heating of a solid is generally well understood and relatively easy to practically apply to ignition. However, the composition and concentrations of gases released from the surface of a material during heating are not directly accounted for in ignition analysis in practical test methods. For the heating and ignition of a thin material such as paint on an inert solid such as concrete block, the chemical kinetics could be very important. Two issues are key in this situation: the amount of flammable material, represented by the amount of paint; and the release of non-flammable gases such as water vapor from the concrete block during heating. The amount of paint on the sample is tied directly to the concentration of the flammable mixture present near the surface to be ignited by an energy source. If there is too little paint on the surface, or if the incident heat flux to the surface is insufficient to release enough pyrolyzate to create a flammable mixture near the energy source, then ignition will not take place. Also, if other non-flammable gases such as water vapor, as may be the case with concrete block or gypsum wallboard, are released by the substrate, the mixture of gases at the energy source may be diluted below the flammable limit to cause ignition. Both of these effects appear to be present for the heating of painted concrete block. In many cases, noticeable release of fuel gases did not lead to ignition at relatively high heat fluxes, or the gases above the surface of the material flashed but did not sustain flaming. In some cases, off-gassing desisted relatively early at high heat fluxes for low coating levels and ignition could not occur. At high heat fluxes surface temperatures would be high enough for ignition, but the concentration of flammable mixture would not be high enough because not enough material is available to be pyrolyzed.

The ignition scenario dependence on concentration of fuel gases suggests the importance of mass loss rate of paint on a substrate before ignition. Relating this mass loss to heat flux or temperature is difficult. It is usually determined via an Arrhenius equation for a chemical reaction:

$$\dot{m}''' = Ae^{E/RT} \ . \tag{8}$$

This analysis is beyond the scope of this study. It is indicated for qualitative and explanatory purposes.

The concentration of fuel gases is also affected by the release of water vapor from the substrate. The release and subsequent mixing of non-flammable gases from a substrate with flammable fuel gases is affected by the path and ease of travel from within the material to the surface and then, in vaporized form, near the surface. For a material like painted concrete block, a few things affect this path and ease of travel of non-flammable vapors. The content of material within the block that decomposes into non-flammable vapors, for example, the water content of the concrete block, or the water content of the paint, affects how much total non-flammable vapor can be released. The porosity of the concrete also affects the ability of non-flammable gases to be released at the surface. Also, the permeability of the dried paint on the surface of the block will affect the penetration of non-flammable vapors to the area near the surface. According to the manufacturer's technical data, oil-based paint is less permeable than latex paint. If that is taken into account along with the fact that latex paint uses water as a solvent, then more water can be released through the paint and more water vapor is released when the paint is heated. These qualitative descriptions can explain why latex paint ignites at a higher critical heat flux than oil-based paint. No quantitative analysis of these effects can be offered at this point.

The temperature data collected during the ten tests with thermpocouples shows that release of water vapor plays a role in the heating of painted concrete block. The plots of measured temperature (Appendix B) show that the thermocouples placed inside the middle of the sample and the thermocouples at the bottom of the sample relative to the incident heat flux plateau at approximately 100°C, or the vaporization temperature of water. This would indicate that the conducted heat wave through the sample is being absorbed to vaporize the water within the sample, thus delaying the time for the material to reach a steady state of conduction through the sample. This is illustrated in Figure *25*.

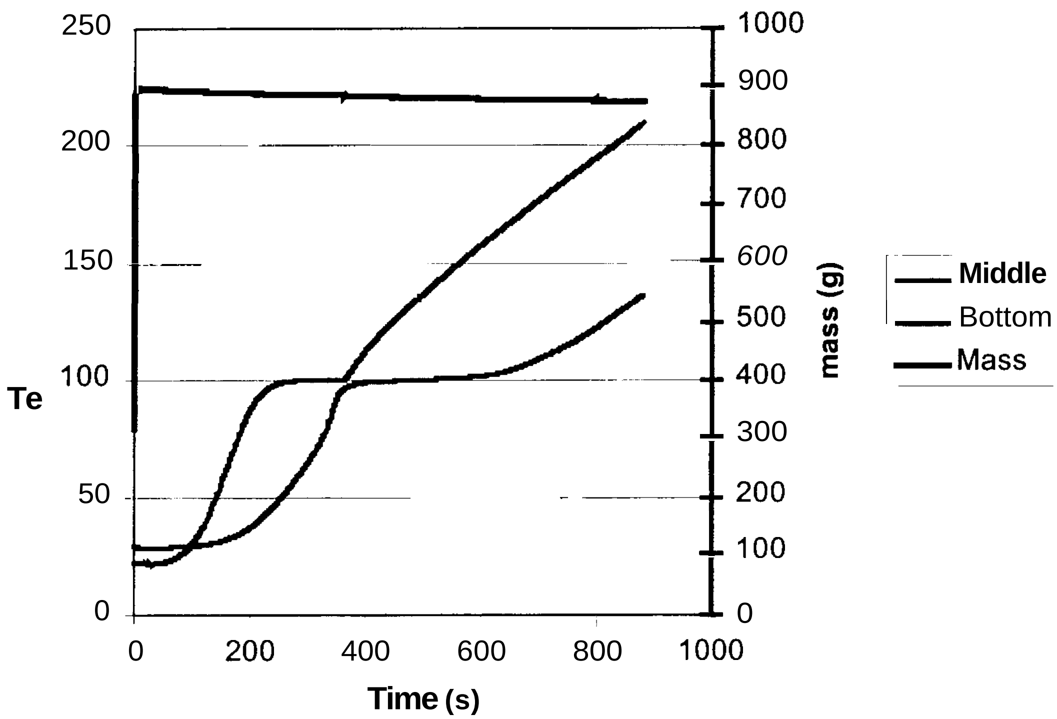

Figure 25: Middle and Bottom Thermocouple and Mass Data

VII. CONCLUSION

This study has characterized some flammability parameters of painted concrete block. Two different types of paint were tested and compared in relation to their respective ignitibility. Tests revealed that latex painted samples are more difficult to ignite than oil-based painted samples. The critical heat flux for ignition increased as the number of coats of paint applied decreased. It was also shown that time to ignition increased and the peak unit heat release rate decreased with a decrease in the number of coats applied. However, those relationships were not found with a decrease in total mass of paint applied. The tests also demonstrated critical heat fluxes that were relatively high compared with other painted wall surfaces and burning durations that were relatively short, suggesting a low propensity for flame spread according to Quintiere's flame spread parameter.

The method by which characteristic ignition temperatures are typically calculated was evaluated for applicability to painted concrete block. This evaluation included calculation of ignition temperature from experimentally determined critical heat flux for ignition and from the heat conduction equation and comparison with directly measured ignition temperature via thermocouples placed on the surface of painted concrete block samples and subjected to a constant imposed heat flux. This comparison has concluded that the heat conduction equation for semi-infinite solids exposed to **a** constant incident heat flux with surface convection and reradiation, closely approximates the surface temperature during heating using handbook thermal properties and more accurately estimates the ignition temperature compared with the method used in ASTM **E1321.** However, the phenomenon of ignition in the case of painted concrete block is not fully described by any method available. This is because of the release of water vapor from the substrate and/or paint depletion that dilutes the flammable mixture above the surface. **A** quantitative description of this effect was beyond the scope of this study.

Further work should include a detailed analysis of the water content in concrete block before, during and after testing under imposed heat fluxes. Dried painted concrete block should be tested to compare with tests of environmentally exposed samples. A more detailed mass loss measurement should be included in further testing for both unpainted and painted samples. Also, in order to more completely verify the effective ignition temperature calculation described in Chapter V, surface temperature should be directly measured and/or compared during heating of other painted and unpainted wall materials. Samples of painted concrete block should be tested at other heat fluxes so direct surface temperature measurements can be obtained to compare with measurements made during this study.

VIII. APPENDIX A

#	Density (g/cm³)	Coats	Paint Mass g	HF (kW/m²)	t_{ig} (s)	t_b (s)	Peak HRR KW/m²	Total HR MJ/m²	b	Comments
1	2.13	2	1.5	35	∞	∞	-	-	-	Pin-head size bubbles @ 45s, blackening @ 480s
2	2.14	2	2.2	35	∞	∞	-	-	-	Pin-head size bubbles @ 60s, blackening @ 420s
3	2.18	2	3.5	35	∞	∞	-	-	-	15min test, vapor @ 45s, bubbles @ 55s, blackening @ 420s
4	2.15	4	5.7	35	∞	∞	-	-	-	15min test, vapor/bubbles @ 20-25s
5	2.15	4	2.4	35	∞	∞	-	-	-	10min test, DAQ froze @ 285s, vapor/bubbles @ 55s
6	2.12	4	1.3	35	∞	∞	-	-	-	5min test, vapor/bubbles @ 35s
7	2.12	6	2.5	35	∞	∞	-	-	-	15min test, vapor/bubbles @ 20-25s
8	2.10	6	4.0	35	∞	∞	-	-	-	10min test, vapor/bubbles @ 20-25s
9	2.15	6	4.1	35	∞	∞	-	-	-	5min test, vapor/bubbles @ 20-25s
10	2.11	8	7.9	35	∞	∞	-	-	-	15min test, DAQ error @ 12:45min, no data acquired
11	2.11	8	4.5	35	∞	∞	-	-	-	5min test
12	2.07	8	6.5	60	107	25	64.24	1.63	-4.64	black spots @ 60s
13	2.14	10	10.0	35	∞	∞	-	-	-	15min test
14	2.20	10	8.9	60	150	25	77.54	1.93	-6.22	Flash @133s
15	2.12	10	10.3	55	198	25	77.40	1.93	-8.15	Flashes @ 170, 176, 189s
16	2.10	2	7.6	50	∞	∞	-	-	-	15min test, blistering @ 540s
17	2.13	2	6.9	80	∞	∞	-	-	-	390s test, flashes 110s-150s
18	1.97	2	9.3	85	106	18	19.44	0.33	-6.69	
19	2.14	4	6.4	50	∞	∞	-	-	-	blistering @ 600s
20	2.13	4	8.3	65	∞	∞	-	-	-	450s test, flashes around 180s

#	Density (g/cm^3)	Coats	Paint Mass g	HF (kW/m^2)	t_{ig} (s)	t_b (s)	Peak HRR KW/m^2	Total HR MJ/m^2	b	Comments
21	2.10	4	8.9	70	∞	∞	-	-	-	420s test, flashes 120s-180s
22	2.03	6	10.7	50	∞	∞	-	-	-	blistering @ 450s, DAQ error @ 840s, no data acquired
23	2.12	6	9.5	60	∞	∞	-	-	-	520s test, black spots around 80s
24	1.95	6	9.9	65	147	25	58.87	1.48	-6.29	
25	2.06	8	11.8	55	171	25	80.76	2.03	-7.03	black spots @90s
26	2.06	8	9.6	50	∞	∞	-	-	-	600s test
27	1.97	8	11.5	75	69	37	65.89	2.48	-2.21	
28	2.13	10	10.4	50	∞	∞	-	-	-	10min test, flashing during 4th minute
29	2.11	10	10.1	50	∞	∞	-	-	-	11min test, flashing 180-300s, DAQ error
30	2.14	10	10.3	75	65	32	70.57	2.31	-2.33	Flashes from 30s to ign
31	2.15	2	6.0	75	∞	-	-	-	-	6min test, no vapors emanating after 330s
32	2.07	2	5.9	85	∞	-	-	-	-	5 min test, DAQ error
34	2.17	4	5.5	75	121	25	40.87	1.03	-5.43	Timing incorrect, add 10s to DAQ data
35	2.15	4	6.3	75	N/A	-	-	-	-	DAQ error, no data acquired
36	2.13	4	5.7	75	∞	-	-	-	-	5min test, flashes from 105-180s, DAQ error
37	2.12	6	6.0	75	79	25	62.65	1.55	-3.53	Flashing @ 73s, t_{bo}=138s
38	2.13	6	8.6	75	97	25	55.95	1.40	-4.23	Flashes from 86s
39	2.17	6	7.6	75	114	23	54.34	1.21	-5.41	
40	2.02	8	7.6	75	62	37	65.44	2.44	-2.02	Flashing @ 22s, 35s, 59s; t_{bo}=147s
41	2.09	8	10.2	65	103	32	62.01	2.01	-3.60	Flashes from 60s to ign
42	2.06	8	9.0	65	113	25	73.28	1.83	-4.79	Flashes from 60s to ign
43	2.22	10	9.4	75	64	37	67.29	2.51	-2.06	Many flashes after 20s until ignition, t_{bo}=147s
44	2.12	10	9.5	65	127	30	[illegible]	[illegible]	[illegible]	[illegible]

Latex										
	Density		**Paint Mass**	**HF**	t_{ig}	t_b	**Peak HRR**	**Total HR**		
#	**(g/cm^3)**	**Coats**	**g**	**(kW/m^2)**	**(s)**	**(s)**	**KW/m^2**	**MJ/m^2**	**b**	**Comments**
45	2.19	10	9.8	65	123	30	75.04	2.25	-4.35	Flashes from 90s to ign
114	2.13	4	13.9	75	70	37	60.65	2.29	-2.29	
115	2.12	4	14.4	75	87	37	64.60	2.40	-2.71	

	Oil Based									
	Density		Paint Mass	HF	t_{ig}	t	Peak HRR	Total HR		
#	g/cm^3	Coats	g	kW/m^2	s	s	kW/m^2	MJ/m^2	b	Comments
49	2.13	4	7.7	60	∞	-	-	-	-	430s test
50	2.01	4	9.0	75	109	-	-	-	-	No data, did not start DAQ
51	2.17	4	8.3	65	283	35	32.22	1.12	-8.76	small flame directly under spark 40-47s, see #52
52	2.16	6	8.6	55	327	40	47.80	1.92	-8.70	Began as 1cm dia flame and grew radially
53	2.04	6	10.5	85	26	50	69.20	3.45	-0.83	
54	2.10	6	9.1	85	21	50	71.34	3.55	-0.71	
55	2.16	8	10.1	45	∞	-	-	-	-	900s test, bubbles @ 30s, vapors emanating from edge
56	2.15	8	9.4	50	∞	-	-	-	-	720s test, bubbles @ 25s, flashes @ 318s, 346s, 368s
57	2.06	8	12.0	55	180	40	84.78	3.40	-4.65	t_{bo}=263s, flash @ 168s
58	2.15	10	13.0	45	∞	-	-	-	-	840s test, bubbles @ 25s, flashes @ 373s, 393s, 723s, 766s
59	2.08	10	14.2	50	234	40	94.94	3.38	-5.90	bubbles @20s, small flames lead to entire surface
60	2.16	10	11.7	75	29	50	104.55	5.25	-0.53	
64	1.99	4	8.6	50	∞	-	-	-	-	10min test, fingertip size bubbles @ 20s, DAQ error
65	2.10	4	8.3	75	212	25	34.05	0.85	-9.14	
66	2.09	4	8.4	75	132	40	52.45	2.08	-3.77	
67	2.12	6	9.9	50	∞	-	-	-	-	DAQ error, no data acquired
68	2.05	6	9.7	85	22	45	70.46	3.15	-0.78	
70	2.18	8	9.6	50	324	37	65.78	2.48	-9.10	Flashing from 262s
71	2.23	8	9.1	75	32	55	64.18	3.52	-0.94	
72	2.11	8	10.1	75	28	55	71.39	3.91	-0.80	
73	2.13	10	10.7	50	240	37	73.73	2.78	-6.75	Local flame @ ruptured bubble
74	2.19	10	9.1	75	19	37	122.68	4.61	-0.29	

Oil Based										
	Density		Paint Mass	HF	t_{ig}	t_b	Peak HRR	Total HR		
#	g/cm^3	Coats	g	kW/m^2	s	s	kW/m^2	MJ/m^2	b	Comments
75	2.19	10	7.5	75	33	50	74.77	3.75	-0.91	
82	1.86	6	11.6	75	85	40	77.08	3.08	-2.35	Flashes @ 75s, 80s
83	2.11	6	11.1	75	30	50	53.61	2.7	-1.06	
84	2.13	6	10.0	75	100	-	-	-	-	Flash @ 80s, 90s
85	2.04	8	13.0	65	109	37	81.38	3.04	-3.13	
86	1.91	8	13.3	65	41	50	67.84	3.40	-1.14	Local ignition leads to full involvement slowly
87	2.08	8	12.4	65	38	55	69.41	3.80	-1.00	
88	2.11	10	11.7	65	33	60	83.84	5.04	-0.71	
89	2.01	10	11.2	65	45	50	77.97	3.90	-1.12	
90	2.16	10	7.0	65	33	40	85.99	3.44	-0.97	

IX. APPENDIX B

Sample #100 (unpainted) @ 75 kW/m2

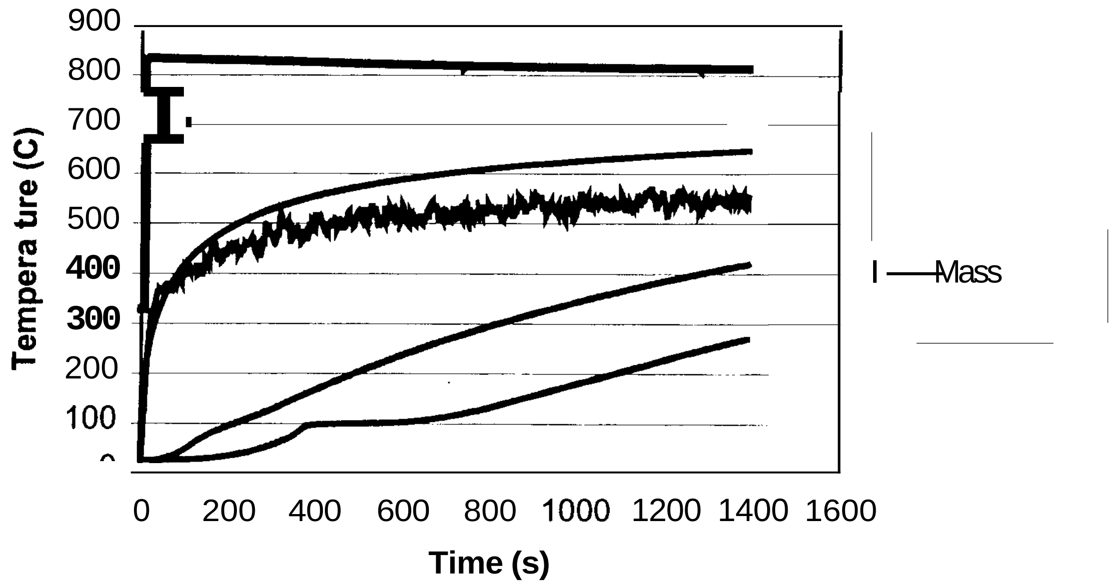

#144 (10 coats Latex) @ 75kW/m2

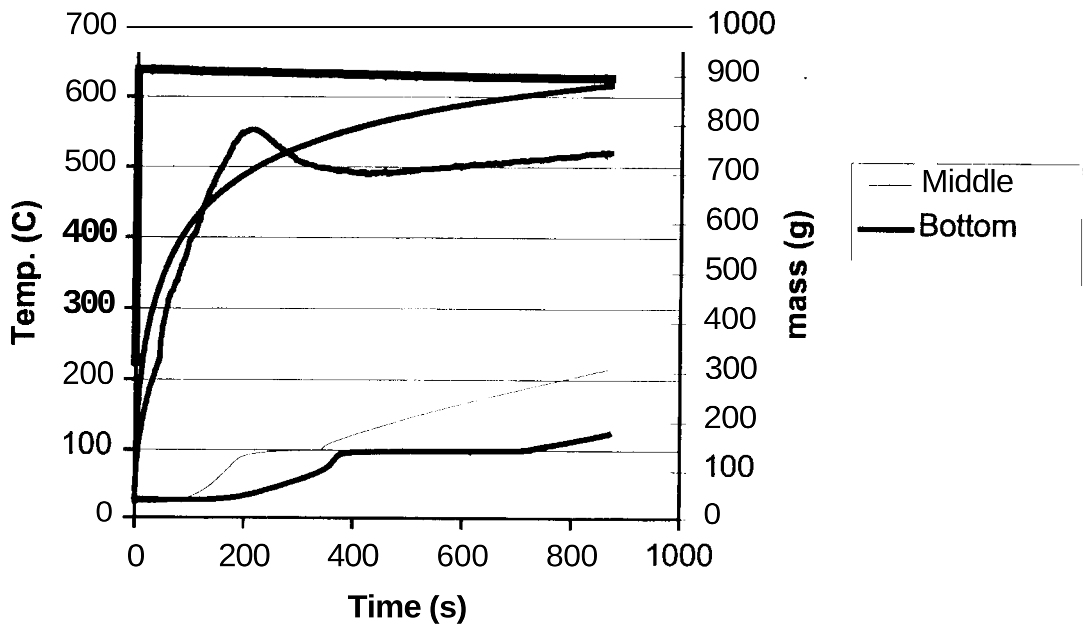

#145 (10 coats OB) @ 75kW/m2

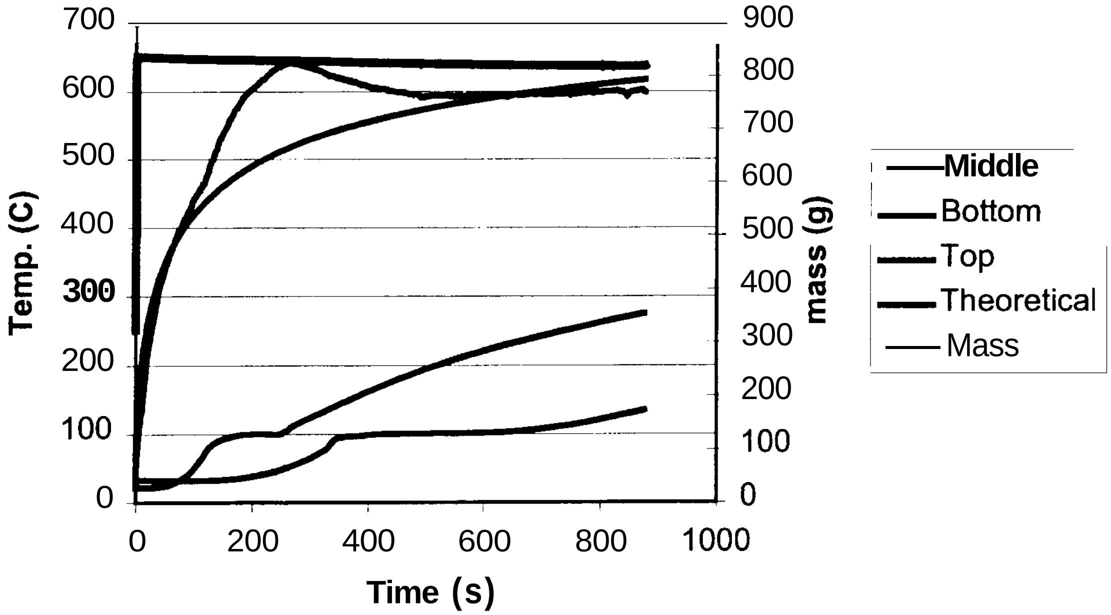

#146 (6 coats Oil Based) @ 75 kW/m2

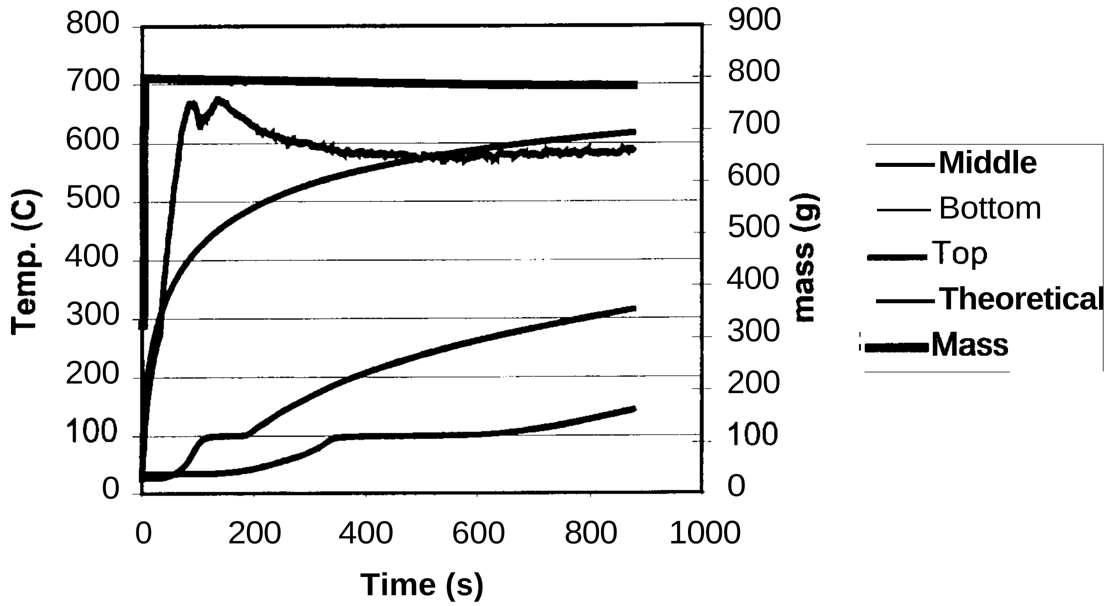

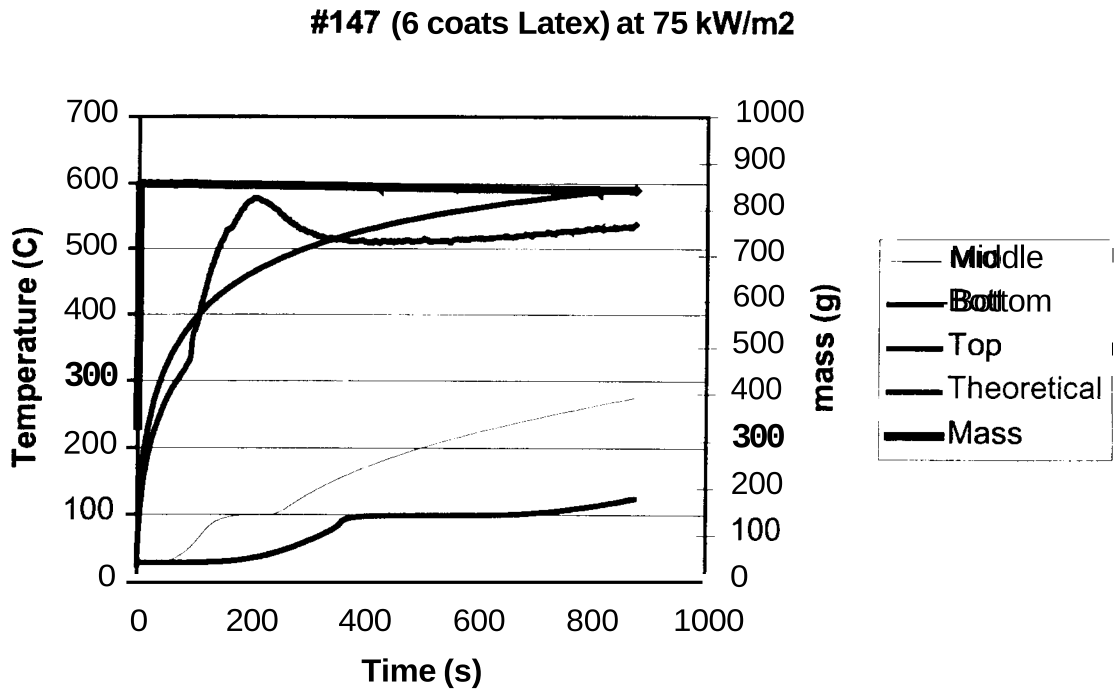
#147 (6 coats Latex) at 75 kW/m2
Temperature (C)
mass (g)
Time (s)
Middle
Bottom
Top
Theoretical
Mass

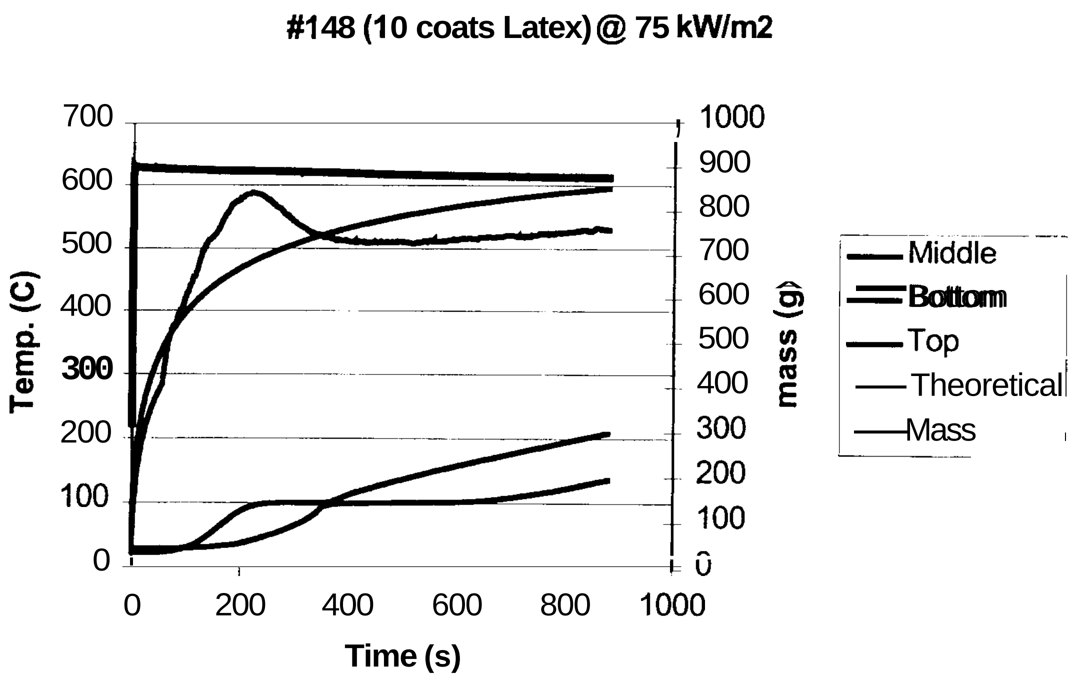
#148 (10 coats Latex) @ 75 kW/m2
Temp. (C)
mass (g)
Time (s)
Middle
Bottom
Top
Theoretical
Mass

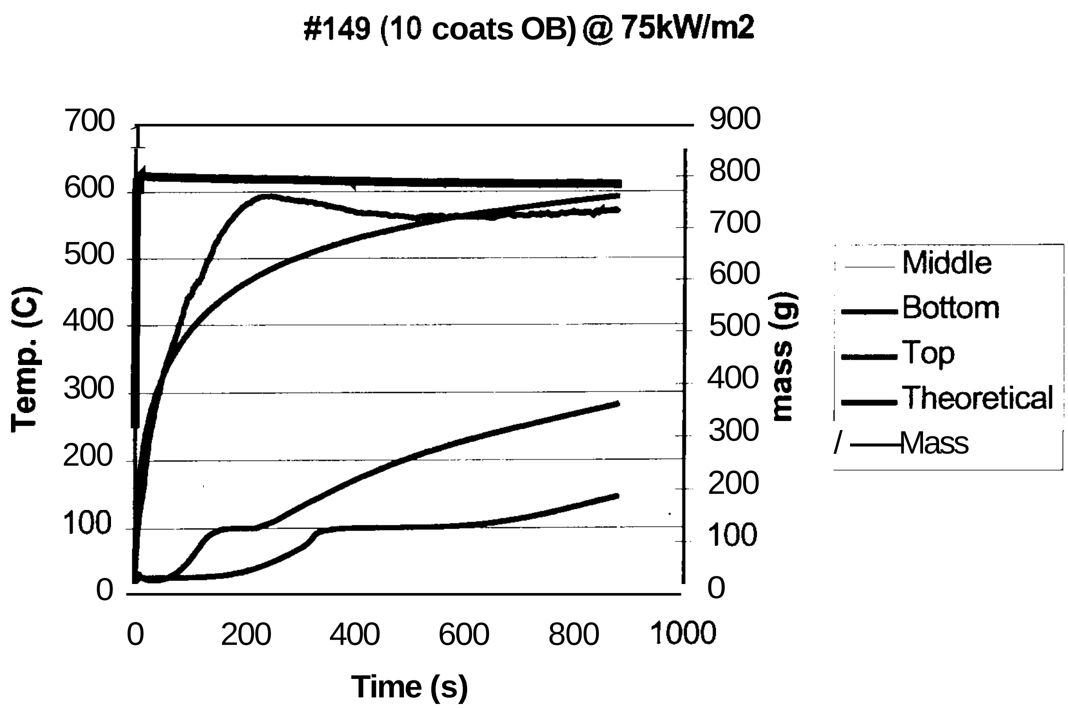
#149 (10 coats OB) @ 75kW/m2
700
600
500
400
300
200
100
0
Temp. (C)
900
800
700
600
500
400
300
200
100
0
mass (g)
0
200
400
600
800
1000
Time (s)
Middle
Bottom
Top
Theoretical
Mass

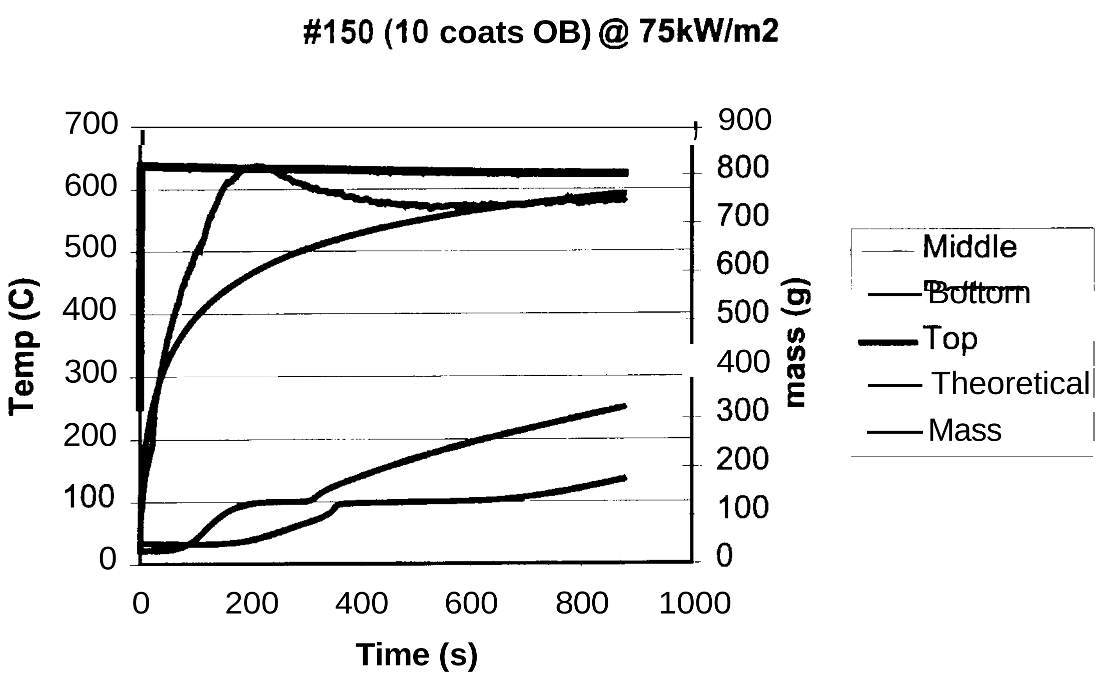
#150 (10 coats OB) @ 75kW/m2
700
600
500
400
300
200
100
0
Temp (C)
900
800
700
600
500
400
300
200
100
0
mass (g)
0
200
400
600
800
1000
Time (s)
Middle
Bottom
Top
Theoretical
Mass

#151 (6 coats OB) @ 75 kW/m2

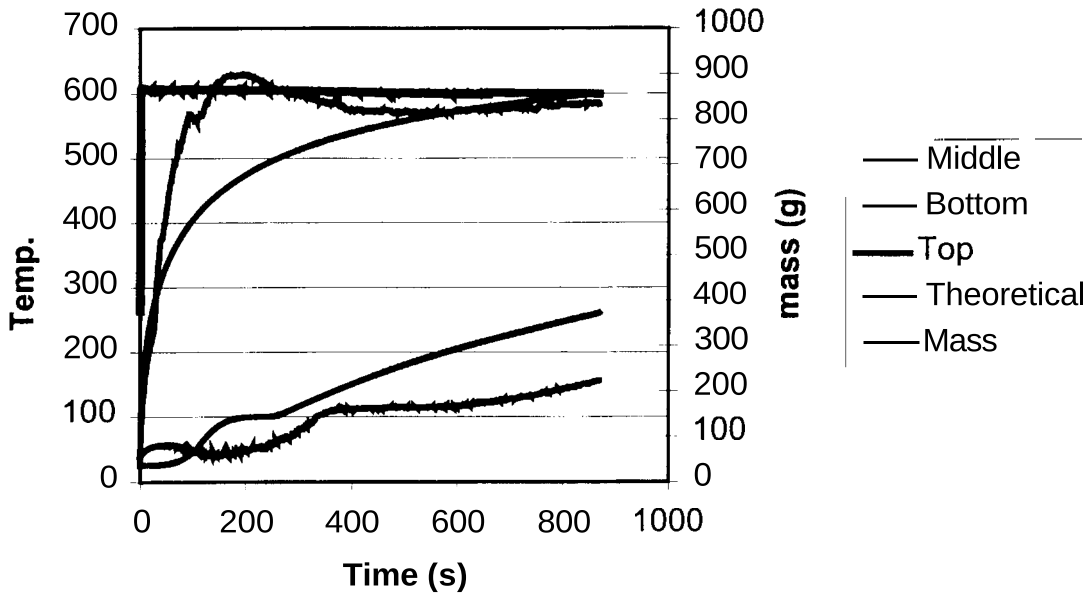

#152 (10 coats Latex) @ 75 kW/m2

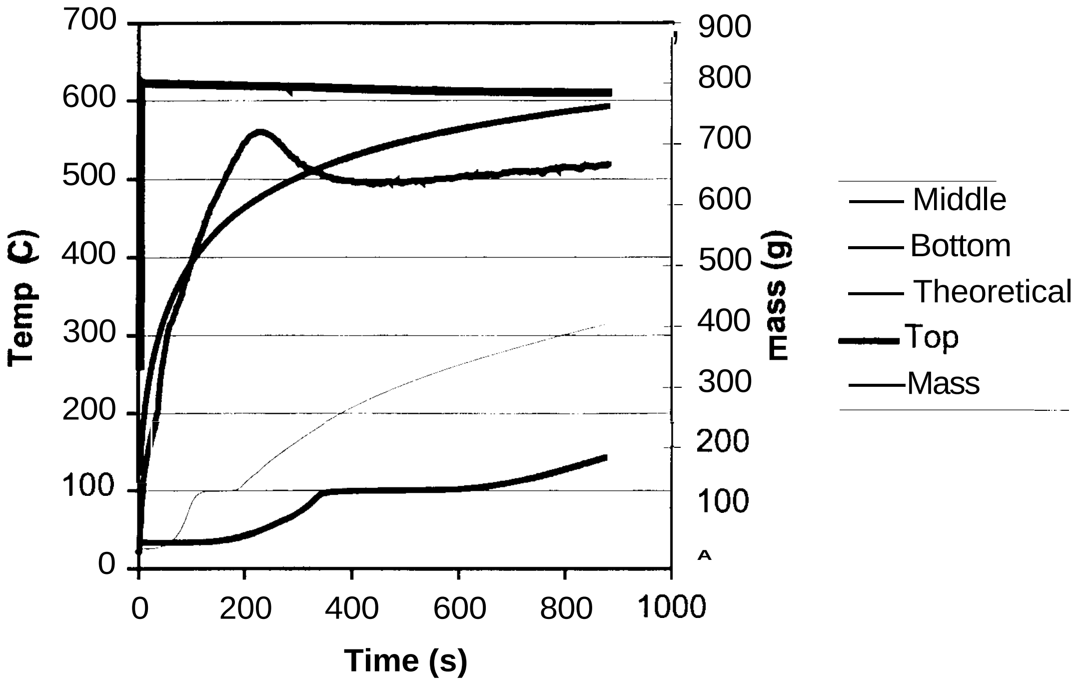

#153 (6 coats Latex)@ 75 kW/m2

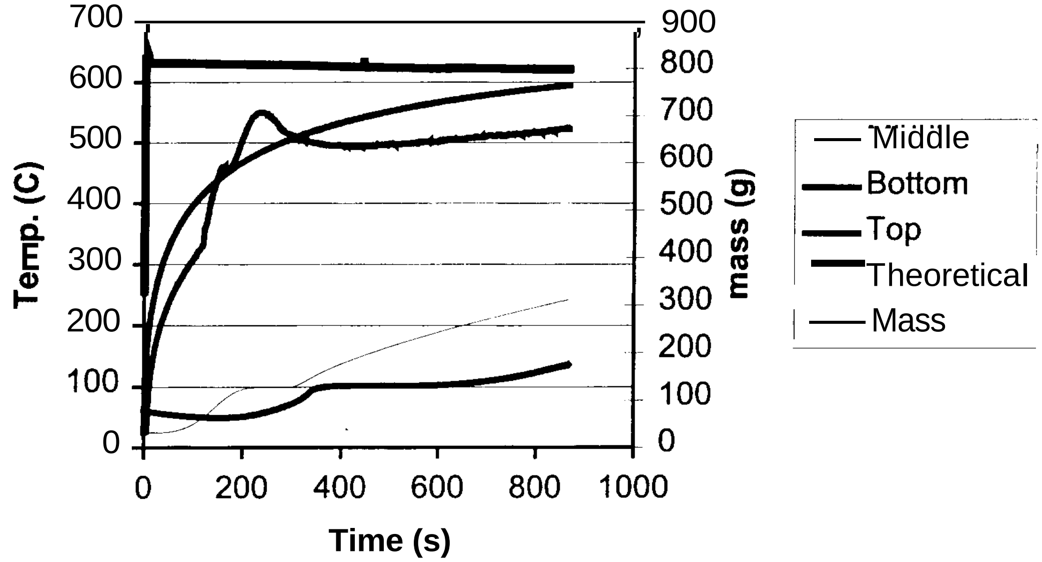

Measured versus Calculated Surface Temperature Using Conduction Equation at 35 kW/m^2 - #157 (unpainted)

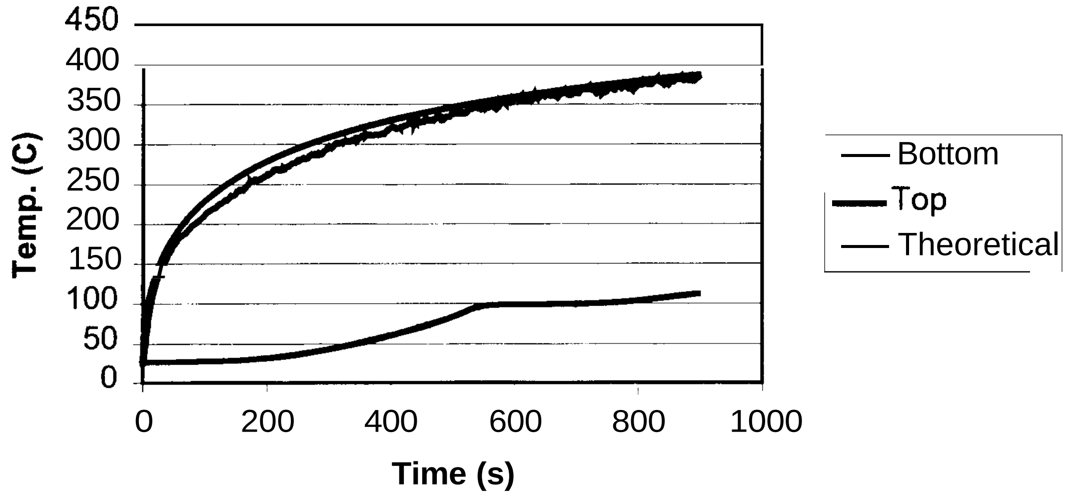

Measured versus Calculated Surface Temperature Using Conduction Equation at 35 kW/m^2 - #158 (unpainted)

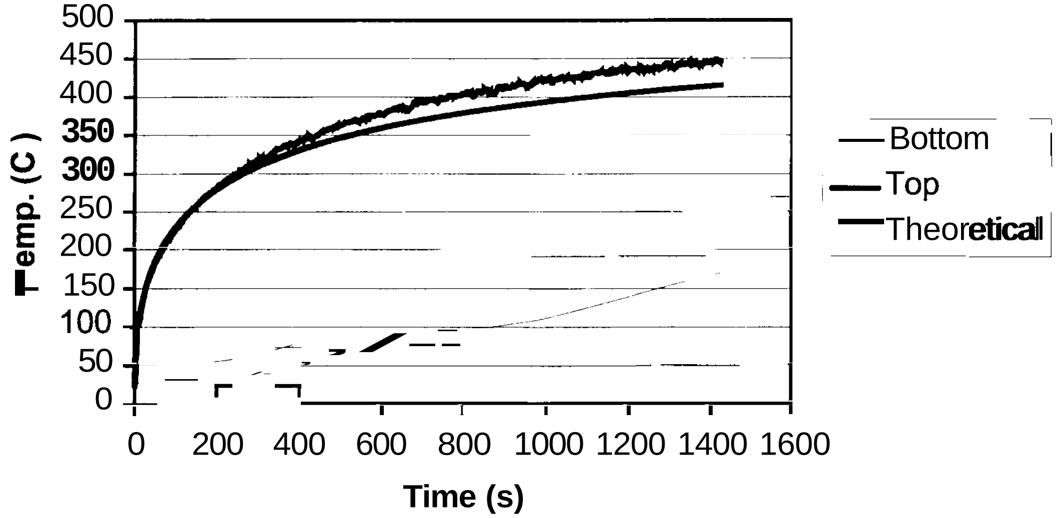

Measured versus Calculated Surface Temperature Using Conduction Equation at 50 kW/m^2 - #159 (unpainted)

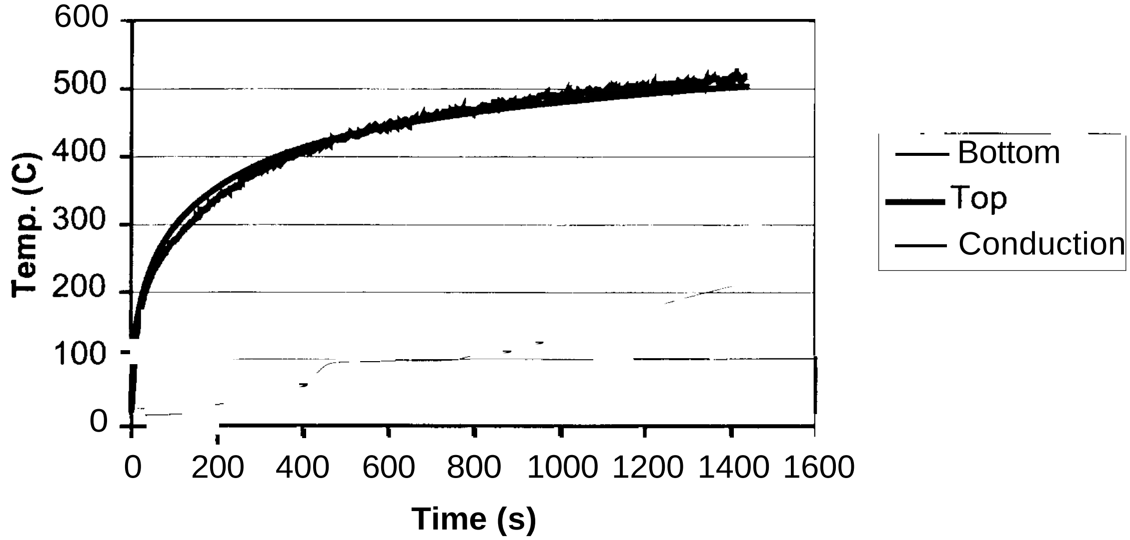

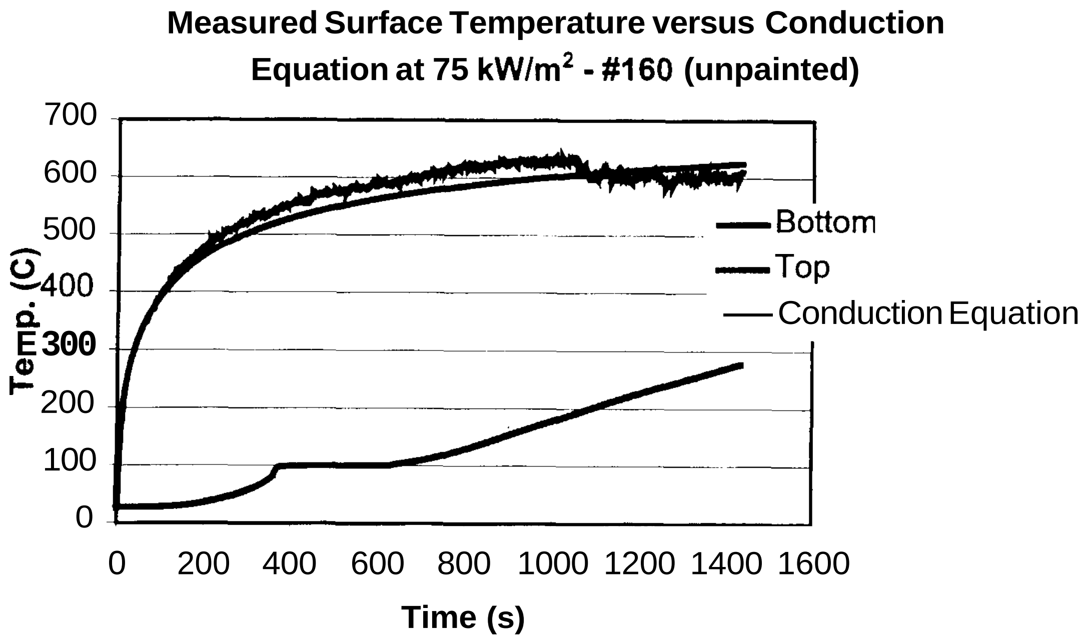
Measured Surface Temperature versus Conduction Equation at 75 kW/m2 - #160 (unpainted)
700
600
500
400
300
200
100
0
Temp. (C)
0
200
400
600
800
1000
1200
1400
1600
Time (s)
Bottom
Top
Conduction Equation

X. APPENDIX C

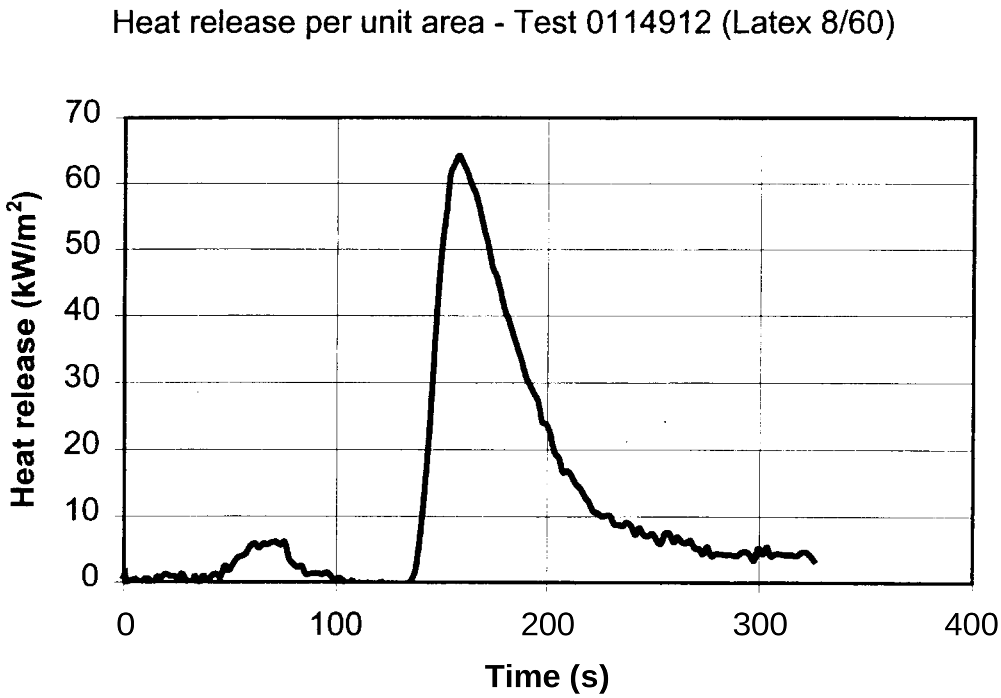
Heat release per unit area - Test 0114912 (Latex 8/60)
Heat release (kW/m²)
70
60
50
40
30
20
10
0
0
100
200
300
400
Time (s)

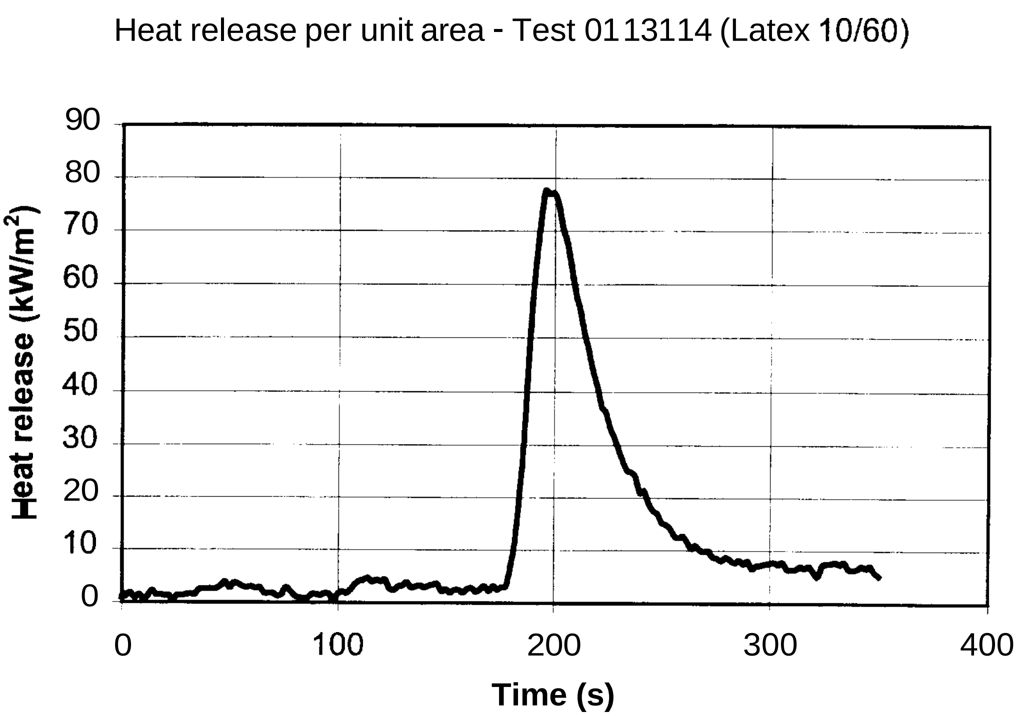
Heat release per unit area - Test 0113114 (Latex 10/60)
Heat release (kW/m²)
90
80
70
60
50
40
30
20
10
0
0
100
200
300
400
Time (s)

Heat release per unit area - Test 0113115 (Latex 10/55)

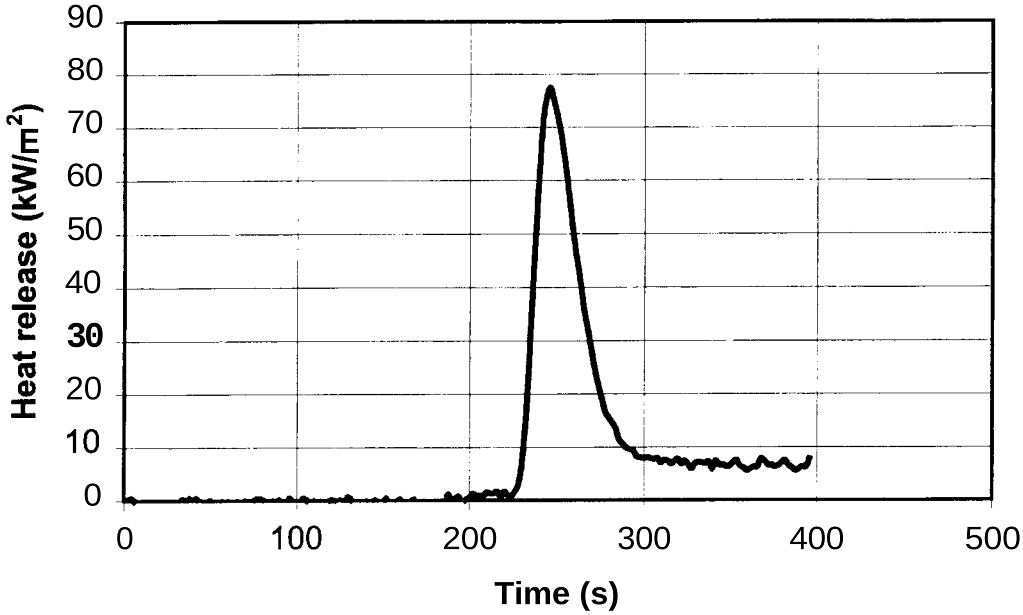

Heat release per unit area - Test 0119018 (Latex 2/85)

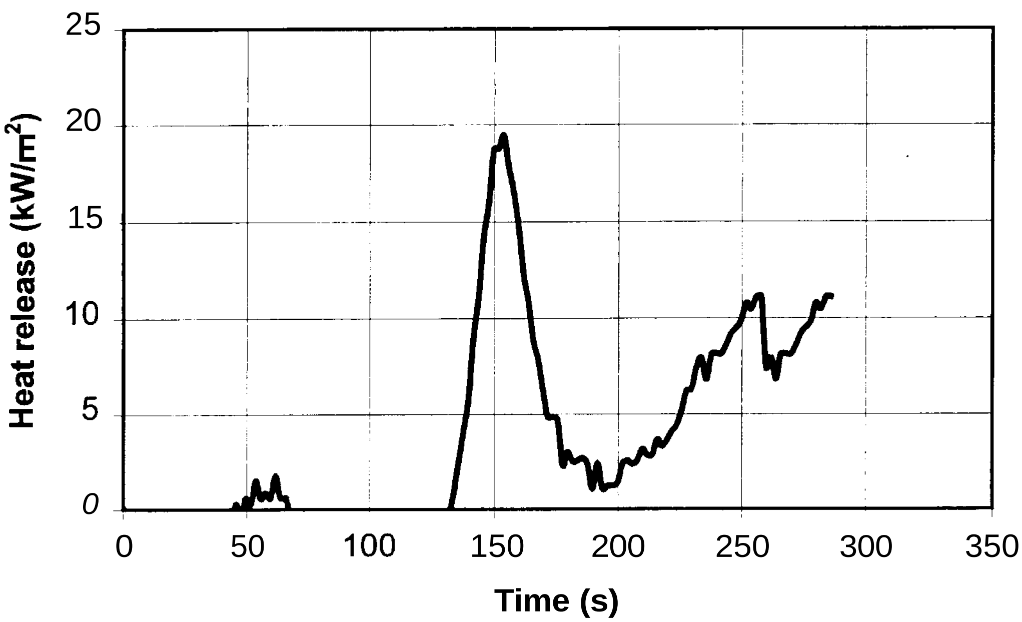

Heat release per unit area - Test 0114924 (Latex 6/65)

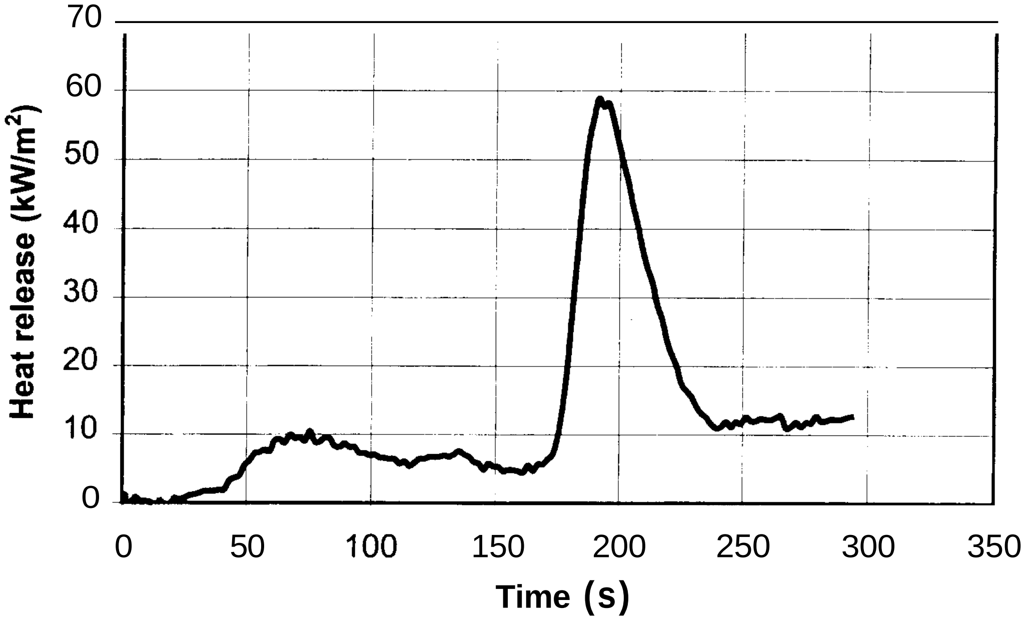

Heat release per unit area - Test 0114925 (Latex 8/55)

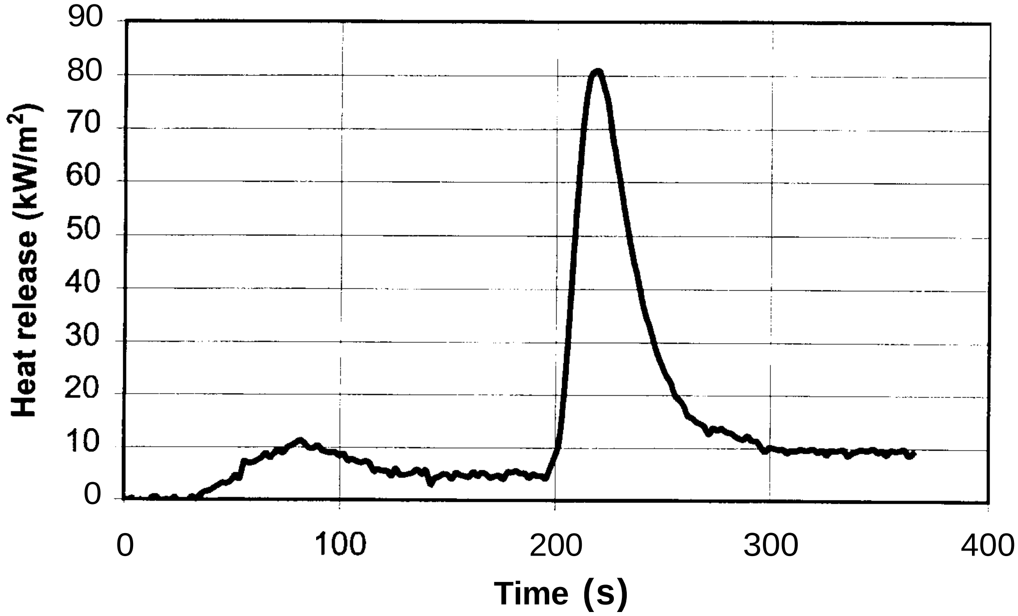

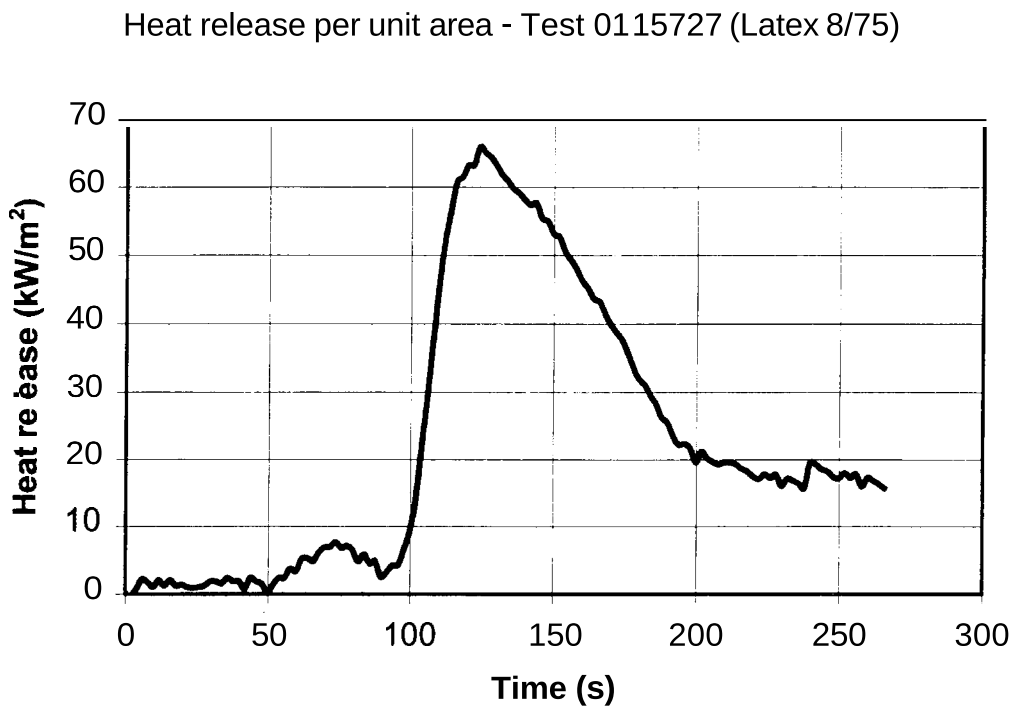
Heat release per unit area - Test 0115727 (Latex 8/75)
Heat re ease (kW/m²)
0
10
20
30
40
50
60
70
0
50
100
150
200
250
300
Time (s)

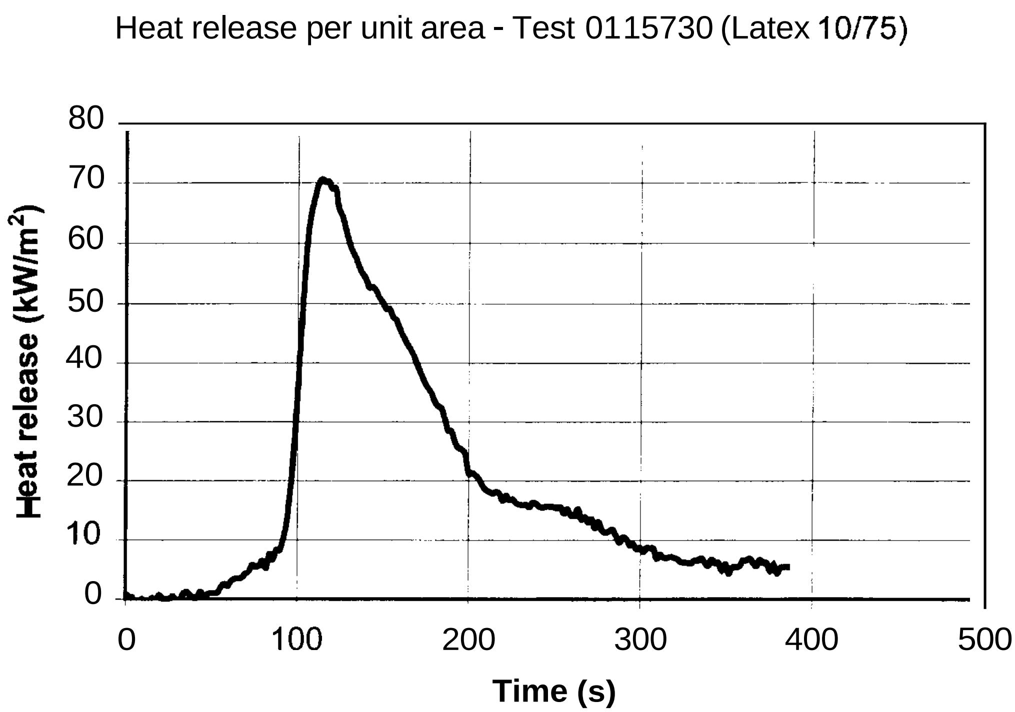
Heat release per unit area - Test 0115730 (Latex 10/75)
Heat release (kW/m²)
0
10
20
30
40
50
60
70
80
0
100
200
300
400
500
Time (s)

Heat release per unit area - Test 0110034 (Latex 4/75)

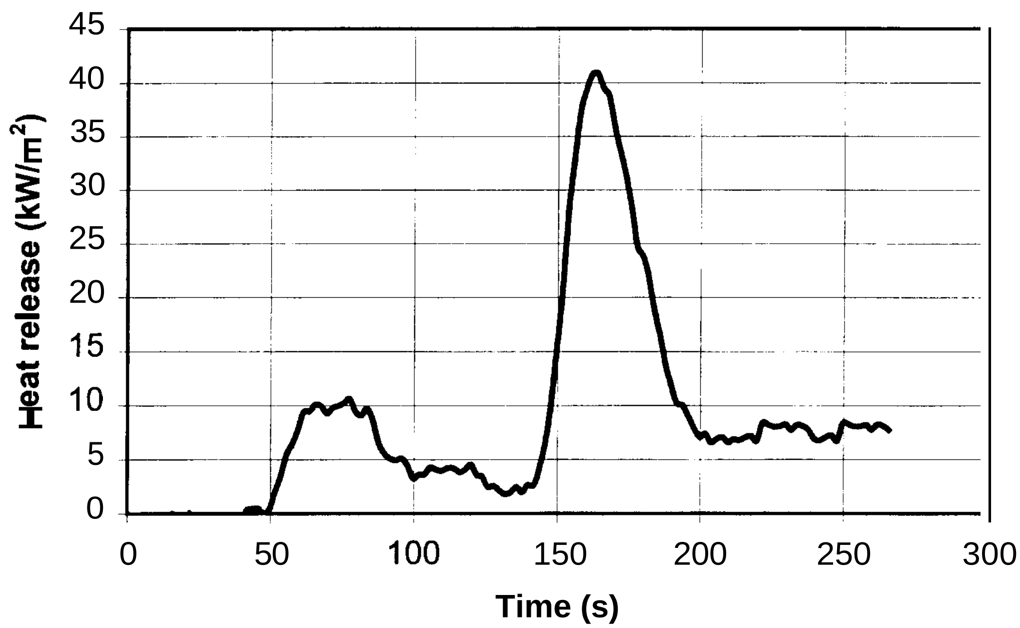

Heat release per unit area - Test 0110037 (Latex 6/75)

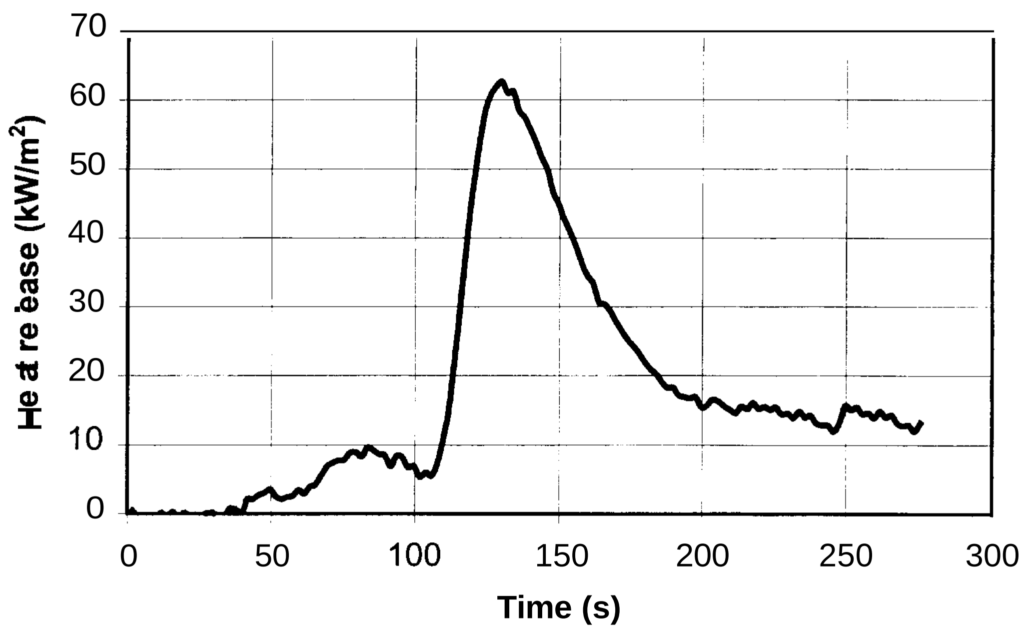

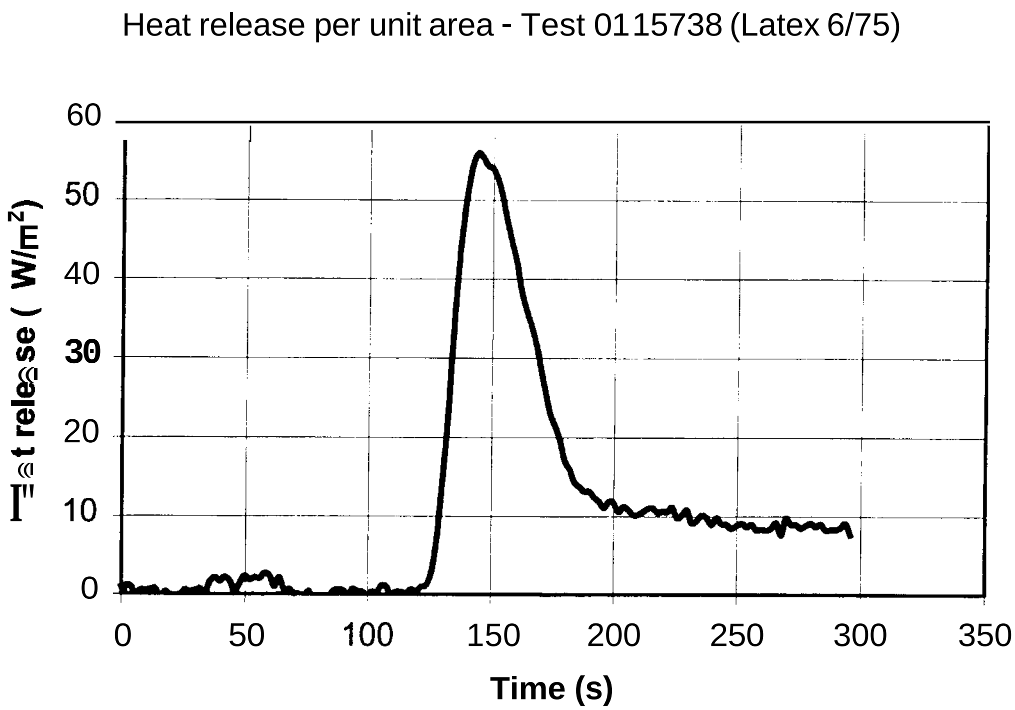
Heat release per unit area - Test 0115738 (Latex 6/75)
60
50
40
30
20
10
0
0
50
100
150
200
250
300
350
Time (s)

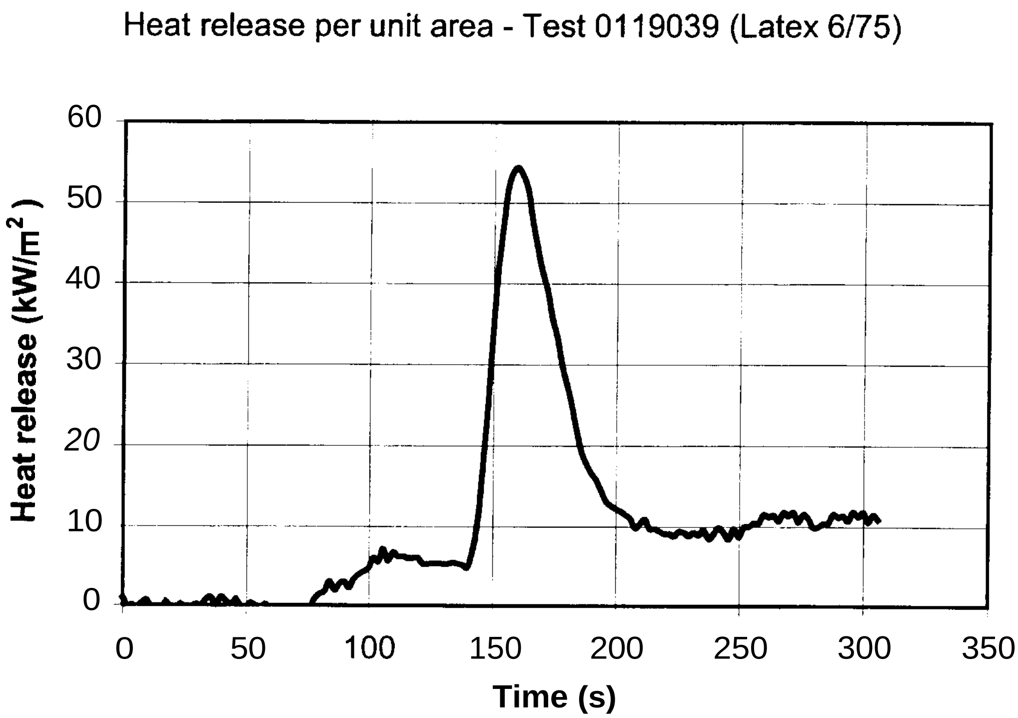
Heat release per unit area - Test 0119039 (Latex 6/75)
Heat release (kW/m2)
60
50
40
30
20
10
0
0
50
100
150
200
250
300
350
Time (s)

Heat release per unit area - Test 0110040 (Latex 8/75)

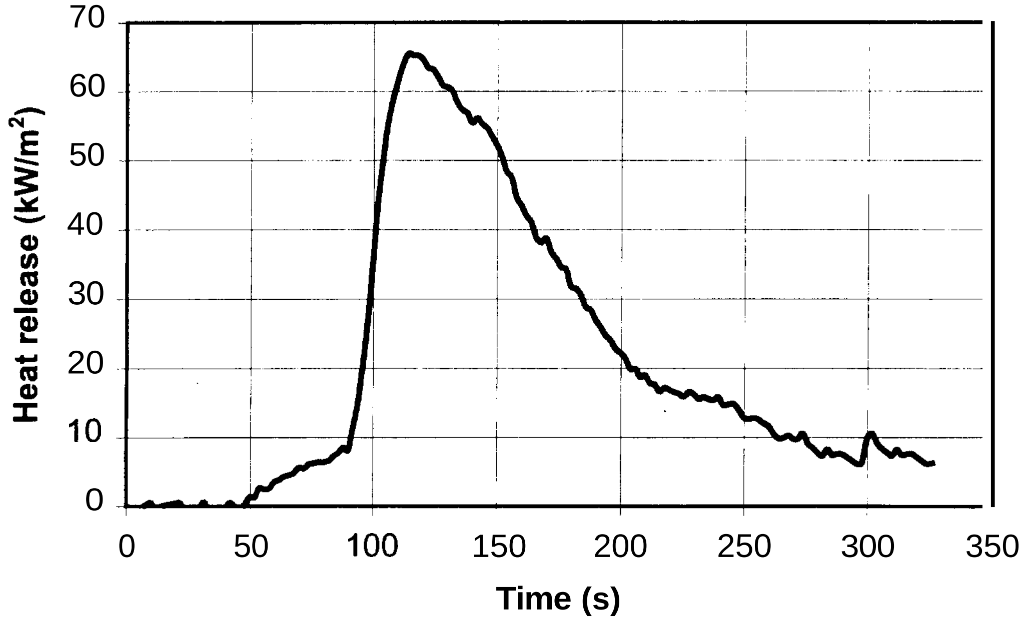

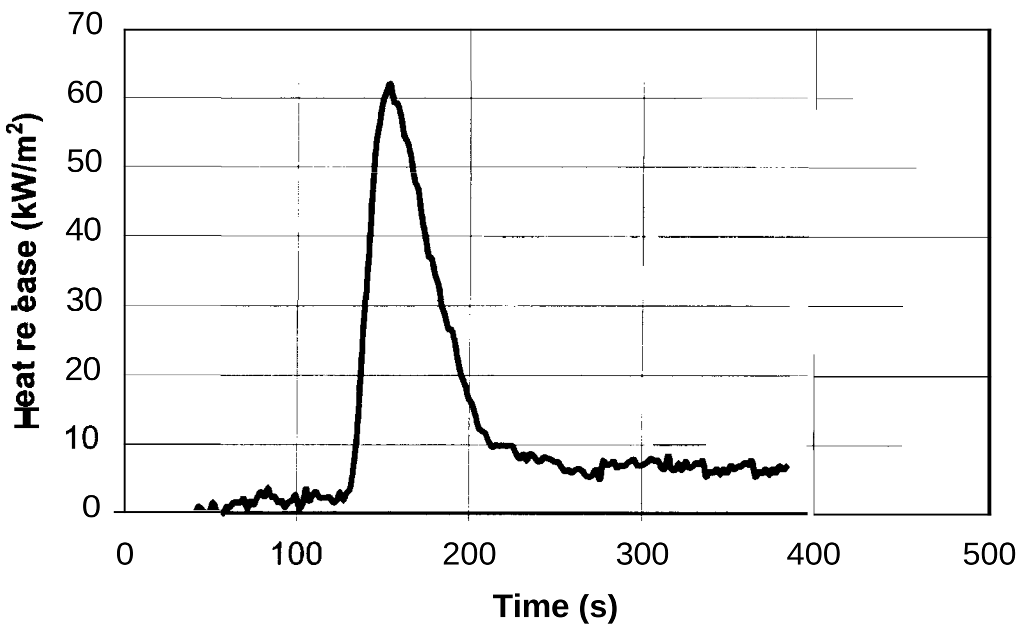

Heat release per unit area - Test 0115742 (Latex 8/65)

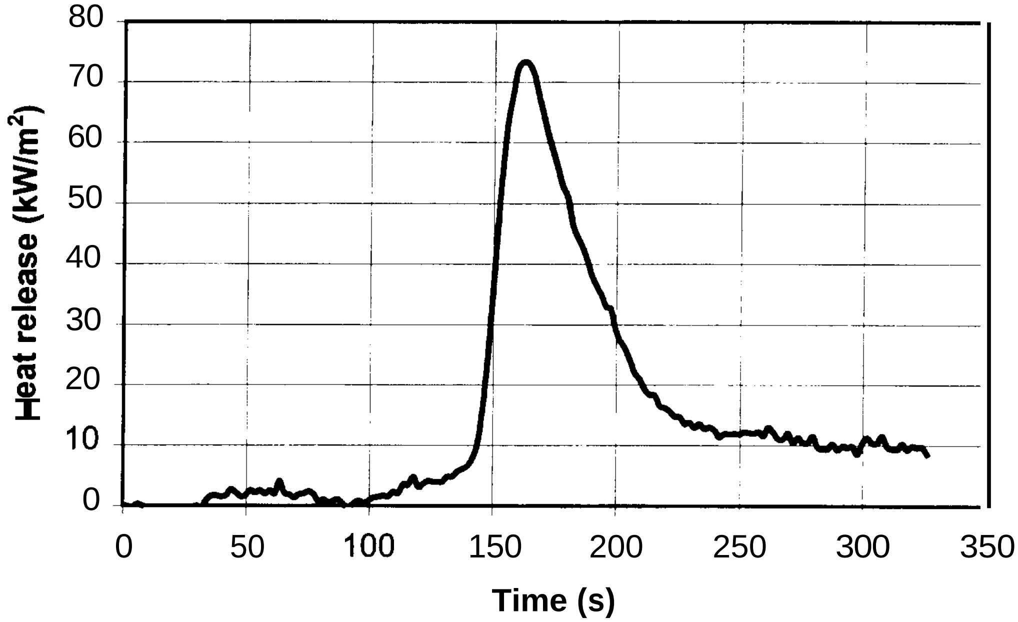

Heat release per unit area - Test 0110043 (Latex 10/75)

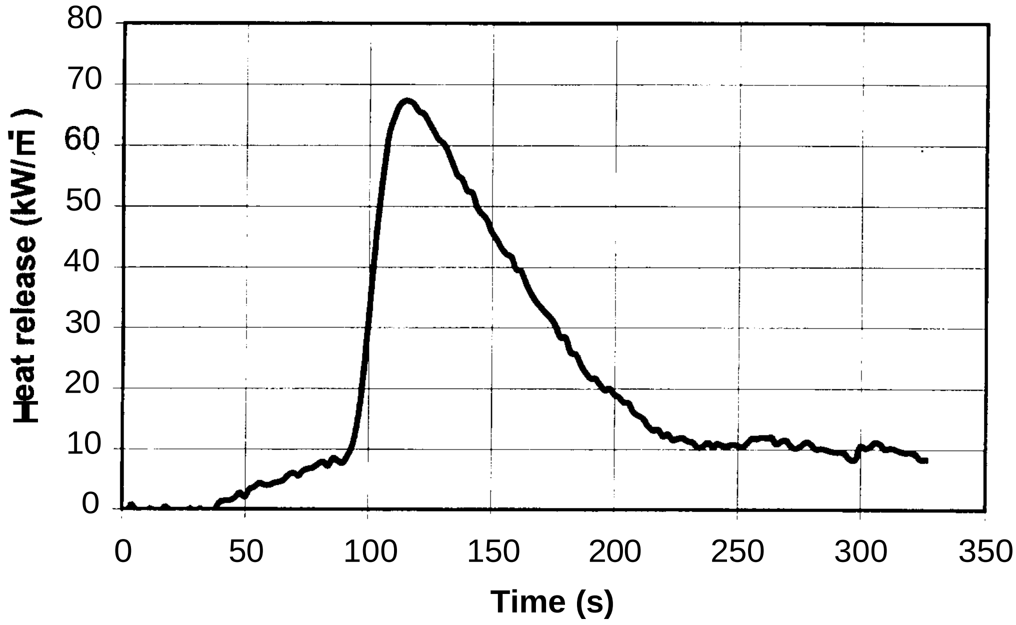

Heat release per unit area - Test 0115744 (Latex 10/65)

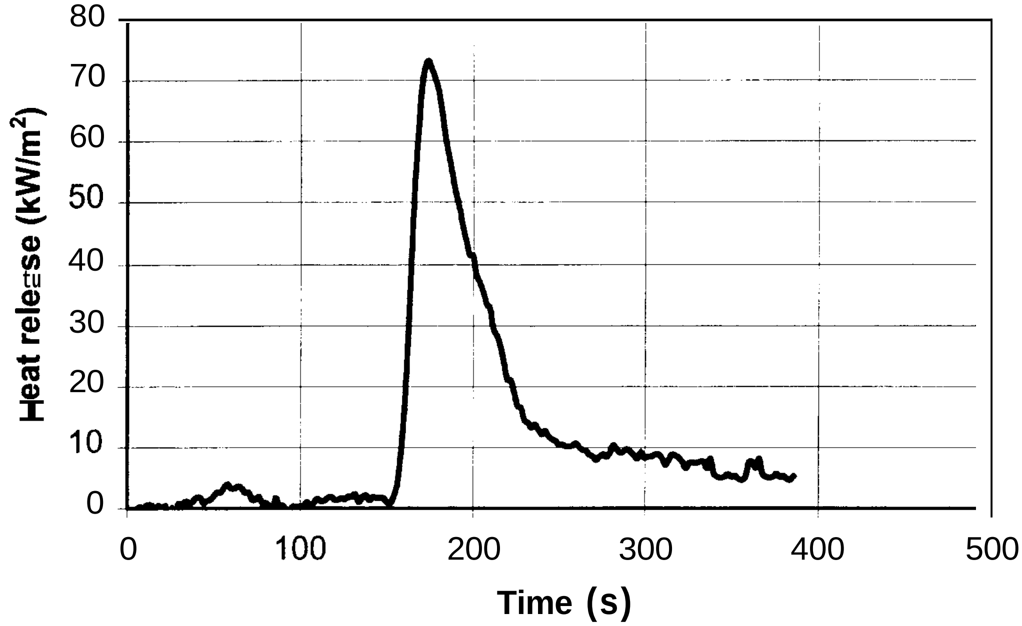

Heat release per unit area - Test 0115745 (Latex 10/65)

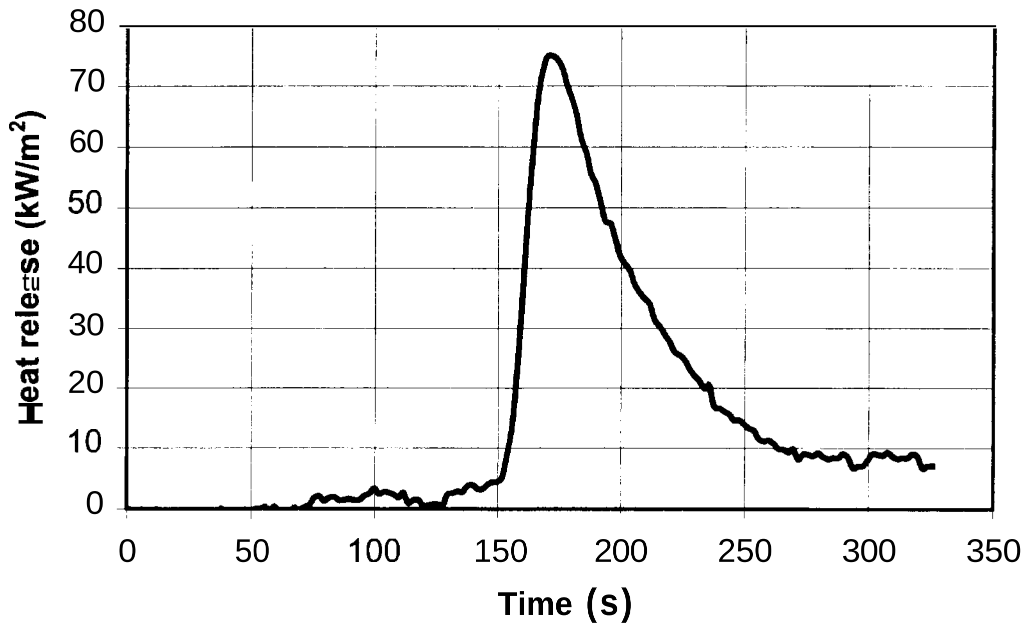

Heat release per unit area - Test 0119011 4 (Latex 4/75)

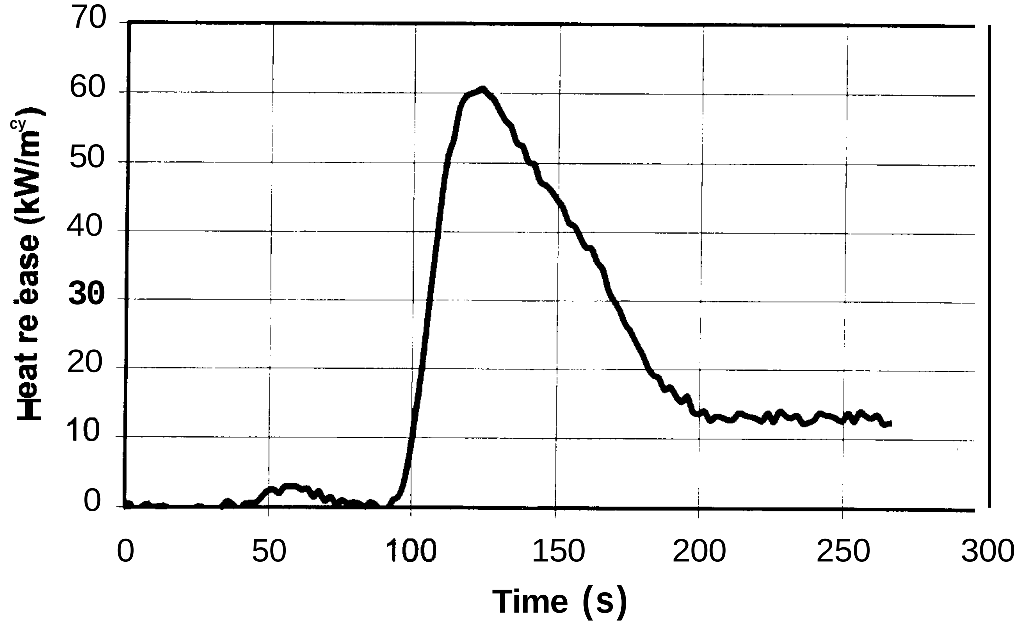

Heat release per unit area - Test 0119011 5 (Latex 4/75)

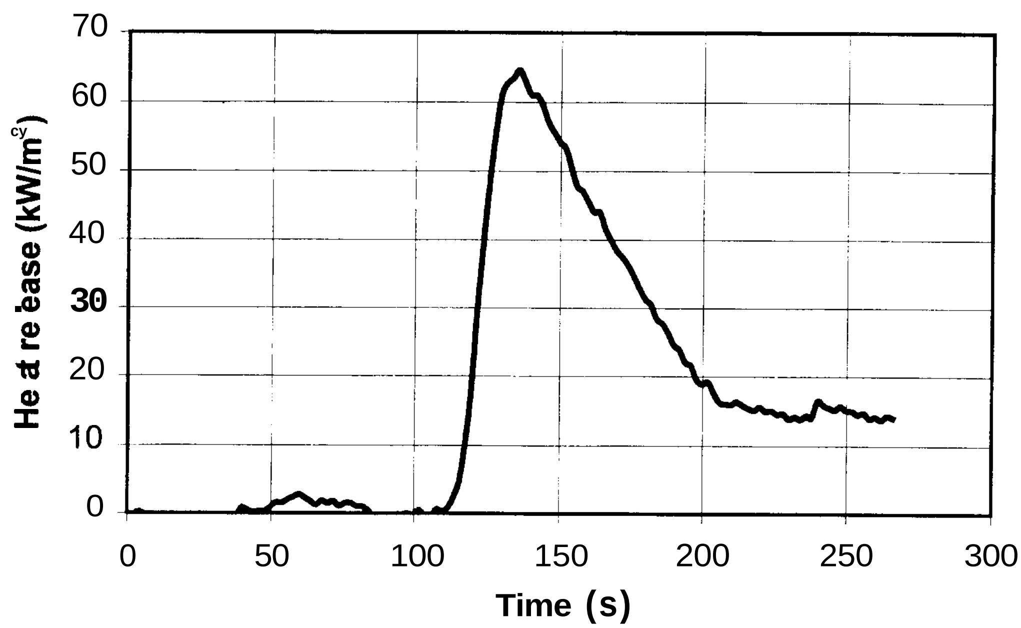

Heat release per unit area - Test 0115151 (Oil 4/65)

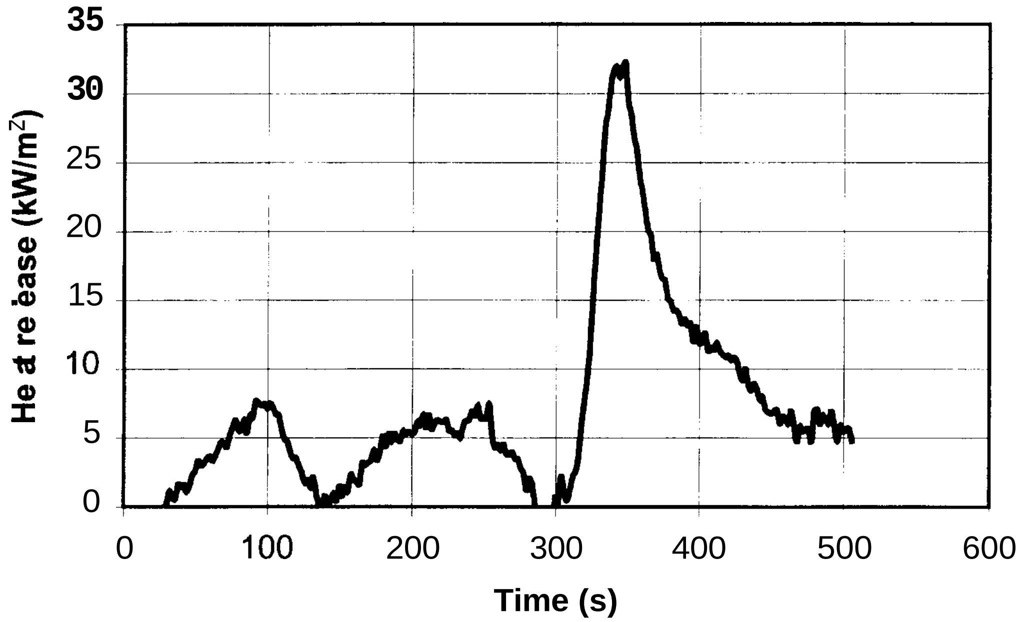

Heat release per unit area - Test 0115152 (Oil 6/55)

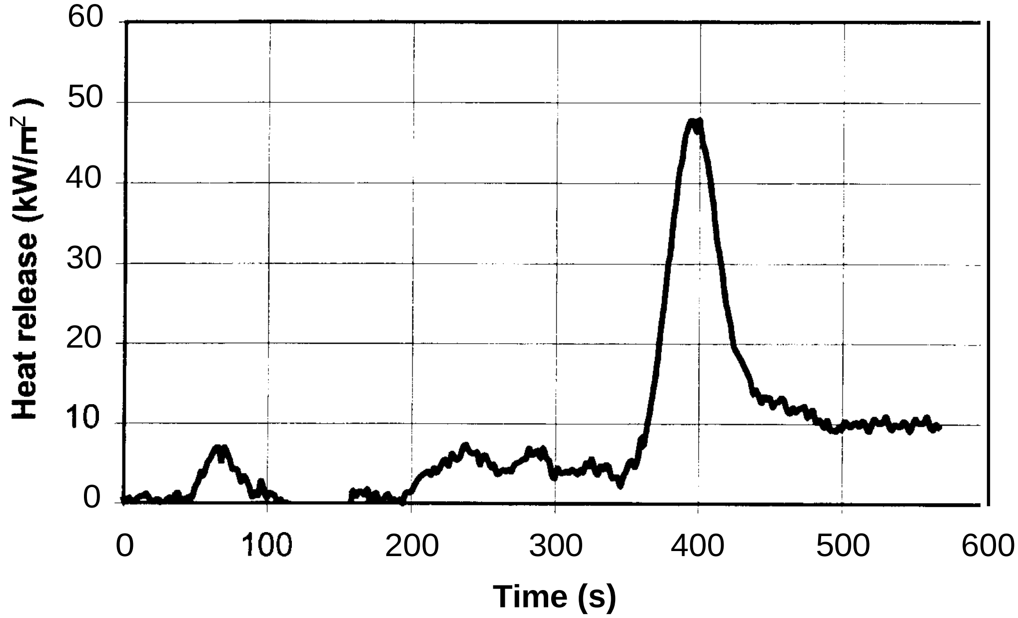

Heat release per unit area - Test 0119053 (Oil 6/85)

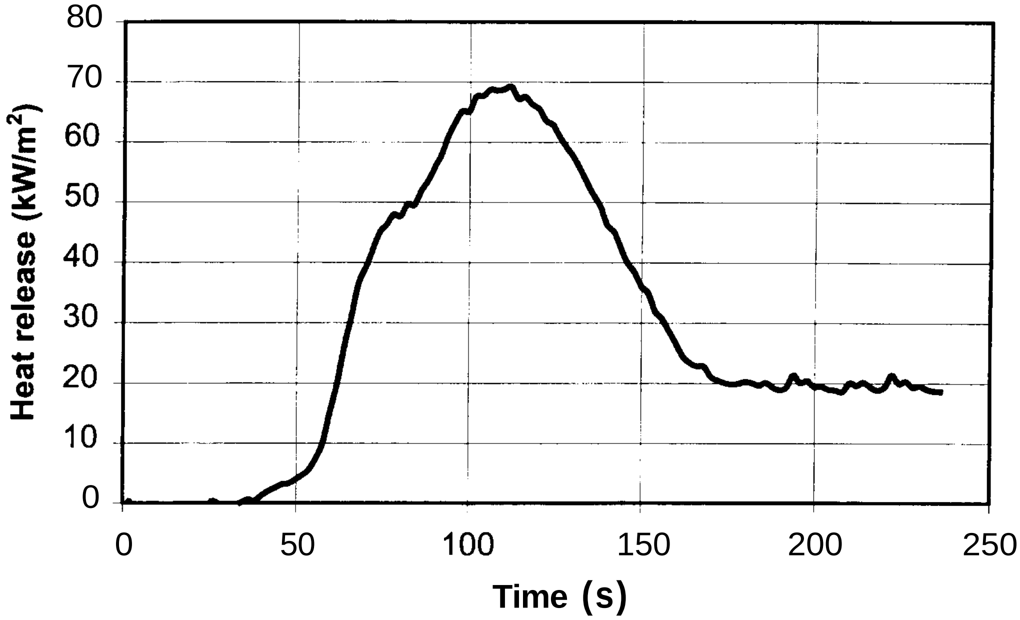

Heat release per unit area - Test 0119054 (Oil 6/85)

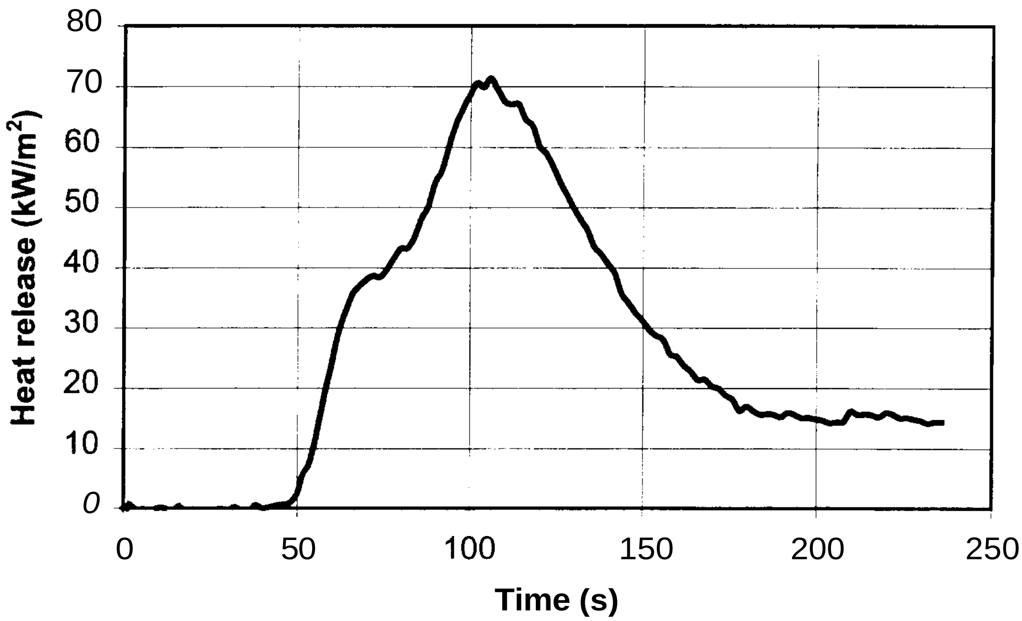

Heat release per unit area - Test 0115157 (Oil 8/55)

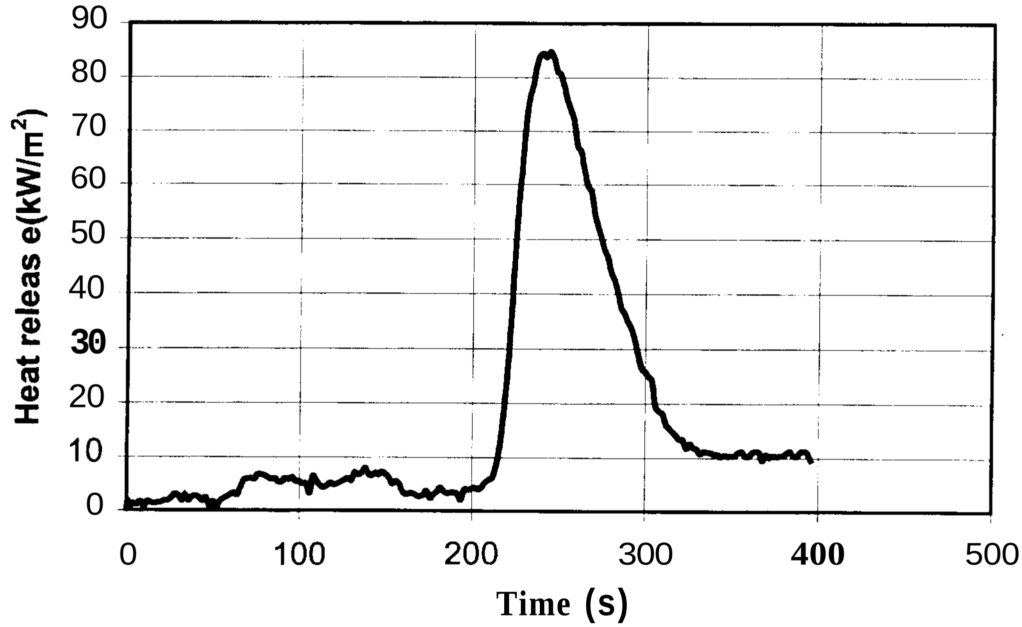

Heat release per unit area - Test 0115159 (Oil 10/50)

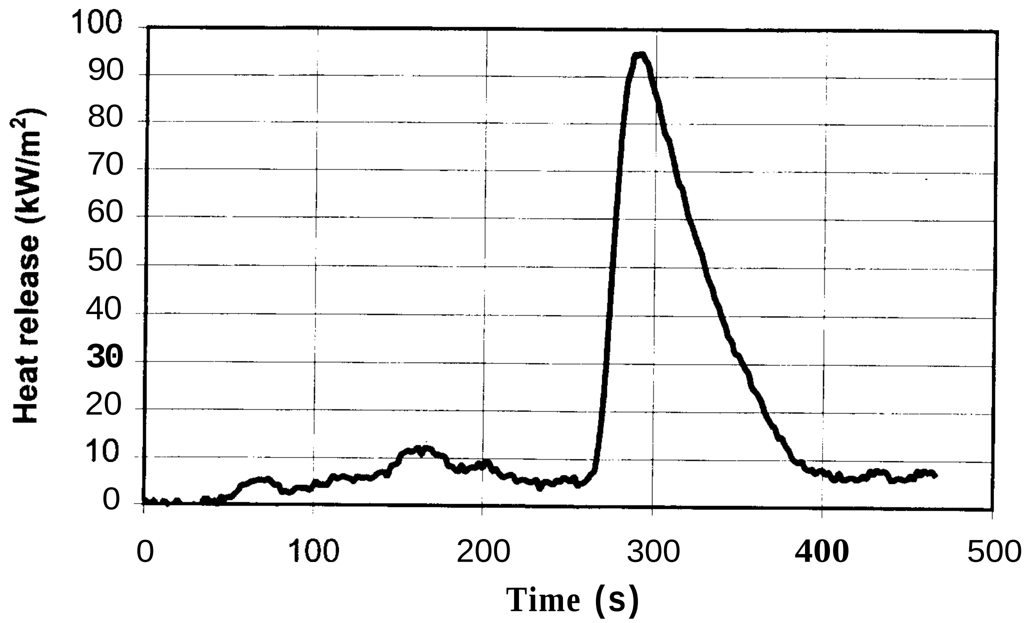

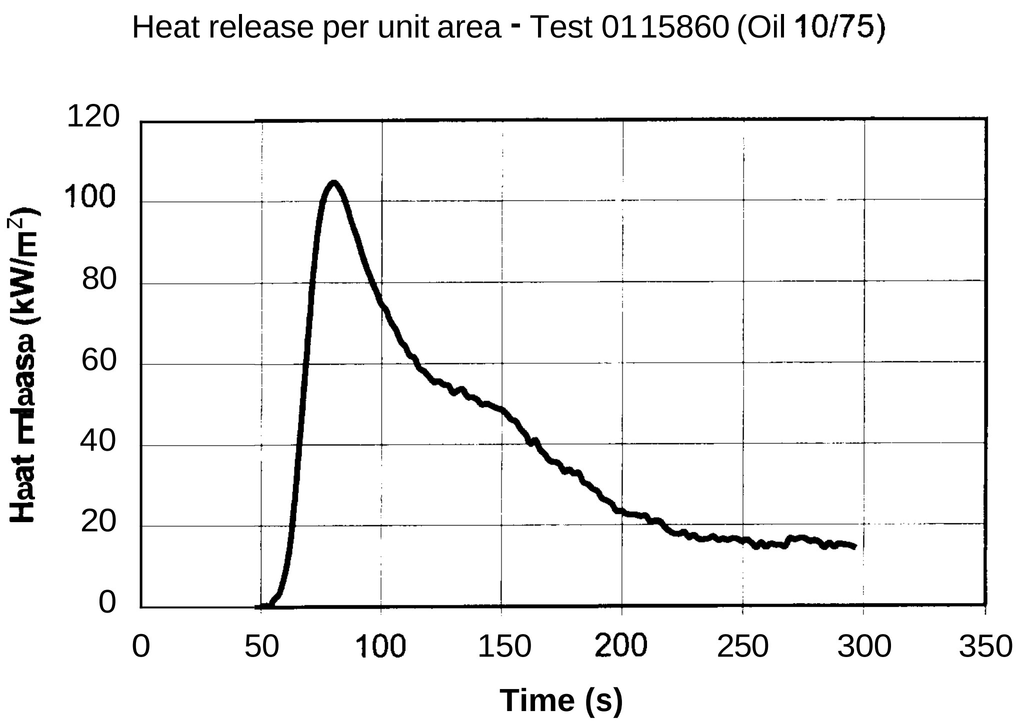
Heat release per unit area - Test 0115860 (Oil 10/75)
Heat release (kW/m2)
Time (s)
0
20
40
60
80
100
120
0
50
100
150
200
250
300
350

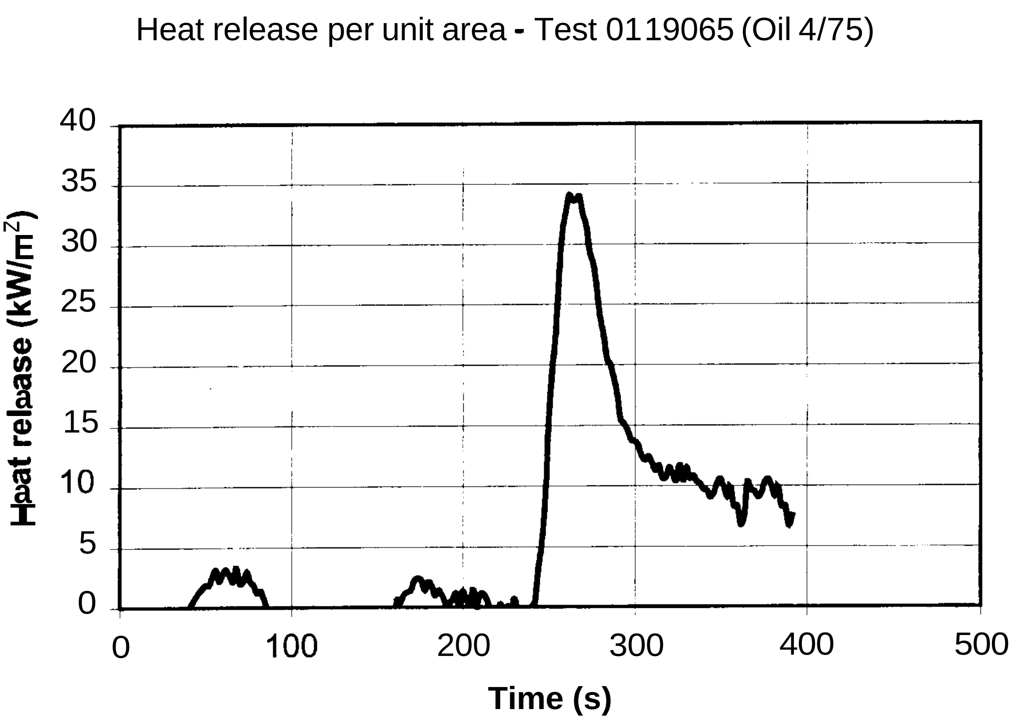
Heat release per unit area - Test 0119065 (Oil 4/75)
Heat release (kW/m2)
Time (s)
0
5
10
15
20
25
30
35
40
0
100
200
300
400
500

Heat release per unit area - Test 0119066 (Oil 4/75)

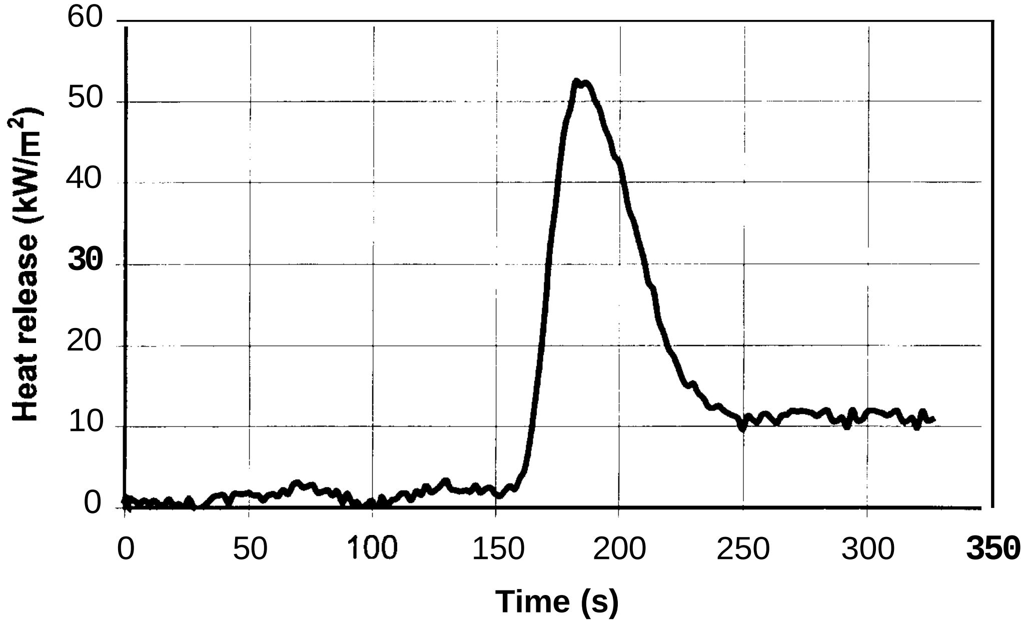

Heat release per unit area - Test 0119068 (Oil 6/85)

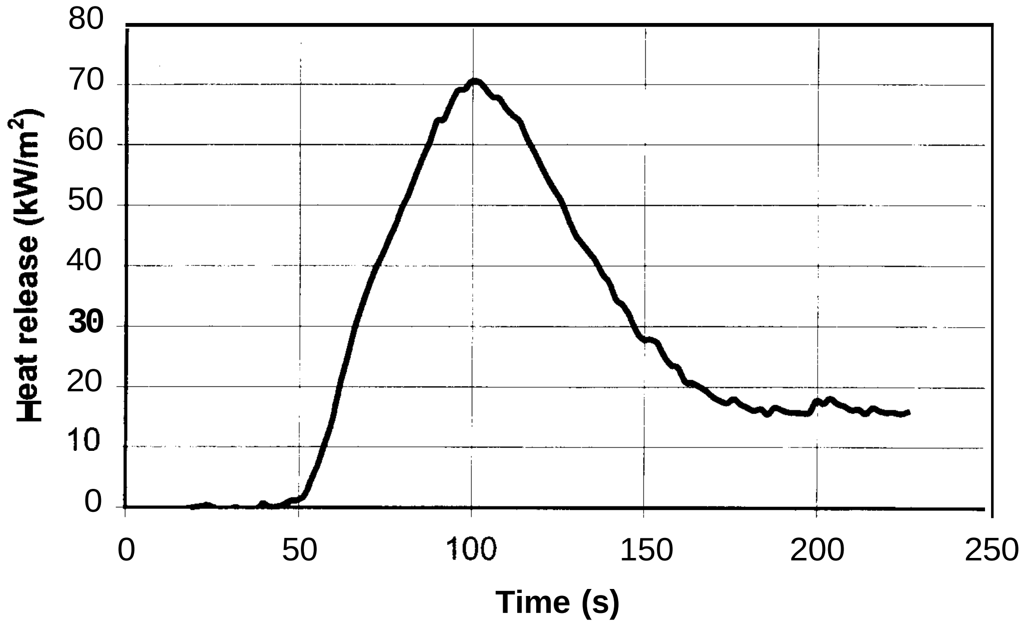

Heat release per unit area - Test 0112170 (Oil 8/50)

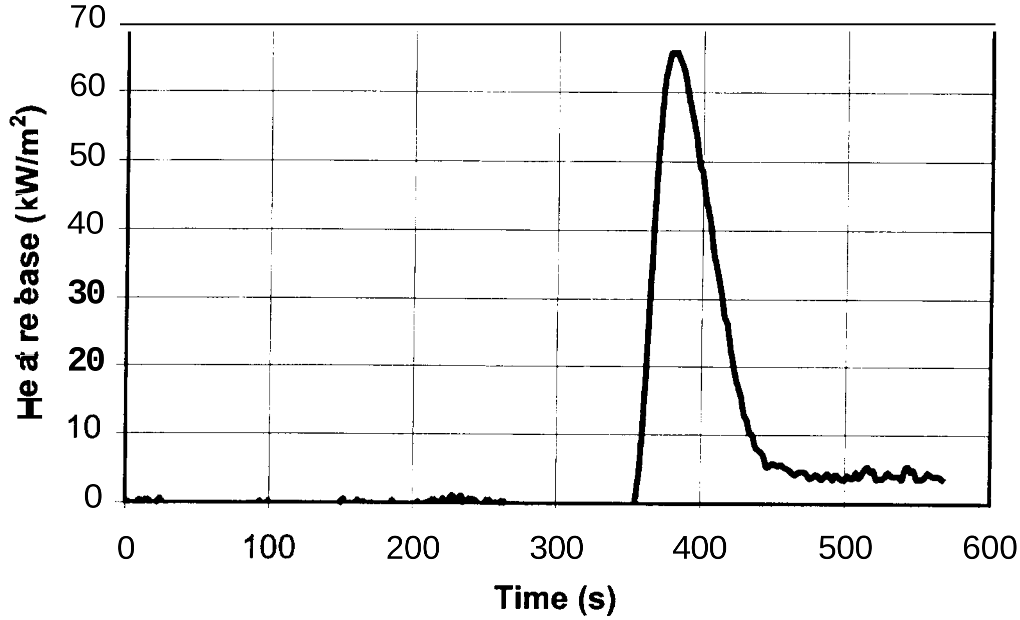

Heat release per unit area - Test 0115871 (Oil 8/75)

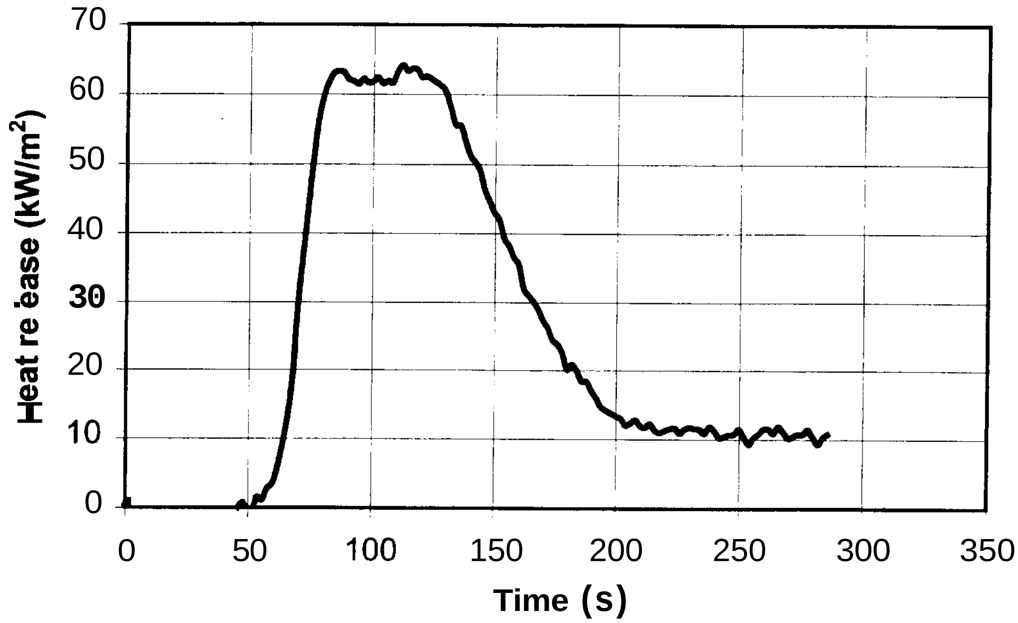

Heat release per unit area - Test 0115872 (Oil 8/75)

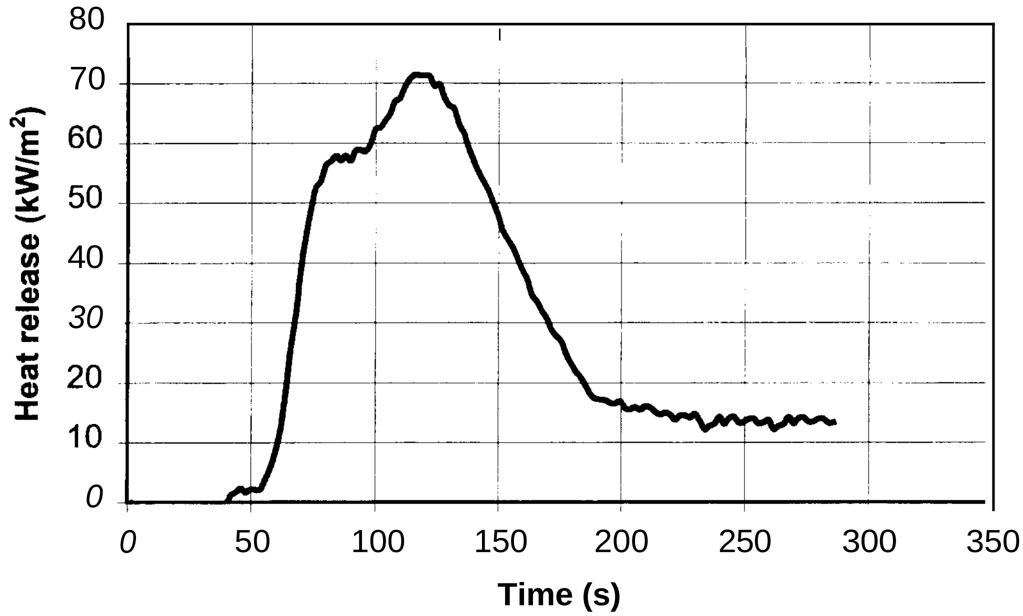

Heat release per unit area - Test 0112173 (Oil 10/50)

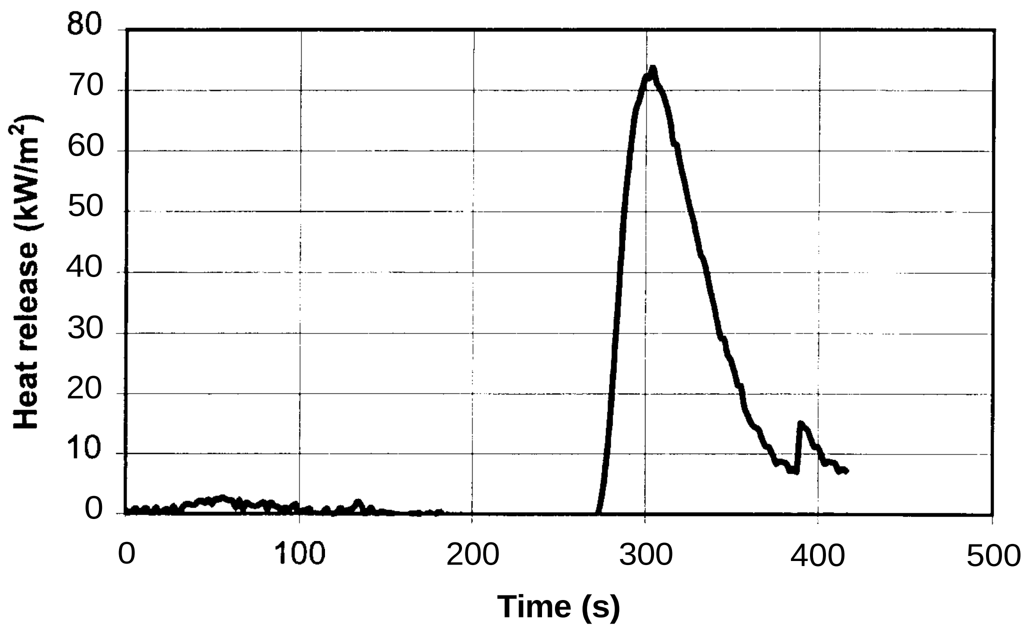

Heat release per unit area - Test 0115874 (Oil 10/75)

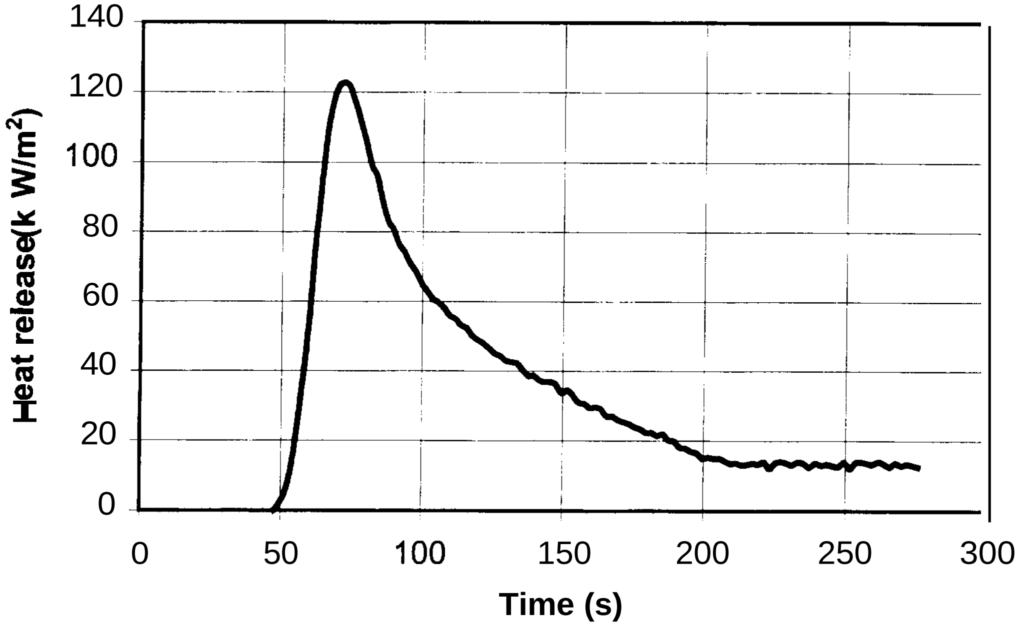

Heat release per unit area - Test 0115875 (Oil 10/75)

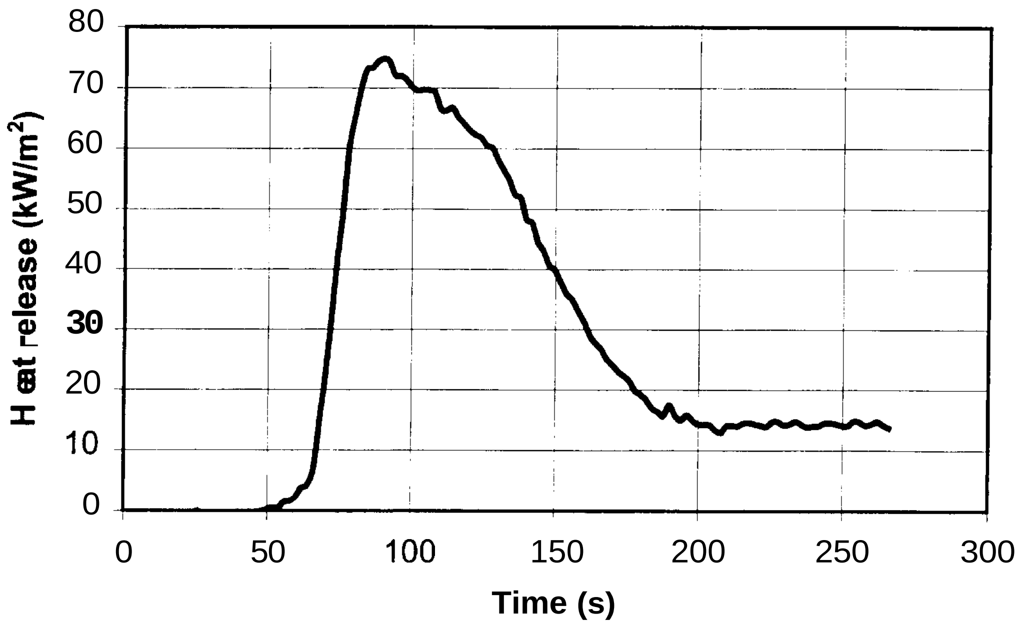

Heat release per unit area - Test 0115882 (Oil 6/75)

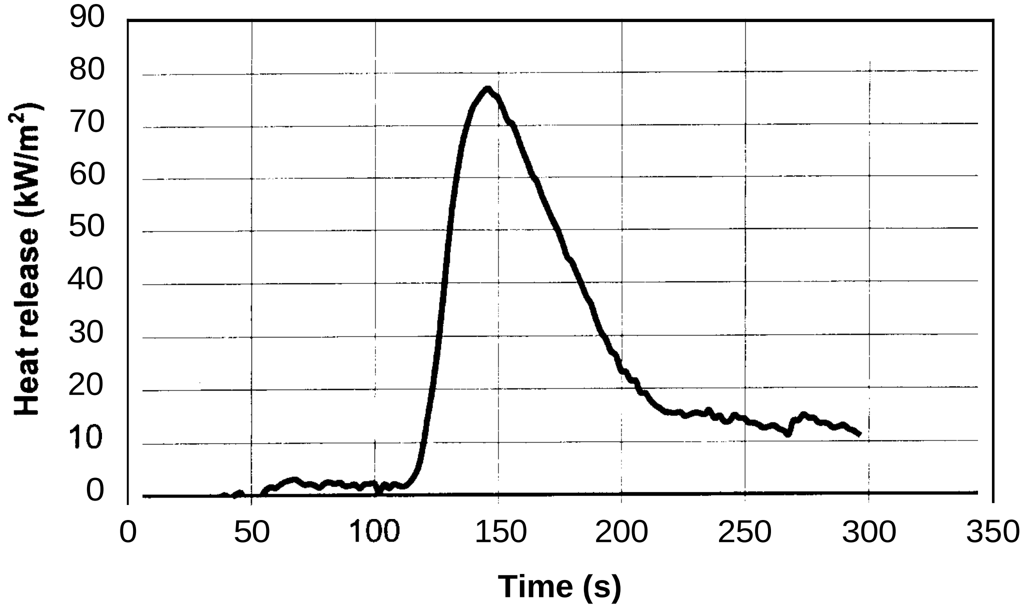

Heat release per unit area - Test 0115883 (Oil 6/75)

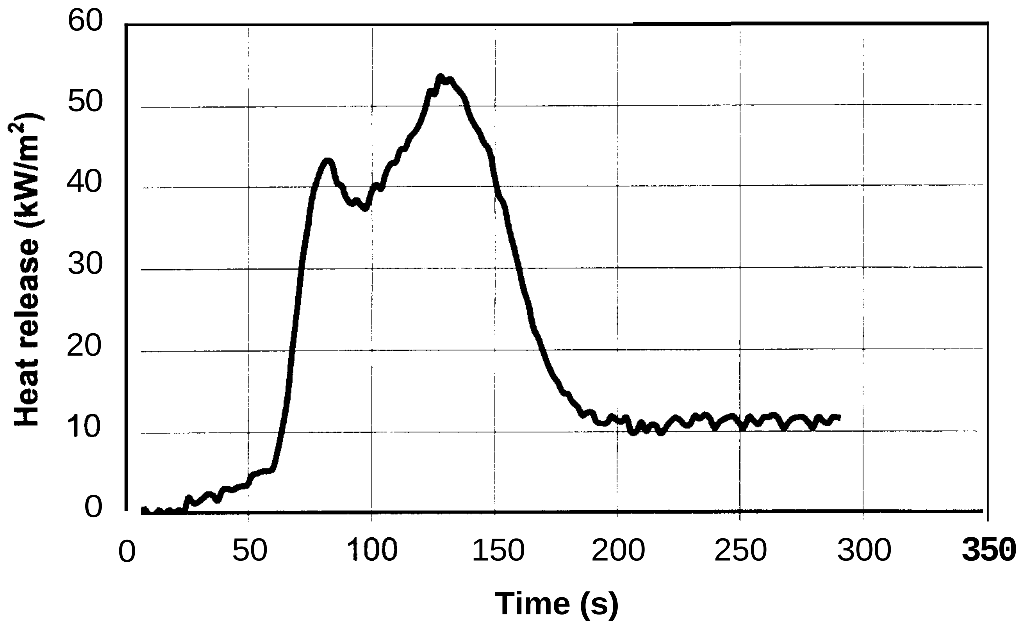

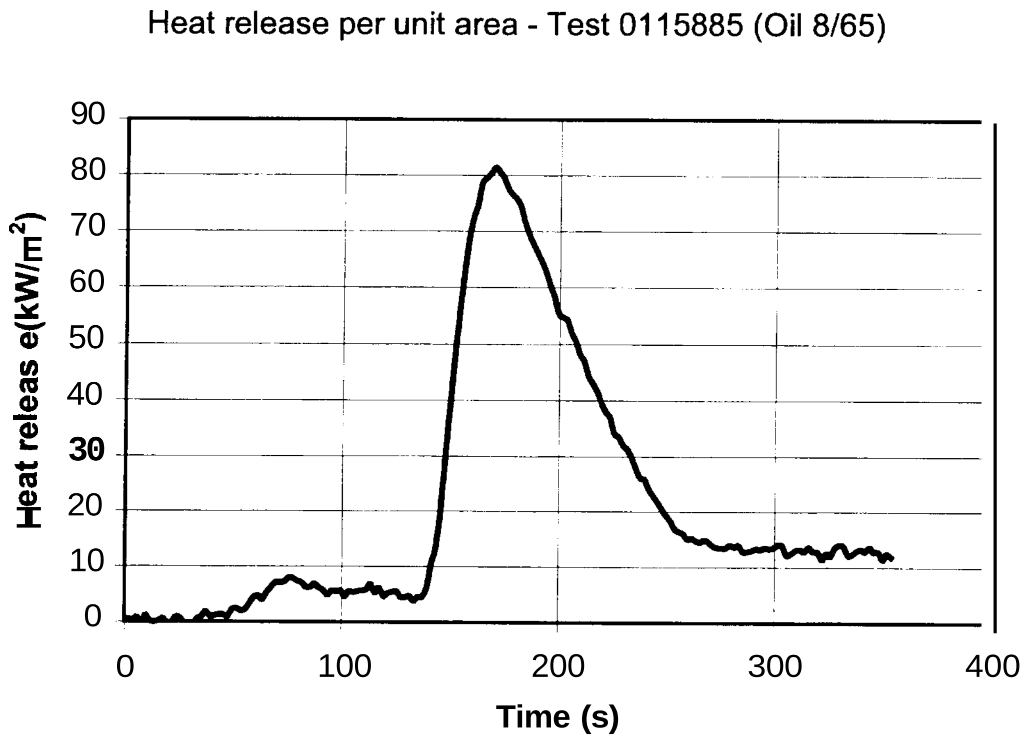
Heat release per unit area - Test 0115885 (Oil 8/65)
Heat releas e(kW/m2)
90
80
70
60
50
40
30
20
10
0
0
100
200
300
400
Time (s)

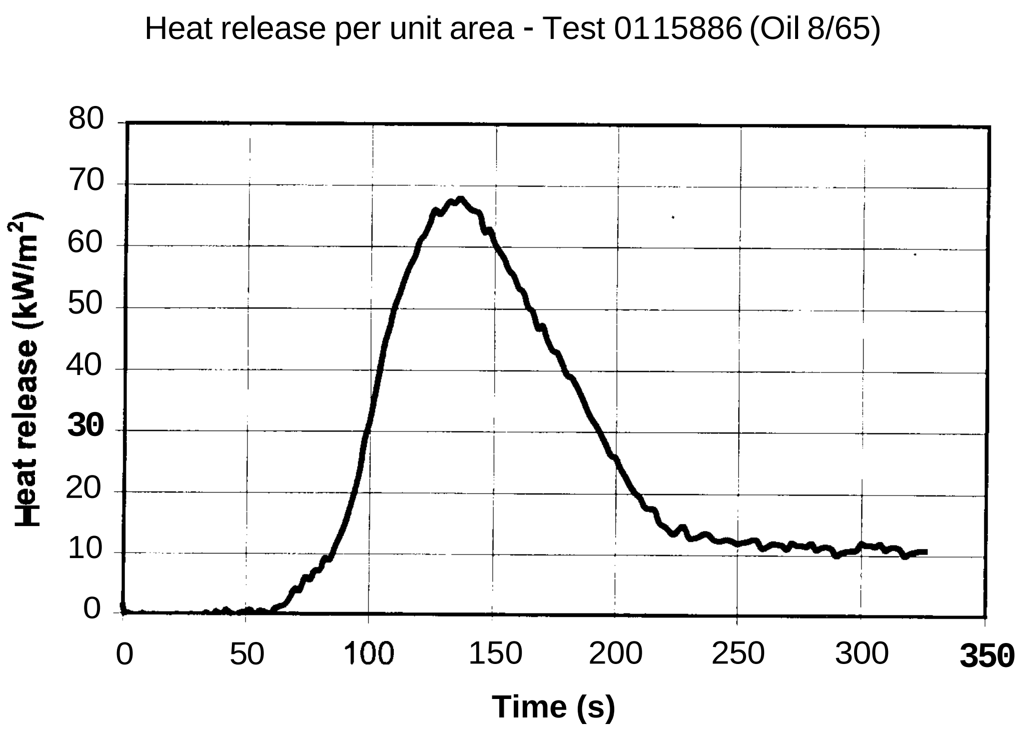
Heat release per unit area - Test 0115886 (Oil 8/65)
Heat release (kW/m2)
80
70
60
50
40
30
20
10
0
0
50
100
150
200
250
300
350
Time (s)

Heat release per unit area - Test 0115887 (Oil 8/65)

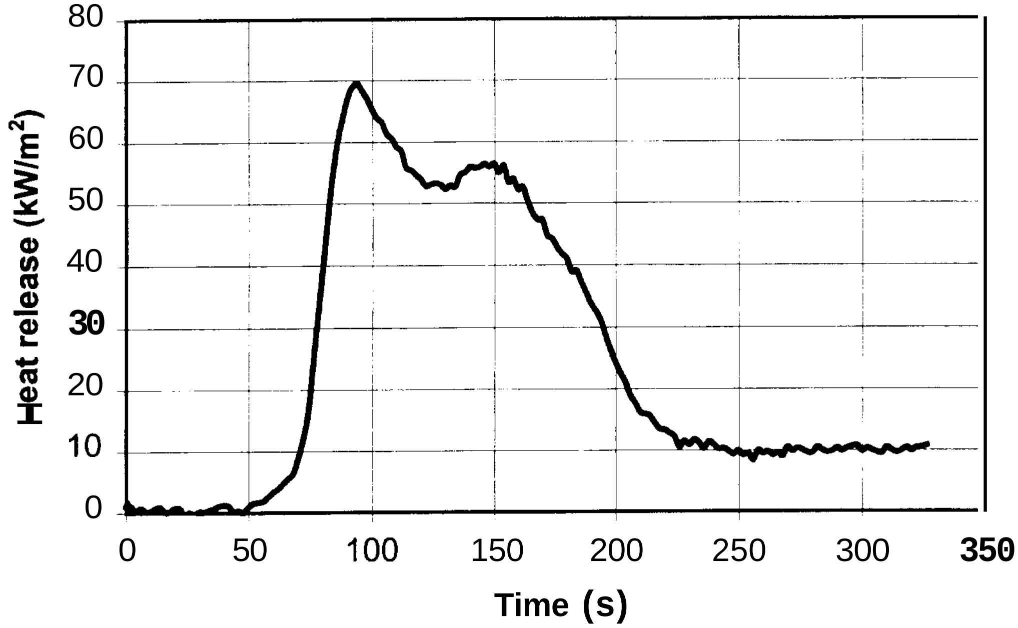

Heat release per unit area - Test 0115888 (Oil 10/65)

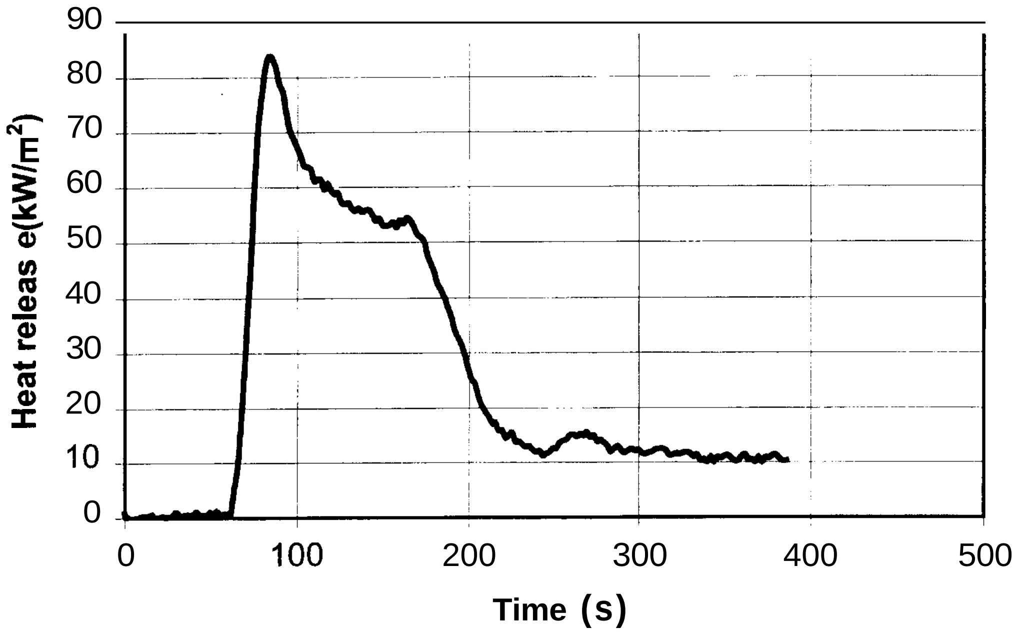

Heat release per unit area - Test 0115889 (Oil 10/65)

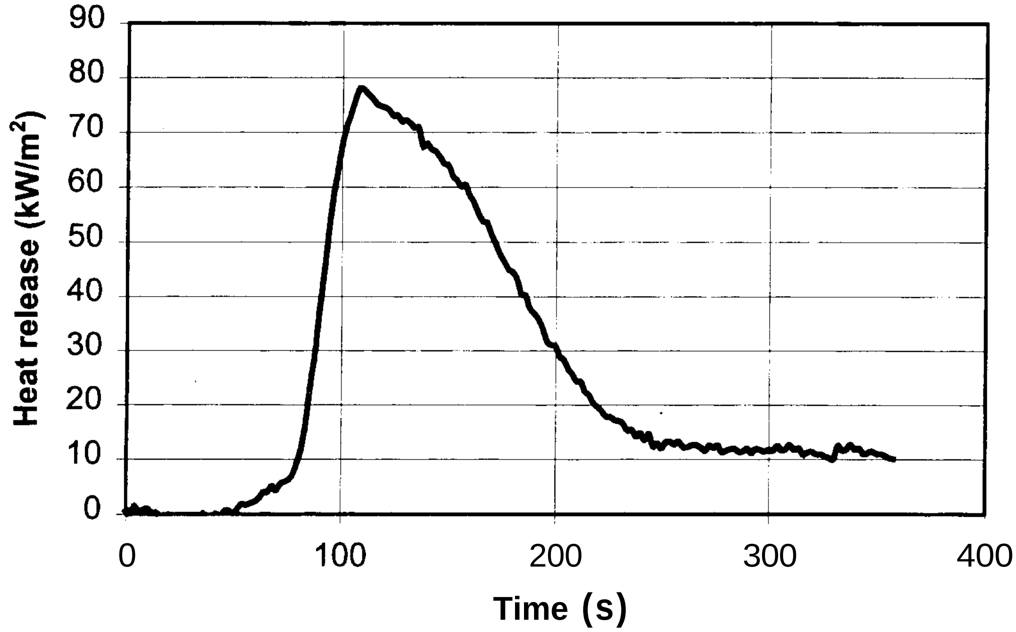

Heat release per unit area - Test 0115890 (Oil 10/65)

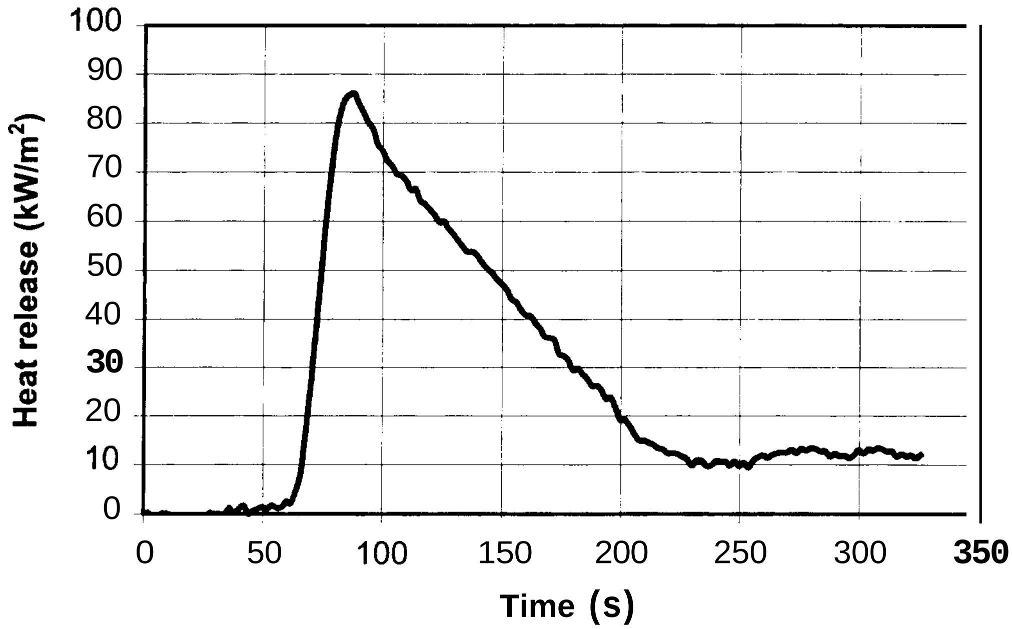

XI. REFERENCES

1. Belles, D., "Interior Finish," Section 7/Chapter 3, *NFPA Fire Protection Handbook,* Arthur E. Cote, ed., NFPA, Quincy, 1997.
2. ASTM E84, *Standard Test Methodfor Surface Burning Characteristics of Building Materials,* American Society for Testing and Materials, West Conshohocken, PA, 2000.
3. Saito, K., Quintiere, J.G., and Williams, F.A., "Upward Turbulent Flame Spread," in *Fire Safety Science – Proc. Of the First International Symposium,* eds. C.E. Grant and P.J. Pagni, Hemisphere, Washington, DC, 1986.
4. Cleary, T.G., and Quintiere, J.G., "A Framework for Utilizing Fire Property Tests,'' in *Fire Safety Science – Proc. Of the Third International Symposium,* eds. G. Cox and B. Langford, Elsevier, London, 1991.
5. Quintiere, J.G., "A Simulation Model for Fire Growth on Materials Subject to a Room/Corner Test," *Fire Safety Journal*, Vol. 18, 1992.
6. NFPA 271, *Standard Method of Testfor Heat and Smoke Release Ratesfor Materials and Products Using and Oxygen Consumption Calorimeter,* National Fire Protection Association, Quincy, 2001.
7. ASTM E1321, *Standard Test Methodfor Determining Material Ignition and Flame Spread Properties,* American Society for Testing and Materials, West Conshohocken, PA, 1997.
8. Janssens, M.L., Dillon, S.E., "Balanced Approach to the Fire Performance Evaluation of Interior Finish Materials," U.S./Japan Government Cooperative Program on Natural Resources (UJNR), Fire Research and Safety, 15th Joint

Panel Meeting, Volume 1, Proceedings, March 1-7,2000, San Antonio, TX, Bryner, S. L., Editor, 2000.

9. Dillon, S. E., Kim, W. H., Quintiere, J. G., "Determination of Properties and the Prediction of the Energy Release Rate of Materials in the ISO 9705 Room-Comer Test," NIST GCR 98-753, July 1998.

10. ISO 9705, "Fire Tests - Full Scale Room Fire Test for Surface Products," International Organization for Standardization, 1993.

11. Torero, J.L., Mowrer, F.W., **"A** New Approach to Interpreting LIFT Ignition Test Data," to be published, University of Maryland, College Park, MD, 2001.

12. Delichatsios, **M.A.,** Panagiotou, Th., Kiley, F., "The Use of Time to Ignition Data for Characterizing the Thermal Inertia and the Minimum (Critical) Heat Flux for Ignition and Pyrolysis," *Combustion and Flame,* **84,** 1991.

13. McGraw, J.R. Jr., Mowrer, F.W., "Flammability of Painted Gypsum Wallboard Subjected to Fire Heat Fluxes," *Proc. – Interflam 2999,* Vol. *2*, Interscience Communications Ltd., London, 1999.

14. Mowrer, F.W., "The Effect of "Blistering" on the Ignition and Flammability of Painted Gypsum Wallboard," *Proc. – Fire and Materials 2002,* San Fransisco, 2001.

15. Mowrer, F.W., Williamson, R.B., "Flame Spread Evaluation for Thin Interior Finish Materials," in Fire Safety Science – Proc. Of the Third International Symposium, eds. G. Cox and B. Langford, Elsevier, London, 1991.

16. *SFPE Handbook of Fire Protection Engineering,* Society of Fire Protection Engineers, ed. Philip DiNenno, Bethesda, 1995.

17. McGrattan, K. B., Forney, G. P., "Fire Dynamics Simulator: User's Manual,", NISTIR 6469, January 2000.

18. *ASHRAE Handbook – Fundamentals,* American Society of Heating, Refrigerating, and Air-conditioning Engineers, Atlanta, 1997.

19. Tewarson, A., "Generation of Heat and Chemical Compounds in Fires," Section 3/Chapter 4, *SFPE* ***Handbook*** *of Fire Protection Engineering,* Society of Fire Protection Engineers, ed. Philip DiNenno, Bethesda, MD, 1995.